Technische Universität München
TUM School of Medicine and Health

Identification of Ewing Sarcoma specific T Cell Receptors for adoptive Transfer
-
Exploring LIPI, GPR64, PAX7, and CHM1 as Targets

Hannah Hüls

Vollständiger Abdruck der von der TUM School of Medicine and Health

der Technischen Universität München zur Erlangung einer

Doktorin der Medizin (Dr. med.)

genehmigten Dissertation.

Vorsitz: Prof. Dr. Marcus Makowski

Prüfende der Dissertation:

1. Priv.-Doz. Dr. Uwe Thiel
2. Priv.-Doz. Dr. Josef Mautner

Die Dissertation wurde am 04.07.2024 bei der Technischen Universität München eingereicht und durch die TUM School of Medicine and Health am 06.11.2024 angenommen.

Table of Contents

List of Figures

List of Tables

Abbreviations

AEC	3-Amino-9-ethyl-carbazole
AKT/PKB	Protein Kinase B
ALL	Acute lymphocytic leukemia
Allo-SCT	Allogeneic stem cell transplantation
APC	Allophycocyanin
auto-SCT	autologous stem cell transplantation
BCP	1-Bromo-3-Chloro-Propane
BCR	B cell receptor
BLAST	Basic Local Alignment Search Tool
Bp	Base pair
BSA	Bovine serum albumin
BuMel	busulfan, melphalan
CAR	Chimeric antigen receptor
cDNA	Copy deoxyribonucleic acid
CDR	Complementarity-determining regions
CHM1	Chondromodulin 1
CLL	Chronic lymphocytic leukemia
CRISPR/Cas9	Clustered regularly interspaced palindromic repeats/Cas9
CRS	cytokine release syndrome
CTLA-4	Cytotoxic T-Lymphocyte-Associated Protein 4
DC	Dendritic cell
DEPC	Diethylpyrocarbonate
DMEM	Dulbecco's modified eagle's medium
DMF	Dimethylformamide
DMSO	Dimethyl sulfoxide
DNA	Deoxyribonucleic acid
dNTP	Deoxynucleotides triphosphate
DPBS	Dulbecco's phosphate-buffered saline
DRK	Deutsches Rotes Kreuz
EBV	Epstein-Barr Virus

EDTA	Ethylenediaminetetraacetic acid
ELISpot	Enzyme-linked immunosorbent spot
ERK	Extracellular signal-regulated kinase
ETS	E26 transformation-specific
EwS	Ewing Sarcoma
FACS	Fluorescent activated cell sorting
FBS	Fetal bovine serum
FCS	Fetal calf serum
FITC	Fluorescein isothiocyanate
FLI1	Friend leukaemia integration
FLU	Influenza peptide
FUS	Fused in Sarcoma
GM-CSF	Granulocyte-macrophage colony-stimulating factor
GPR64	G protein-coupled receptor 64
GvHD	Graft versus host disease
HBSS	Hank's balanced salt solution
HLA	Human leukocyte antigen
IE	ifosfamide, etoposide
IFN	Interferon
IGF-1	Insulin-like Growth Factor 1
IGF-1R	Insulin-like growth factor 1 receptor
IL	Interleukin
LCL	Lymphoblastoid cell line
LDH	Laktat-Dehydrogenase
LIPI	Lipase I
mAb	Monoclonal antibody
MACS	Magnetic activated cell sorting
MAPK	Mitogen-activated protein kinase
MEK	Mitogen-activated protein kinase
MEM	Minimum essential medium
MHC	Major histocompatibility complex
NEAA	Non-essential amino acid
NK	Natural killer

ORF	Open Reading Frame Finder
p53	p53-Protein
PAX7	Paired Box 7
PBL	Peripheral blood lymphocytes
PBMC	Peripheral blood mononuclear cell
PBS	Phosphate-buffered saline
PCR	Polymerase chain reaction
PD-L1	programmed death-ligand 1
PD1	programmed cell death protein 1
PE	Phycoerythrin
Pen Strep	Penicillin, Streptomycin
PGE2	Prostaglandin E2
PI3-K	Phosphoinositide 3-kinase
RAF	Rapidly accelerated fibrosarcoma
RAS	Rat sarcoma virus
RB	retinoblastoma protein
RNA	ribonucleic acid
rpm	Rounds per minute
RT-PCR	Real-time polymerase chain reaction
scRNAseq	Single-cell ribonucleic acid sequencing
Steap1	Six-transmembrane epithelial antigen of the prostate 1
TAA	Tumour-associated antigen
TCR	T-cell receptor
TIL	Tumor-infiltrating lymphocytes
TNF	Tumour necrosis factor
TSA	tumour specific antigens
UV	Ultraviolet
VAC	vincristine, actinomycin D, cyclophosphamide
VAI	vincristine, actinomycin D, ifosfamide
VC	vincristine, cyclophosphamide
VDC	vincristine, doxorubicin, cyclophosphamide
VIDE	vincristine, ifosfamide, doxorubicin, etoposide

1 Introduction

1.1 Ewing Sarcoma

1.1.1 Introduction

Ewing Sarcoma is a highly malignant, small-round cell basophilic tumor affecting the bone and soft tissue. It is the second most common primary malignant bone tumor after osteosarcoma, accounting for 10-15%. Children and adolescents between 10 and 20 are mainly affected. It is prone to metastasize. First described in 1921 by Dr. James Ewing, the tumor's origin is still mysterious, with undifferentiated mesenchymal cells of the bone or neural-crest-derived cells often considered. It mainly presents without many prior symptoms but becomes apparent due to pain, swelling, or pathological fractures. (Balamuth & Womer, 2010; Bernstein et al., 2006; Bosma et al., 2018; Burchill, 2003; Grünewald et al., 2018; Tu et al., 2017)

1.1.2 Genetic Alterations

In general, the genomic background of EwS is quiet, with a low mutation burden. (Crompton et al., 2014; Gröbner et al., 2018)

However, the EWS-FLI1 fusion gene is characteristic for EwS. It typically results from the translocation t(11;22)(q24;12) and is found in 85% of Ewing tumors. Similar translocations can be detected in the remaining cases, which also fuse EWS or other FET gene family members to other ETS family of transcription factors members. Therefore, EWS-FLI1 and other ETS proteins could function as potential treatment targets, though this has proven difficult up until now due to a lack of enzymatic activity and potentially problematic small molecule binding. (Delattre et al., 1992; Grünewald et al., 2018; Hsing et al., 2020; Toomey et al., 2010; Zöllner et al., 2021)

EWS-FLI1 encodes for an oncoprotein that acts as an aberrant transcription factor where the N-terminal transactivation domain of EWS is combined with the C-terminal FLI1 DNA-binding domain. Normally, the ETS family of which FLI1 is a member, as transcription factors regulate cell differentiation, proliferation, migration, apoptosis, and angiogenesis. (Balamuth & Womer, 2010; Delattre et al., 1992;

Grünewald et al., 2018; Hsing et al., 2020; Mackintosh et al., 2010; Scotlandi et al., 2020; Toomey et al., 2010)

1.1.3 Epidemiology and Presentation

Ewing sarcoma is most common in children and adolescents, primarily affecting those aged 10 to 24. With an incidence of 2.93 per one million people per year, it is relatively rare. The disease is most prevalent among white males, with the lower incidences in African and Asian populations. (Balamuth & Womer, 2010; Bernstein et al., 2006; Burchill, 2003; Ozaki, 2015)

Ewing sarcomas typically occur in flat bones like the pelvis and long bones of the legs and arms, with a predilection for the diaphysis of long bones and early soft tissue involvement. The bones of the chest wall can also be affected. Extraskeletal Ewing sarcoma is rarer but can be found anywhere, mainly in the soft tissues of the upper thigh, buttocks, upper arm, and shoulders. (Abboud et al., 2021; Bernstein et al., 2006; Bosma et al., 2018; Burchill, 2003) Ewing sarcomas can metastasize to other bones and/or the bone marrow, lungs, and other organs. Metastasis into the liver, central nervous system, or lymph nodes is rare—about 25% of patients present with metastatic disease at diagnosis (Balamuth & Womer, 2010; Bernstein et al., 2006).

1.1.4 Prognosis

Prognostic factors in Ewing sarcoma include patient characteristics, tumor specifics, and treatment response. Age does not appear to be a significant variable in most studies, but sometimes, younger patients seem to have more favorable outcomes. Ethnicity may also play a role in prognosis. Some studies suggest that non-white patients, while less likely to develop Ewing Sarcoma, have a poorer outcome if they do. (Bosma et al., 2018; Cotterill et al., 2000; Worch et al., 2010) Another important prognostic factor is the tumor size at diagnosis. Larger tumors (>8 cm or > 200 mL) are associated with a worse prognosis. (Bosma et al., 2018; Gaspar et al., 2015) Moreover, metastases, especially at diagnosis, impact the outcome negatively (Bosma et al., 2018; Cotterill et al., 2000; Gaspar et al., 2015). The lungs are the most common site of metastatic disease. Interestingly, patients with only lung metastases have a better prognosis than those with metastases at other sites or multiple sites of metastases. (Balamuth & Womer, 2010; Bosma et al., 2018; Cotterill et al., 2000;

Gaspar et al., 2015) Furthermore, tumors in the extremities have a better prognosis than those in the pelvis or axis (Bosma et al., 2018; Cotterill et al., 2000). The histological response and the serum LDH level are also discussed as possible prognostic factors. (Bosma et al., 2018) Patients with localized disease have survival rates exceeding 70%, whereas those with advanced Ewing Sarcoma (approximately 30% 5-year survival rate for patients with metastases) and early (<24 months post-diagnosis: 4-8,5% 5-year survival rate) or multiple relapses have poorer prognoses. Despite all therapeutic advancements, the relapse rate of patients, in general, is 30-40%, with a 5-year survival rate in late occurrences of 23-35%. (Bernstein et al., 2006; Grünewald et al., 2018)

1.1.5 Clinical Symptoms

Ewing sarcoma symptoms are often nonspecific, leading to delayed diagnosis. Pain and swelling are common. The pain is typically recurring, exacerbated by physical activity, and continues at night. (Bernstein et al., 2006; Widhe & Widhe, 2000) Both parents and physicians often think it is due to bone growth or a sports injury. This frequently results in a trial of conservative management with anti-inflammatory or antibiotic medication before making the correct diagnosis. These diagnosis delays range from weeks to years, with a median of 160 days. (Bernstein et al., 2006; Goedhart et al., 2016; Khan et al., 2021) Systemic symptoms like fever, malaise, and weight or appetite loss may also occur, especially in metastatic disease (Bernstein et al., 2006).

A pathologic fracture can also be the first symptom, especially in tumors of the lower extremity, with 15% of patients having one at diagnosis. Tumors in the spine can cause back pain and can escalate to spinal paralysis. (Ozaki, 2015; Zöllner et al., 2021)

1.1.6 Treatment

Historically, patients had a dismal prognosis. Until the late 1970s, the survival rate for patients was approximately 10%. (Balamuth & Womer, 2010; Bernstein et al., 2006; Hesla et al., 2021)

However, the introduction of chemotherapy into the multimodal treatment strategy significantly improved survival rates to > 70% for localized disease. This is

thought to be due to the fact that the systemic treatment of Ewing Sarcoma eradicates micrometastasis, which is crucial for improving long-term survival. Patients are usually enrolled in clinical trials, which allows for the continuous modification and improvement of treatment protocols. One example is the Euro-Ewing 2012 trial, which provides the current treatment protocol in Europe. (Anderton et al., 2020; Balamuth & Womer, 2010; Bernstein et al., 2006; Gaspar et al., 2015; Grünewald et al., 2018; Hesla et al., 2021; Zöllner et al., 2021)

The standard treatment protocol for Ewing sarcoma relies on a combination of cyclic, multi-agent chemotherapy, surgery, and radiation (Balamuth & Womer, 2010; Bernstein et al., 2006; Hesla et al., 2021).

The neoadjuvant, or induction chemotherapy, lasts at least 12 weeks with six cycles of vincristine, ifosfamide, doxorubicin, and etoposide (VIDE) in three-week intervals. The aim is to shrink the primary tumor and eradicate possible metastases. (Anderton et al., 2020; Grünewald et al., 2018; Hesla et al., 2021)

After a disease response evaluation, patients undergo surgery and/or radiation. Surgical resection is critical for managing the primary tumor. The complete removal of it with a wide enough margin should always be the aim to improve the prognosis of patients. Limb-sparing surgeries should be favored over amputation whenever possible. Endoprosthesis, allo- or autologous bone grafts, or rotationplasty can be employed should reconstruction be necessary. (Anderton et al., 2020; Bernstein et al., 2006; Gaspar et al., 2015; Grünewald et al., 2018; Hesla et al., 2021; Zöllner et al., 2021)

Radiation therapy can be used either alone or together with surgery, as EwS is a very radiosensitive tumor. It can be utilized for inoperable tumors, in the case of small operating margins, or intralesional resection. It can also be used palliatively to alleviate symptoms such as pain. (Bernstein et al., 2006; Gaspar et al., 2015; Zöllner et al., 2021) Local treatment with surgery, radiotherapy, or a combination thereof should also include the resection or irradiation of metastatic lesions (Haeusler et al., 2010; Zöllner et al., 2021).

Following local treatment, patients are randomized into risk groups depending on tumor response and disease progression and receive consolidation chemotherapy with either vincristine, actinomycin D, and ifosfamide (VAI) or vincristine, actinomycin D, and cyclophosphamide (VAC). Alternatively, Busulfan and Mephalan can be applied in poor risk groups. (Anderton et al., 2020)

Arm B of the Euro-Ewing 2012 trial tests the North American model, which includes induction therapy with vincristine, doxorubicin, and cyclophosphamide alternating with ifosfamide and etoposide (VDC/IE) followed by consolidation with vincristine and cyclophosphamide in turns with ifosfamide and etoposide or vincristine, actinomycin D, ifosfamide, busulfan and melphalan (IE/VC/VAI/BuMel). (Anderton et al., 2020; Hesla et al., 2021)

In advanced cases, autologous (auto-SCT) or allogeneic stem cell transplantation (allo-SCT) can be considered, particularly for relapsed patients. Patients are treated with high-dose chemotherapy and or irradiation, followed by the infusion of their own or donor stem cells to restore the bone marrow and regular blood cell production. In allo-SCT, there is also the hope for a Graft versus Tumor effect, although this remains debatable and is often tied to toxic GvHD. (Bernstein et al., 2006; Burdach, 2004; Burdach et al., 2000; Grünewald et al., 2018; Hesla et al., 2021)

However, all these treatments come with significant morbidities that can be divided into acute and chronic adverse effects, which is especially important as most patients are young and must live with them for a long time, and over 70% of EwS survivors report impairments. (Ginsberg et al., 2010; Grünewald et al., 2018) Among others, chemotherapy can cause short-term toxicity, such as nausea and myelosuppression, and long-term effects, such as cardiotoxicity, infertility, and secondary malignancies. Surgical risks include infection and functional impairments, while radiation can cause tissue damage, growth impairments in pediatric patients, and secondary neoplasms. (Allo-) SCT carries a significant risk of graft-versus-host disease and severe infections. (Bernstein et al., 2006; Burdach et al., 2000; Caruso et al., 2019; DANIEL KELLY BENJAMIN et al., 2002; Friberg et al., 2002; Fuchs et al., 2003; Ginsberg et al., 2010; Grünewald et al., 2018; Hardes et al., 2010; Hesketh, 2008; Hesla et al., 2021; Hudson, 2010; Paulino & Fowler, 2005; Simbre et al., 2005; Zöllner et al., 2021)

1.1.7 Novel Therapeutic Approaches

Due to the still poor prognosis of advanced Ewing Sarcoma cases and the toxicities that accompany the current treatments, new, more effective, and less harmful ones are needed.

One attractive option are targeted therapies, which include new drugs that target more specific molecular structures, such as EWS-FLI1 or targets thereof, as targeting the fusion protein has proven challenging, other mutations, like those affecting the IGF-1 pathway, and the tumor microenvironment. Agents include monoclonal antibodies and “small molecules.” These drugs are investigated in preclinical and clinical trials to see if they could provide effective yet less toxic treatment options. (Fayzullina et al., 2022; Gaspar et al., 2015; Tsimberidou, 2015; Wu et al., 2006; Zöllner et al., 2021)

Immunotherapy, which leverages the immune system to target and eliminate cancer cells, plays a huge part in targeted therapy. Some of the most prominent agents are checkpoint inhibitors, such as anti-PD1/PD-L1 or anti-CTLA-4, which block the ability of cancer cells to block the immune system. Immunotherapy and checkpoint inhibitors, in particular, have already shown promising results in various malignancies, especially hematologic ones, and slowly in solid ones. However, they have shown limited success in treating Ewing sarcoma, characterized by a low mutation burden, a lack of HLA class I expression, and an immunosuppressive tumor microenvironment. (Couzin-Frankel, 2013; Hesla et al., 2021; Morales et al., 2020; Waldman et al., 2020; Zöllner et al., 2021)

Another immunotherapeutic approach is adoptive T cell transfer. Chimeric antigen receptor (CAR-T) cell therapies modify a patient’s T cells to express a synthetic receptor that recognizes and attacks cancer cells. They have also proven effective in other cancers, especially hematologic malignancies. However, success in solid tumors has been limited due to a lack of tumor infiltration and immunosuppressive microenvironment. T-cell receptor (TCR) Therapy is another form of T-cell therapy and the focus of this thesis. (Morales et al., 2020; Rohaan et al., 2019; Sterner & Sterner, 2021; Waldman et al., 2020)

Oncolytic virus therapy could be another promising approach. It utilizes viruses, which are pro-inflammatory and have cytolytic properties, either directly via replication-associated necrosis or oncolysis or by initiating the release of antigens that can trigger the immune system. Preclinical studies, even in our laboratory, have shown the potential effectiveness of these therapies in targeting Ewing sarcoma, especially when administered together with other treatments, such as targeted T-cell therapy. (Morales et al., 2020; Schober et al., 2024)

Epigenetic therapy could also be interesting, considering the importance of epigenetic modifications in Ewing sarcoma (Grünewald et al., 2018). Epigenetic therapies for cancer, including DNA methyltransferase inhibitors (DNMTi), histone deacetylase inhibitors (HDACi), and histone methyltransferase inhibitors (HMTi), could be combined with current immunotherapies to make these therapies more effective, maybe even reversing immune evasion. The potential of HDACi has been shown by Sakimura et al. (2005), who showed that FK228 can reduce tumor growth and even induce apoptosis in Ewing's family tumors. (Gomez et al., 2020; Sakimura et al., 2005)

Current research indicates that a combination of new therapies among themselves and with traditional therapy regimes will likely garner the best results. (Gomez et al., 2020; Hesla et al., 2021; Waldman et al., 2020)

1.2 Tumor Immunology and Adoptive T-Cell Therapy

1.2.1 Cancer and the Immune System

The immune system plays an important role in preventing the development and growth of cancer by monitoring the body's tissues by recognizing and eliminating pre-cancerous and cancerous cells through a differing antigen profile. This phenomenon is described in the immunosurveillance hypothesis. (Schreiber et al., 2011; Waldman et al., 2020)

It has been shown that lymphocytes specific for tumor antigens can be found in tumors as tumor-infiltrating lymphocytes (TILs) and even correlate with patient outcomes. This has led to the idea of purposefully "creating" those cells in one way or another to generate an effective immune response against cancer—adoptive cell therapy. (Husby et al., 1976; Morotti et al., 2021; Rohaan et al., 2019; Rosenberg & Restifo, 2015; Rosenberg et al., 1986)

However, cancer cells, in turn, can develop ways to avoid being recognized and destroyed by the immune system. This is known as immune evasion and plays an important role in cancer progression and the failure of immunotherapies, especially after initial tumor regression. Mechanisms can relate to a dysfunctioning immune system or the tumor itself and include a loss of tumor antigens, the loss of MHC class I, and an increased resistance to immune measures, for example, by blocking apoptosis. Other strategies include the development of an immunosuppressive environment. The discovery of these mechanisms has led to the evolution of the

immunosurveillance theory to the immunoediting theory, which acknowledges a back-and-forth of elimination, equilibrium, and escape between the neoplasm and the immune system. This has to be taken into consideration when devising new strategies for treatment. (Muenst et al., 2016; Schreiber et al., 2011; Seliger, 2005)

1.2.2 Adoptive T-Cell Therapy and TCR - Therapy

Adoptive cell therapy represents a pioneering approach to cancer treatment. Based on the findings described above, it strives to utilize immune cells, as an autologous or allogeneic transplant, introduced into the patient to target malignancies more directly and effectively. It is an interesting anti-cancer approach as the T cells can be expanded *in vitro* and even be selected based on their avidity and desired effector functions, to ensure the best possible combination. Once administered, as living treatments, the cells even grow and can sustain their anti-tumor effects *in vivo*. The oldest modality is Tumor-Infiltrating Lymphocyte Therapy, which relies on the isolation of immune cells and their expansion *ex vivo* and reintroduction into the patient. Natural Killer Cell Therapy follows the same process but tries to harness the ability of NK cells to target un-processed, un-presented antigens, which facilitates their rapid and potent anti-tumor response, maybe even in an “off-the-shelf manner.” Next to utilizing naturally occurring cells, Chimeric Antigen Receptor T Cell Therapy and T Cell Receptor Therapy rely on genetically engineered T cells. This enables the generation of larger quantities of specific cells with a potentially more potent anti-tumor response. T-cell receptor therapy, the focus of this thesis, engineers T cells to express a specific TCR. (Chruściel et al., 2020; Liu et al., 2021; Morotti et al., 2021; Restifo et al., 2012; Rohaan et al., 2019; Rosenberg & Restifo, 2015)

However, clinical application of TCR-engineered T-cell therapy in Ewing sarcoma is still at its nascent stage, where both preclinical and clinical trials evaluate its antitumor efficacy and potential toxicity. Major hurdles to be tackled include the need for an appropriate target and the TCRs’ specificity to avoid “on-target off tumor” and off-target effects, respectively. Moreover, there is the precondition for MHC expression and the necessity to overcome the previously mentioned immune-suppressive environment, antigen escape, and an adequate T-cell infiltration of the tumor. (Biele et al., 2021; Blaeschke et al., 2016; Chruściel et al., 2020; Rath & Arber, 2020; Rohaan et al., 2019; Rosenberg & Restifo, 2015; Thiel et al., 2017)

1.2.3 T-Cell Receptors (TCRs)

T-cell receptors are responsible for the fact that T cells, which are constantly searching the organism, can recognize antigens on target cells and induce the adaptive immune response. (Davis & Bjorkman, 1988; Mazzotti et al., 2022; Shah et al., 2021)

TCRs consist of two different heterodimers composed of an alpha (α) and a beta (β) chain, or rarely a gamma (γ) or delta (δ) chain, each containing variable (V) and constant (C) domains (Davis & Bjorkman, 1988; Shah et al., 2021). Structurally similar to immunoglobulins, TCR V domains have a highly variable complementarity-determining region (CDR) responsible for antigen binding and recognition. The variable region of the chains is generated through somatic recombination of V, J, and D gene segments. The constant (C) domain is essential for intracellular signaling as it facilitates the interaction with CD3. The TCR forms a complex with the ε/γ/δ/ζ subunits of CD3 signaling proteins. (Davis & Bjorkman, 1988; Rudolph et al., 2006; Shah et al., 2021)

Importantly, T cells undergo positive and negative selection, to ensure the safety and specificity of the T cells. Positive selection refers to the fact, that T cells need to be able to recognize MHC molecules, whereas negative selection removes self-reactive T cells. (Davis & Bjorkman, 1988; Shah et al., 2021; Viret & Janeway, 1999)

TCRs must be presented with the antigen by an antigen-presenting molecule, usually a major histocompatibility complex (MHC) molecule, to be able to recognize it. A distinction can be made between MHC class I, which is recognized by CD8+ cells, and MHC class II, which is recognized by CD4+ cells. CD8 and CD4 act as coreceptors in this context and increase the sensitivity for the antigen. (Davis & Bjorkman, 1988; Pishesha et al., 2022; Rudolph et al., 2006; Shafer et al., 2022; Shah et al., 2021)
Before being presented, antigens need to be processed. In the case of MHC class I, this usually happens as proteolysis in the cytosol and endoplasmic reticulum, whereas MHC class II presents antigens that were extracellularly captured and then processed in endolysosomal compartments. (Pishesha et al., 2022) This work focuses on Human leukocyte antigen (HLA)-A*0201, Europe's most common HLA allele (Gonzalez-Galarza et al., 2011).

The MHC molecules can activate the T cell upon binding. In that case, a signaling cascade is initiated by the phosphorylation of immunoreceptor tyrosine-based activation motifs in the CD3 complex, which activates the T cell and enables effector functions like proliferation, differentiation, the secretion of cytokines, and cytotoxicity. (Mariuzza et al., 2020; Pishesha et al., 2022; Shafer et al., 2022; Shah et al., 2021)

In conclusion, TCRs are responsible for guiding T cells to their targets by recognizing and distinguishing between diverse peptides bound to MHC molecules. This makes TCRs attractive for genetic engineering. They can be modified to direct T cells specifically to a desired target, that needs to be destroyed. (Mariuzza et al., 2020; Shafer et al., 2022; Shah et al., 2021)

1.2.4 TCR Engineering

Over the years, different strategies have been developed to engineer T cells. Viral vector systems, such as retroviral and lentiviral vectors, were the main delivery forms. These vectors enable a more or less efficient gene transfer and expression of these genes in the transduced T cells. Nevertheless, safety concerns are associated with them. Mispairing between the introduced and endogenous TCR may occur, leading to non-productive T cells in the best-case scenario and causing cross-reactivity and graft versus host disease (GvHD) in the worst-case scenario. Furthermore, the endogenous TCR can suppress the newly introduced one, also hampering the T cells' functionality. Insertional mutagenesis is another problem that can arise when using a vector transfer strategy. (Bendle et al., 2010; Ghosh et al., 2020; Howe et al., 2008; Schober et al., 2019; Shafer et al., 2022; Xue et al., 2022) CRISPR-Cas9 is an alternate strategy that has more recently be used in TCR engineering. This method lowers the possibility of side effects by ensuring precise alpha- and beta-chain pairing, knocking out the endogenous TCR and regulating insertion sites, allowing for example for a more physiological TCR expression. (Foy et al., 2023; Schober et al., 2019; Xue et al., 2022)

The most common method is transducing a natural, or only minimally altered, antigen-specific TCR into the T cell using either of the methods described above (Schober et al., 2019; Shafer et al., 2022; Tsimberidou et al., 2021). However, other approaches like introducing a single-chain TCR consisting of the TCR α and β chains

fused together by a flexible linker region and a Cβ domain have also been explored to avoid the risk of mispairing. (Aggen et al., 2012; Knies et al., 2016; Shafer et al., 2022)

Moreover, TCRs can be chosen and enhanced for example regarding levels of functionality. Efforts have shifted towards developing TCRs with high affinity for target antigens, as cytotoxicity relates to affinity, for example by introducing amino acid sequence variations into TCRs. However, some studies have shown that higher affinity can potentially lead to higher cross-reactivity. Furthermore, a too-strong affinity can provoke early T-cell exhaustion, limiting the continuous recognition of tumor cells. (Baulu et al., 2023; Campillo-Davo et al., 2020; Shafer et al., 2022)

1.2.5 Molecular Targets

T-cell recognition and killing of tumor cells in T-cell therapy is an antigen-specific event. Therefore, identifying the ideal tumor-specific T-cell target is crucial. The chosen antigen must significantly impact the tumor, affecting growth or metastasis, and, at best, only be expressed on the tumor to avoid cross-reactivity (Leko & Rosenberg, 2020; Rath & Arber, 2020; Shafer et al., 2022).

Tumor-associated antigens (TAA) are present on tumor cells, but also on some normal cells. Tumor-specific antigens (TSA) are expressed only on tumor cells. Further, it can be differentiated between differentiation antigens, overexpressed antigens, cancer germline antigens, viral antigens, or neoantigens. (Leko & Rosenberg, 2020; Rath & Arber, 2020; Shafer et al., 2022) Due to the MHC restriction of CD8+ and CD4+ T cells, the TAA/TSA gene product must be processed and presented to T cells by MHC molecules (Pishesha et al., 2022; Rudolph et al., 2006; Szeto et al., 2020).

The antigens chosen and investigated for this study are the following:

LIPI

LIPI, a lipase, plays a significant role in oncogenesis and metastasis. Mahlendorf and Staege (2013) showed that it is specific for and overexpressed in Ewing family tumor cells. (Mahlendorf & Staege, 2013; Pirson, 2010; Staege et al., 2004)

GPR64

GPR64 is a G protein-coupled receptor relevant to the development, progression, invasiveness, and metastasis of several cancers, including Ewing sarcoma. Studies have shown that GPR64 is overexpressed in Ewing sarcoma cells and is only normally expressed in human epididymis. It is also overexpressed in nephroblastoma. (Pirson, 2010; Richter et al., 2013; Schirmer et al., 2018)

PAX7

PAX7 is a transcription factor known for its crucial role during fetal development and cancer growth. It is over-expressed in Ewing sarcoma and not present in normal tissue. It can also be found in alveolar rhabdomyosarcoma and synovial sarcoma. (Baldauf et al., 2018; Charville et al., 2017)

CHM1

Chondromodulin 1, a glycoprotein, is an angiogenesis inhibitor and is normally involved in enchondral bone formation. In Ewing sarcoma, CHM1 facilitates invasiveness and induces metastasis, especially in the lung. It is a downstream target of EWS-FLI1. It is virtually not expressed on normal tissue and is highly expressed in Ewing sarcoma. (Blaeschke et al., 2016; Hiraki & Shukunami, 2000; Pirson, 2010; U. Thiel et al., 2011; von Heyking et al., 2017)

2 Aim

This doctoral thesis aimed to identify TCRs targeting Ewing sarcoma tumor-associated antigens essential for tumor metastasis and/or tumor survival for adoptive transfer. The antigens are the Ewing sarcoma-specific antigens CHM1 (von Heyking et al., 2017) and LIPI (Mahlendorf & Staege, 2013; Staege et al., 2004) (Grünewald et al., unpublished data), PAX7, specific for both Ewing sarcoma and alveolar rhabdomyosarcoma (Baldauf et al., 2018) , and GPR64, specific for Ewing sarcoma and nephroblastoma (Richter et al., 2013), to address tumor-specific targets that are present in more than one tumor entity.

T cells with suitable TCRs were tested in interferon-gamma (IFNγ) ELISpots and FACS analyses and identified and subsequently sequenced in a standard approach with the help of PCR primers for various Vα- and Vβ-chains. Single-cell RNA sequencing was used as a second method to identify and verify relevant TCR sequences in a more streamlined manner.

Figure 1 provides an overview of the workflow to identify TCR sequences for transgenic T cells.

The identified TCRs can be used for further testing *in vitro* and *in vivo* and will provide parts of a toolbox for CRISPR/Cas9 and retroviral-mediated T-cell engineering within our research group. They could form the basis for a possible TCR library to deliver precise, targeted patient therapy to improve outcomes and reduce the side effects affecting patients of (advanced) Ewing Sarcoma now.

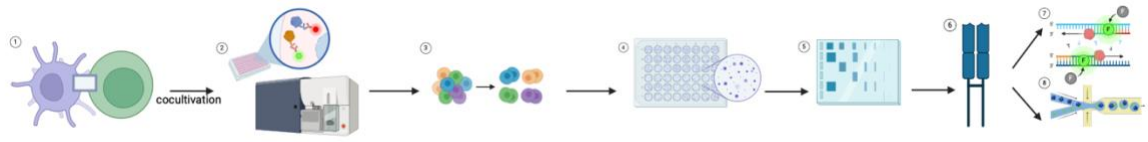

Figure 1 Workflow. *With selected peptides pulsed HLA-A*0201+ dendritic cells were used to prime HLA-A*0201-CD8+ T cells (1). After two weeks of cocultivation, proliferating T cells were multimer-stained, sorted (2), and expanded through a single-cell dilution process (3). The selected clone populations were evaluated for HLA-A*0201/peptide specificity in ELISpot assays (4). Selected EwS-specific candidates were further expanded, and the DNA sequence of the TCR (6) was analyzed using electrophoresis (5) and PCR (7). ScRNAseq was employed to comprehensively analyze T cells (8), created with BioRender.com.*

3 Materials

3.1 Technical Equipment

Table 1 *Technical Equipment*

Name	Manufacturer
Autoclave V95/ VX95	Systec GmbH & Co. KG, Linden, Germany
Balance (analytical) 770	Kern & Sohn GmbH, Balingen-Frommern, Germany
BD IMagTM Cell separation system	BD, New Jersey, USA
Cell counting chamber Neubauer	Brand, Wertheim, Germany
Cell counting chamber Neubauer	Paul Marienfeld GmbH & Co KG, Germany
Cell Sorter MoFlow Astrios S2	Beckmann Coulter GmbH, Brea, USA
Centrifuge 5427R	Eppendorf SE, Hamburg, Germany
Centrifuge Biofuge fresco	Heraeus, Hanau, Germany
Centrifuge MIKRO 220-R	Andreas Hettich GmbH & Co KG, Tuttlingen, Germany
Centrifuge Multifuge 3 S-R	Haraeus, Hanau, Germany
Centrifuge Sorvall RC6	Thermo Fisher Scientific, Waltham, USA
Controlled-freezing box	Nalgene, Rochester, USA
Electrophoresis chamber Easy cast	Thermo Fisher Scientific, Waltham, USA
Erlenmeyer Flask	Sarstedt AG & Co. KG, Nümbrecht, Germany
ELISpot reader AID iSpot Reader Unit	AID GmbH, Straßberg, Germany
FACS Aria Cell Sorter	BD, New Jersey, USA
Flow cytometer FACSCaliburTM	BD, New Jersey, USA
Flow cytometer MACS Quant10	Miltenyi Biotec, Bergisch Gladbach, Germany

Freezer/Refrigerator (- 20 °C/ +4°C)) cool vario	Siemens, Munich, Germany
Freezer (- 80 °C) Hera freeze	Heraeus, Hanau, Germany
Freezer (-80°C) TDE40086FV	Thermo Fisher Scientific, Waltham, USA
Freezer (-80°C) HLE series	Thermo Fisher Scientific, Waltham, USA
Fridge (+ 4 °C) cool vario	Siemens, Munich, Germany
Fridge (+4°C) KG28XM4	Siemens, Munich, Germany
Fume Cupboard Airflow	Köttermann GmbH, Uetze, Germany
Gamma-Bestrahlungsgerät Biobeam GM	Gamma-Service Medical GmbH, Leipzig, Germany
Hairdryer ZWT LS1202D	Z.W.T.
Heating block Thermomixer Comfort	Eppendorf, Hamburg, Germany
Hybrid graphic printer UP-X898MD	Sony, Tokyo, Japan
Ice machine AF 100	Scotsman Ice Systems, Vernon Hills, IL, USA
Ice machine Flake line	Wessamat Eismaschinenfabrik GmbH, Kaiserslautern, Germany
Incubator Hera cell	Heraeus, Hanau, Germany
Liquid nitrogen tank L-240 K series	Taylor-Wharton, Theodore, USA
Liquid nitrogen tank Level Controller type	Worthington Industries, Columbus, USA
Micropipets (0,5 – 10 µL, 10 – 100 µL, 20 – 200 µL, 100 – 1000 µL)	Eppendorf SE, Hamburg, Germany
Microscope Axiovert 100	Zeiss, Jena, Germany
Microscope DMIL LED	Leica Camera AG, Solms, Germany
Microwave oven	Siemens, Munich, Germany
MidiMACS Separator	Miltenyi Biotech, Bergisch-Gladbach, Germany
Mini-Centrifuge Sprout	Kisker Biotech GmbH & Co KG, Steinfurt, Germany
Mini-Centrifuge Mini Star	VWR International, Radnor, USA

MS2 Minishaker	Janke & Kunkel IKA-Werke GmbH & Co. KG, Staufen, Germany
Multichannel pipette (10-100 µL)	Eppendorf SE, Hamburg, Germany
NanoPhotometer	Implen, Munich, Germany
Pipetting assistant Easypet	Eppendorf SE, Hamburg, Germany
Pipetting assistant Integra	Integra Biosciences GmbH, Biebertal, Germany
Power supplier Standard Power Pack P25 Biometra	Analytik Jena, Jena, Germany
Precision balance Explorer	Ohaus, Parsippany, USA
Rotary	Kisker Biotech GmbH & Co. KG
Sterile Bench Hera	Haraeus, Hanau, Germany
Thermal cycler iCycler	BioRad, Richmond, CA, USA
Thermocycler Mastercycler epgradient	Eppendorf SE, Hamburg, Germany
UV transilluminator Gene Genius	Syngene, Cambridge, UK
Vortexer Vortex-Genie2	Janke & Kunkel IKA-Werke GmbH & Co. KG, Staufen, Germany
Water bath	GFL, Burgwedel, Germany
Water purification system TKA GenPure	TKA GmbH, Niederelbert, Germany

3.2 Consumable Supplies

Table 2 *Consumable Supplies*

Name	**Manufacturer**
Butterfly Safety-Multifly-Cannula	Sarstedt AG & Co. KG, Nümbrecht, Germany
Cell culture flasks 25/75/175 mL	Greiner Bio-One GmbH, Kremsmünster, Austria
Cell culture flasks 25/75/175 mL	TPP, Trasadingen, Switzerland
Cell strainer	BD, New Jersey, USA
Cryo tubes 1,6 mL	Greiner Bio-One GmbH, Kremsmünster, Austria

Falcons 15/50 mL	Greiner Bio-One GmbH, Kremsmünster, Austria
Filters (sterile) Minisart	Sartorius, Göttingen, Germany
Gloves latex	Meditrade Medicare, Kufstein Austria
Gloves nitrile	Sempermed, Vienna, Austria
Gloves nitrile	Medline, Northfield, USA
LS columns	Miltenyi Biotech, Bergisch-Gladbach, Germany
MultiScreen Filterplates (ELISpot)	Merck KgaA, Darmstadt, Germany
Parafilm	Eppendorf SE, Hamburg, Germany
Pipet tips ARTR Aerosol resistant tips	Thermo Fisher Scientific, Waltham, USA
Pipet tips ARTR Aerosol resistant tips	Starlab GmbH, Hamburg, Germany
Plates for cell culture (96 wells)	BD, New Jersey, USA
Plates for cell culture (96 wells)	TPP (Techno Plastic Products AG), Trasadingen, Switzerland
Pointed bottom plates (96 wells)	Greiner Bio-One GmbH, Kremsmünster, Austria
Reservoir for reagents	VWR, Ismaning, Germany
Round bottom FACS tubes	BD, New Jersey, USA
Round bottom FACS tubes	Sarstedt AG & Co. KG, Nümbrecht, Germany
Scalpels	Braun, Tuttlingen, Germany
Serological pipets Cellstar R	Greiner Bio-One GmbH, Kremsmünster, Austria
Sterifilter 0,45 qn	Omnilab, Germany
Syringe Original Perfusor 50mL	B-Braun Melsung SE, Melsung, Germany
Omnifix-F 1mL	B-Braun Melsung SE, Melsung, Germany
Tubes 0,5/1,5/2 mL	Eppendorf SE, Hamburg, Germany
Tubes 0,5/1,5/2 mL	Sarstedt AG & Co. KG, Nümbrecht, Germany
Twin.tec real time PCR plate 96	Eppendorf SE, Hamburg, Germany

3.3 Chemicals and Reagents

Table 3 *Chemicals and Reagents*

Name	Manufacturer
100 mM dNTP Set	Invitrogen, Life Technologies, Darmstadt, Germany
1 kb plus DANN ladder	Invitrogen, Life Technologies, Darmstadt, Germany
2-Propanol	Roth, Karlsruhe, Germany
3-Amino-9-ethylcarbazole	Sigma-Aldrich, St. Louis, Missouri, USA
5% trypsine	Gibco, Thermo Fisher Scientific, Waltham, USA
6x DNA loading dye	Fermentas, St. Leon-Rot, Germany
MEM NEAA 100x	Gibco, Thermo Fisher Scientific, Waltham, USA
Acetate	Sigma-Aldrich, St. Louis, Missouri, USA
AEC	Sigma-Aldrich, St. Louis, Missouri, USA
Agarose	Invitrogen, Life Technologies, Darmstadt, Germany
AIM V medium	Gibco, Thermo Fisher Scientific, Waltham, USA
Anti-PE Microbeads	Miltenyi Biotech, Bergisch-Gladbach, Germany
AutoMACS TM Rinsing Solution	Miltenyi Biotech, Bergisch-Gladbach, Germany
Anti Human CD 14 Magnetic Particles	BD, New Jersey, USA
ß2-Microglobuline from human urine	Sigma-Aldrich, St. Louis, Missouri, USA
BCP (1-Bromar-3-Chloro-Propane)	Sigma-Aldrich, St. Louis, Missouri, USA
BD IMag Buffer (10x)	BD, New Jersey, USA
CD8 MicroBeads, human	Miltenyi Biotech, Bergisch-Gladbach, Germany
CD8+ T Cell Isolation Kit human	Miltenyi Biotech, Bergisch-Gladbach, Germany
DEPC Water	Ambion, Darmstadt, Germany

Desoxyribonuclease A	Invitrogen, Life Technologies, Darmstadt, Germany
DMEM medium	Gibco, Thermo Fisher Scientific, Waltham, USA
DMSO	AppliChem GmbH, Darmstadt, Germany
DPBS (10x)	Gibco, Thermo Fisher Scientific, Waltham, USA
EDTA	Merck KgaA, Darmstadt, Germany
Erythrocyte Lysis Buffer	Pharmacy of Klinikum rechts der Isar, Munich, Germany
Erythrocyte Lysis Buffer	Thermo Fisher Scientific, Waltham, USA
Ethanol	Roth, Karlsruhe, Germany
Ethidium Bromide	Sigma-Aldrich, St. Louis, Missouri, USA
FACS TM Clean	BD, New Jersey, USA
FACS TM Flow	BD, New Jersey, USA
FACS TM Rinse	BD, New Jersey, USA
Fetal bovine serum (FBS)	Gibco, Thermo Fisher Scientific, Waltham, USA
Ficoll-Paque	Sigma-Aldrich, St. Louis, Missouri, USA
GM-CSF	ImmunoTools, Friesoythe, Germany
HBSS	Gibco, Thermo Fisher Scientific, Waltham, USA
HCl	Merck KGaA, Darmstadt, Germany
Heparin-natrium 5000	Ratiopharm, Ulm, Germany
Human Serum Type AB	Lonza, Basel, Switzerland
Hydrogen peroxide solution	Sigma-Aldrich, St. Louis, Missouri, USA
IFNy	R&D Systems, Minneapolis, Minnesota, USA
IL-1ß	R&D Systems, Minneapolis, Minnesota, USA
IL-2	R&D Systems, Minneapolis, Minnesota, USA

IL-4	R&D Systems, Minneapolis, Minnesota, USA
IL-6	R&D Systems, Minneapolis, Minnesota, USA
IL-7	R&D Systems, Minneapolis, Minnesota, USA
IL-12	PAN-Biotech GmbH, Aidenbach, Germany
IL-15	R&D Systems, Minneapolis, Minnesota, USA
Isopropanol	Sigma-Aldrich, St. Louis, Missouri, USA
L-glutamine 200mM	Gibco, Thermo Fisher Scientific, Waltham, USA
MACS R BSA Stock Solution	Miltenyi Biotech, Bergisch-Gladbach, Germany
Multimers for CHM1, LIPI, Pax7, GPR64, STEAP	Provided by Prof Dr. Dirk Busch, Institute for Medical Microbiology, Immunology and Hygiene, Technical University Munich, Munich, Germany
OKT3	BD, Franklin Lakes, USA
Pentamer CHM1 & PAX7	ProImmune, Oxford, UK
N,N-Dimethylformamide	Roth, Karlsruhe, Germany
Pen Strep	Gibco, Thermo Fisher Scientific, Waltham, USA
Peptides CHM1(319), Pax7 (489), LIPI, GPR64 (862), FLU	Thermo Fisher Scientific, Waltham, USA, Ulm, Germany
Peptides Pax7, CHM1, FLU	peptides & elephants GmbH, Henningsdorf, Germany
PGE2	Cayman Chemical Company, Ann Arbor, Michigan, USA
Proleukin (recombinant human interleukin 2)	Novartis, Basel, Switzerland
Proleukin	Clinigen, Germany

Propidium iodide staining solution	BD, New Jersey, USA
Propidium iodide staining solution	Miltenyi Biotech, Bergisch-Gladbach, Germany
RPMI 1640 medium	Gibco, Thermo Fisher Scientific, Waltham, USA
Sodium acetate	Merck KGaA, Darmstadt, Germany
Sodium pyruvate	Gibco, Thermo Fisher Scientific, Waltham, USA
Taq DNA polymerase	Invitrogen, Life Technologies, Darmstadt, Germany
TNF-a	R&D Systems, Minneapolis, Minnesota, USA
Tri Reagent Solution	Ambion, Darmstadt, Germany
Tris (Trishydroxymethylaminomethan)	Merck KGaA, Darmstadt, Germany
Trypan blue	Gibco, Thermo Fisher Scientific, Waltham, USA
Tween 20	Sigma-Aldrich, St. Louis, Missouri, USA
Unlabeled Pro5 R MHC class I Pentamers	ProImmune, Oxford, UK
Labeled Pro5 R MHC class I Pentamers	ProImmune, Oxford, UK
X-vivo 15 medium	Gibco, Thermo Fisher Scientific, Waltham, USA

3.4 Kit

Table 4 *Kits*

Name	**Manufacturer**
BD IMag TM Anti-Human CD14 Magnetic Particles	BD, New Jersey, USA
CD8 + T Cell Isolation Kit	Miltenyi Biotech, Bergisch-Gladbach, Germany
Strataprep DNA Gel Extraction Kit	Agilent Technologies, Böblingen, Germany

High-Capacity Reverse Transcription Kit	Applied Biosystems, Life Technologies, Darmstadt, Germany
AccuPrime R Taq DNA Polymerase System	Invitrogen, Life Technologies, Darmstadt, Germany

3.5. ELISpot Reagents

3.5.1 Capture Antibodies

Table 5 *Capture Antibodies*

Antibody	Working concentration	Manufacturer
Anti-h-IFN-y mAb 1-D1K, purified	10 µg/mL	mABTech, Nacka Strand, Sweden

3.5.2 Detection Antibodies

Table 6 *Detection Antibodies*

Antibody	Working concentration	Manufacturer
Anti-h-IFN-y mAb 7-B6-1, biotinylated	2µg/mL	mABTech, Nacka Strand, Sweden

3.5.3 Enzymes and Buffers

Table 7 *Enzymes and Buffers*

Name	Manufacturer
Streptavidin-Horse Radish Peroxidase	mABTech, Nacka Strand, Sweden
3-Amino-9-ethl-carbazole (AEC)	Sigma-Aldrich, St. Louis, Missouri, USA

Name	Composition
Acetate buffer	37,5 mL distilled H2O + 3,75 mL 0,2 N-acetic acid + 8,8 mL 0,2 N-sodium acetate
AEC solution	1 AEC tablet (20mg) + 2,5 mL DMF + 47,5 mL acetate buffer

Development solution	10ml AEC solution + 25 µL 30 % H2O2

3.6 Flow Cytometry Antibodies

Table 8 *Flow Cytometry Antibodies*

Specificity	Format	Clone	Manufacturer
CD3	FITC/ APC	HIT3A	BD, New Jersey, USA
CD3	PE-Vio 770	REA613	Miltenyi Biotech, Bergisch Gladbach, Germany
CD4	APC-Vio 770	REA623	Miltenyi Biotech, Bergisch Gladbach, Germany
CD4	FITC	RPA-T4	BD, New Jersey, USA
CD8	APC/PE	REA734	Miltenyi Biotech, Bergisch Gladbach, Germany
CD8	FITC/ PE/ APC	RPA-T8	BD, New Jersey, USA
CD83	APC	HB15e	BD, New Jersey, USA
CD83	APC	REA714	Miltenyi Biotech, Bergisch Gladbach, Germany
CD86	FITC	2331 (FUN-1)	BD, New Jersey, USA

HLA-DR	PE	TU36	BD, New Jersey, USA
Anti-human HLA-A2	FITC	BB7.2	BD, New Jersey, USA
Mouse IgG1	FITC/ PE/ APC	X40	BD, New Jersey, USA
IgG1 (Isotype Antibody)	FITC/ PE/ APC		Miltenyi Biotech, Bergisch Gladbach, Germany
Pro 5 Fluorotag	PE (R-PE)		ProImmune, Oxford, UK
Unlabeled Pro5 R MHC class I Pentamers			ProImmune, Oxford, UK
Labeled Pro5 R MHC class I Pentamers	PE (R-PE)		ProImmune, Oxford, UK

3.7 Peptides

The peptides were provided by ThermoFischer TM or peptides & elephants with a purity of >90%. To stock them, they were dissolved in DMSO at a concentration of 10 µg/µL.

Table 9 *Peptides*

Gene	HLA-Allele	Sequence	Position
CHM1	A*0201	VIMPCSWWV	319
CHM1	A*0201	VLISGAVLL	46
CHM1	A*0201	LISGAVLLL	47
CHM1	A*0201	IALVGPDDV	10
CHM1	A*0201	LLFGAIGAF	54
CHM1	A*0201	SSPARLLKV	34

CHM1	A*0201	VVLISGAVL	45
CHM1	A*0201	YTMSINGKL	77
PAX7	A*0201	CLFMESYKV	489
PAX7	A*0201	QLAAFNHLL	280
PAX7	A*0201	ALPGTVPRM	3
Pax7	A*0201	HMNPVSNGL	374
Influenza	A*0201	GILGFVFTL	-
GPR64	A*0201	YLFAIFNTL	862

3.8 Cell Culture Media, Solutions and Buffers

3.8.1 Cell Culture Media and Universal Solutions

Table 10 *Cell Culture Media and Universal Solutions*

Name	**Composition**
Standard Medium	RPMI 1640 10 % FCS 2mM L-glutamine 100 U/mL Pen Strep
293T-Medium	DMEM 10 % FCS 2mM L-glutamine 1mM Sodium pyruvate 1 x NEAA 100 U/mL Pen Strep
LCL medium	RPMI 1640 10 % FCS 2mM L-glutamine 1mM Sodium pyruvate 1 x NEAA 100 U/mL Pen Strep
T-cell medium	AIM V 5% human serum type AB

	2mM L-glutamine 100 U/mL Pen Strep
Standard freezing medium	FCS 10 % dimethyl sulfoxide (DMSO)
Freezing medium for T cells	Human serum type AB 10 % DMSO

3.8.2 Buffer and Gel for DNA electrophoresis

Table 11 *Buffer and Gel for DNA electrophoresis*

Name	**Ingredients**
TAE running buffer	50 x TAE: 2 M Tris, 10 % EDTA (0,5 M), 5,71% HCl
Electrophoresis gel	240 ml TAE buffer (1x), 2% agarose, 5 µL EtBr

3.9 Oligonucleotides

Table 12 *Primers for Vαβ -Repertoire Analysis*

P-5`αST	CTG TGC TAG ACA TGA GGT CT
P-3`αST	CTT GCC TCT GCC GTG AAT GT
3-TCα	GGT GAA TAG GCA GAC AGA CTT GTC ACT GGA
PanVα1	AGA GCC CAG TCT GTG ASC CAG S=C/G
PanVα1.1	AGA GCC CAG TCR GTG ACC CAG R=A/G
Vα2	GTT TGG AGC CAA CRG AAG GAG R=A/G
Vα3	GGT GAA CAG TCA ACA GGG AGA
Vα4	TGA TGC TAA GAC CAC MCA GC
Vα5	GGC CCT GAA CAT TCA GGA
Vα6new	GGT CAC AGC TTC ACT GTG GCT A
Vα7	ATG TTT CCA TGA AGA TGG GAG
Vα8	TGT GGC TGC AGG TGG ACT
Vα9	ATC TCA GTG CTT GTG ATA ATA
Vα10	ACC CAG CTG CTG GAG CAG AGC CCT

Vα11	AGA AAG CAA GGA CCA AGT GTT
Vα12	CAG AAG GTA ACT CAA GCG CAG ACT
Vα13	GAG CCA ATT CCA CGC TGC G
Vα14.1	CAG TCC CAG CCA GAG ATG TC
Vα14	CAG TCT CAA CCA GAG ATG TC
Vα15	GAT GTG GAG CAG AGT CTT TTC
Vα16	TCA CGC GAA GAT CAG GTC AAC
Vα17	GCT TAT GAG AAC ACT GCG T
Vα18	GCA GCT TCC CTT CCA GCA AT
Vα19	AGA ACC TGA CTG CCC AGG AA
Vα20	CAT CTC CAT GGA CTC ATA TGA
Vα21	GTG ACT ATA CTA ACA GCA TGT
Vα22	TAC ACA GCC ACA GGA TAC CCT TCC
Vα23	TGA CAC AGA TTC CTG CAG CTC
Vα24new	GAA CTG CAC TCT TCA ATG C
Vα25	ATC AGA GTC CTC AAT CTA TGT TTA
Vα26	AGA GGG AAA GAA TCT CAC CAT AA
Vα27	ACC CTC TGT TCC TGA GCA TG
Vα28	CAA AGC CCT CTA TCT CTG GTT
Vα29	AGG GGA AGA TGC TGT CAC CA
Vα30	GAG GGA GAG AGT AGC AGT
Vα31new	TCG GAG GGA GCA TCT GTG ACT A
Vα32	CAA ATT CCT CAG TAC CAG CA
P-5`βST	AAG CAG AGA TCT CCC ACA C
P-3`βST	GAG GTA AAG CCA CAG TTG CT
P-3CβII	GAT GGC TCA AAC ACA GCG ACC TC
Vβ1	GCA CAA CAG TTC CCT GAC TTG GCA C
Vβ 2	TCA TCA ACC ATG CAA GCC TGA CCT
Vβ3	GTC TCT AGA GAG AAG AAG GAG CGC
Vβ4	ACA TAT GAG AGT GGA TTT GTC ATT
Vβ5.1	ATA CTT CAG TGA GAC ACA GAG AAA C
Vβ5.2	TTC CCT AAC TAT AGC TCT GAG CTG

Vβ5.2T	TTC CCT AAT TAT AGC TCT GAG CTG
Vβ6.1new	GCC CAG AGT TTC TGA CTT ACT TC
Vβ6.2	ACT CTG ASG ATC CAG CGC ACA S=C/G
Vβ6.3	ACT CTG AAG ATC CAG CGC ACA
Vβ7	CCT GAA TGC CCC AAC AGC TCT C
Vβ8	ATT TAC TTT AAC AAC AAC GTT CCG
Vβ8S3	GCT TAC TTC CGC AAC CGG GCT CCT
Vβ9new	CCT AAA TCT CCA GAC AAA GCT
Vβ10	CTC CAA AAA CTC ATC CTG TAC CTT
Vβ11	TCA ACA GCT TCC AGA ATA AGG ACG
Vβ12	AAA GGA GAA GTC TCA GAT
Vβ12S3	GCA GCT GCT GAT ATT ACA GAT
Vβ13new	TCG ACA AGA CCC AGG CAT GG
Vβ13.1	CAA GGA GAA GTC CCC AAT
Vβ13.2	GGT GAG GGT ACA ACT GCC
Vβ13S5	ATA CTG CAG GTA CCA CTG GCA
Vβ14	GTC TCT CGA AAA GAG AAG AGG AAT
Vβ15	AGT GTC TCT CGA CAG GCA CAG GCT
Vβ16	AAA GAG TCT AAA CAG GAT GAG TCC
Vβ17	CAG ATA GTA AAT GAC TTT CAG
Vβ18	GAT GAG TCA GGA ATG CCA AAG GAA
Vβ19	CAA TGC CCC AAG AAC GCA CCC TGC
Vβ20	AGC TCT GAG GTG CCC CAG AAT CTC
Vβ21	AAA GGA GTA GAC TCC ACT CTC
Vβ22.1	CAT CTC TAA TCA CTT ATA CT
Vβ22.2	AAG TGA TCT TGC GCT GTG TCC CCA
Vβ22.3	CTC AGA GAA GTC TGA AAT ATT CG
Vβ23	GCA GGG TCC AGG TCA GGA CCC CCA
Vβ24new	TC CAG GAG GCC GAA CAC TTC T

3.10 Cell Lines and Primary Cell Lines

Table 13 *Cell Lines & Primary Cell Lines*

Cell line	Description	HLA-Allele	Medium
A673	ES cell line	A*0201 +	Standard Medium
TC71	ES cell line	A*0201 +	Standard Medium
EW7	ES cell line	A*0201 +	Standard Medium
697	B-cell precursor leukemia cell line	A*0201 +	Standard Medium
K562	Chronic myelogenous leukemia cell line	A*0201 -	Standard Medium
LCL	Lymphoblastoid cell line	A*0201 +	LCL - Medium
SB-KMS-KS1	Ewing Tumor (formerly SBSR-AKS)	A*0201 -	Standard Medium
T2	TAP-transporter deficient hybrid of T and B lymphoblastoid cell line	A*0201 +	LCL - Medium
PBMCs	Peripheral blood mononuclear cell derived from a Buffy Coat via Ficoll-Paque	-	TCM
CD8+ T cells	Isolated from PBMCs using negative selection	-	TCM
CD14+ Monocytes	Isolated from PBMCs using positive selection	-	X-Vivo
Pool-PBMCs	Mixed PBMCs from 4 different donors	-	TCM

4 Methods

4.1 General techniques

4.1.1 Cell Culture

Depending on their growth rate, suspension cell lines were split every two days. To that end, half of the medium was removed and replaced with new one.

The medium was carefully aspirated to split adherent cells. The cells were then rinsed with 5 to 10 mL of PBS and, depending on their adherence, incubated with 3 to 5 mL trypsin at 37°C for 3 to 5 minutes. If necessary, the vessel was gently tapped to aid detachment. Afterward, the detachment was verified microscopically. The loose cells were washed by centrifuging at 1500 rpm for 5 minutes and seeded into culture vessels with fresh medium at the appropriate number of cells.

4.1.2 Counting Cells

To count cells, they were diluted 1:2 or higher with trypan blue, depending on the estimated cell count. Ten microliters were then placed into a Neubauer counting chamber.

The cells were counted in the chamber's four outer squares, consisting of 16 small squares. Only the unstained, glowing cells were considered; defective cells are stained blue by trypan blue. Furthermore, only the cells touching the top and left margins of the small squares were counted.

The cell number was calculated by multiplying the cell number/square with the dilution factor and 10^4. Multiplying the result again by the medium volume in milliliters yielded the total cell number in the sample.

4.1.3 Cell Freezing and Thawing

First, the cells were counted. After centrifugation at 1500 rpm for five minutes, the cells were resuspended at 1-2 x 10^6 cells/mL in a suitable freezing medium and transferred into labeled cryovials, filling them with 1 mL each. Human AB serum with 10% DMSO was used for T cells, and other cells were frozen in FCS along with 10% DMSO. The cryovials were placed in a Mr. Frosty for at least 24 hours.

Cells were kept either in the liquid nitrogen freezer or the -80°C.

To defrost cells, they were thawed by mixing them with suitable media and then centrifuged at 1500 rpm for five minutes to wash them. The cell pellet was then transferred into culture media.

4.2 Determining the Binding Properties of Peptides

*4.2.1 HLA-A*0201 Peptide Binding Properties In Silico Prediction*

An *in silico* analysis of PAX7 and CHM1 peptide nonamers was conducted using SYFPEITHI, a database of MHC ligands and peptide motifs, to find suitable targets for adoptive T-cell transfer. The nonamers were checked for HLA-A*0201 binding potential.

Moreover, the ScanProsite tool was used to check for cross-reactivity. The most promising candidates were tested in an HLA*0201 binding assay.

*4.2.2 T2/ HLA-A*0201 Peptide Binding Assay*

T2 cells were centrifuged (1500 rpm, 5 min) and washed with PBS. Cells were counted and reduced to a final concentration of $1x10^6$ cells/mL. Per well, 250 µL of the suspension was used.

Then, the T2 cells were pulsed with peptides in increasing concentrations (10 µg/mL, 50 µg/mL, 100 µg/mL). Non-pulsed cells functioned as a negative control, whereas cells pulsed with an influenza peptide were used as the positive control.
The cells were incubated overnight (16 hours), and the HLA-A*0201 binding efficacy was measured using FACS. The relative bond was determined by dividing the intensity of the fluorescence at a specific concentration by the intensity of fluorescence of the non-pulsed cells. A good epitope was identified by having comparable values to the positive control.

4.3 Specific T Cell Generation

4.3.1 Isolation of Peripheral Blood Mononuclear Cells

Using Ficoll density gradient centrifugation, peripheral blood mononuclear cells (PBMC) were isolated. For this purpose, the blood cell concentrate (buffy coat) was thinned with an equal volume of PBS to facilitate layering over the already added Ficoll (35 mL concentrate to 15 mL Ficoll). The tube was tilted slightly, and the

blood mixture was pipetted gently along the tube's side to prevent mixing. Subsequently, the layered mixture was centrifuged at 2220 rpm for 10 minutes without a break, and the PBMCs, now forming a distinct white layer, were aspirated and transferred to another tube. To remove thrombocytes, PBS was added until a volume of 50 mL was reached, and the tube was centrifuged with breaking at 700 rpm for 7 minutes. Cells were counted and washed with PBS by centrifuging at 1300 rpm for 7 minutes with breaking.

The isolated cells could then be used immediately or were frozen until usage.

The blood concentrates were acquired at the DRK-Blutspendedienst Baden-Württemberg/ Hessen in Ulm. Heparinized whole blood was centrifuged in a 50 mL tube for 10 minutes at 2200 rpm. The serum was aspirated, and the rest was mixed 1:1 with PBS and treated like the buffy coats.

4.3.2 Pool-PBMC Manufacturing

Four blood cell concentrates from four individuals were used as the basis for the pool-PBMCs. First, each concentrate was handled separately, isolating the PBMCs as described above (see 4.3.1.)

Each sample was counted and then standardized to the same number of cells. Afterward, the buffy coats were mixed and centrifuged at 2200 rpm for 10 minutes. The pool PBMCs were then frozen (see 4.1.3) or used immediately.

4.3.3 CD14+ Cell Isolation

CD14+ monocytes were isolated from PBMCs (HLA-A*0201+ healthy blood donor) utilizing the BD Anti-Human CD14 Magnetic Particles kit and the BD IMag following the manufacturer's instructions.

The BD IMag buffer was prepared with sterile, distilled water at 1:10.

The PBMCs were counted and washed with an excess volume of the BD IMag buffer. The supernatant was carefully aspirated.

Per $2x10^7$ cells, 50 µL of thoroughly vortexed BD IMag anti-human CD14 particles were used. After mixing, the cells were incubated at room temperature for 30 minutes. The BD IMag particle labeling volume was then increased to 9 mL with 1x BD IMag buffer, distributed into 3 FACS tubes, and placed on the magnet for 8-10 minutes. The supernatant containing the negative fraction was aspirated with the

tubes still on the magnet. The remaining cells were resuspended in a 4 mL buffer after being removed from the magnet. They were returned to the magnet for 2-4 minutes, and the supernatant was again aspirated. This step was repeated once.

In the end, the stained, positive fraction was resuspended in an appropriate buffer or media.

CD14+ cells were used for the generation of dendritic cells.

4.3.4 Dendritic Cell Generation

After PBMC and CD14+ cell isolation, the identified cells were utilized to generate dendritic cells. They were transferred into a medium of X-VIVO 15 medium containing 1% human serum type AB, 1000 U/mL IL-4, and 800 U/mL GM-CSF. After 2 days, cytokines were added again using the same amount. Medium and serum were renewed if necessary. On days 5-6, naïve dendritic cells were checked microscopically, and maturation-promoting factors (1000 U/mL IL-6, 10 ng/mL IL-1ß, 10ng/mL TNF-alpha and 1ug/mL PGE2) were added into the flask.

The morphology was checked again in the following 1 to 2 days. If the dendritic cells were mature, they displayed distinct dendrites.

Afterward, the immune phenotype was analyzed by flow cytometry, staining for CD86, CD83, and HLA-DR.

Subsequently, the mature DCs were pulsed with the desired peptide (30 µmol/mL) and ß2-microglobulin (20 ng/mL) for 2 to 4 hours and used for T cell priming or frozen and stored at -80°C until further use.

4.3.5 CD8+ T Cell Isolation

CD8+ T cells can be isolated from PBMCs using the CD8+ T Cell Isolation Kit, following the manufacturer's instructions.

First, the buffer was prepared by mixing the MACS BSA Stock Solution (PBS, 0.5% bovine serum albumin (BSA), and 2 mM EDTA with the autoMACS Rinsing Solution in a ratio of 1:20.

Cells of interest were counted, centrifuged, and resuspended in 40 µL buffer per 10^7 total cells. 10 µL/ 10^7 cells of the provided Biotin-Antibody Cocktail were added and incubated for 5 minutes at 2-8°C. Then, 30 µL buffer/ 10^7 cells and 20 µL/10^7 cells

of CD8+ T Cell MicroBead Cocktail were added. The mixture was again incubated for 10 minutes at 2-8°C.

An LS column must be put into a suitable MACS Separator to separate the cells and prepared by rinsing it with 3 mL of buffer. After that, the cell suspension was pipetted into the column. This being a negative selection, the flow-through containing the enriched CD8+ cells had to be collected. Subsequently, the column was washed with 3 mL of buffer, and the flow-through was again collected.

The stained cells were removed from the column by extracting it from the magnet and flushing 5 mL of buffer through the column using a plunger.

4.3.6 In Vitro T-cell Priming

The previously generated and with the desired peptide-pulsed HLA-A*0201+ DCs were co-cultured with HLA-A*0201- CD8- T cells (5 x 10^3 DCs per well: 10^5 CD8+ T cells per well). For that purpose, each well of a labeled 96-well plate was filled with 200 µl T cell medium and the required amount of both cell types. The T-cell medium was enriched with 1000 U/mL IL-6 and 10 ng/mL IL-12.

After one week, the cells were re-stimulated using an equal amount of pulsed DCs, supplemented with 5ng/mL IL-7 and 100 U/mL IL-2.

4.3.7 Cell Sorting and Multimer Staining

The previously primed CD8+ cells were washed and then stained to determine their specificity for CD8 and the multimer in question (for the procedure, see Chapter 4.6.2 Flow Cytometry).

To prepare the cells for sorting, they were washed with T-cell medium and counted.

2 x 10^5 cells were either not stained or stained with the appropriate amount of CD8 antibody (FITC and PE). The remaining cells were stained with CD8 antibody and the specific multimer provided by the working group of Prof. Dirk Busch, Institute for Medical Microbiology, Immunology and Hygiene, Technical University Munich, an unlabeled Pro5 R MHC class I Pentamer by ProImmune or a labeled Pro5 R MHC class I Pentamer by ProImmune and used according to their protocols and indication of quantity. In the end, there were four samples per sorting.

The sorting took place in the laboratory of Prof. Dirk Busch, Institute for Medical Microbiology, Immunology and Hygiene, Technical University Munich, using a FACS Aria. The cells were filtered on-site, and propidium iodide (1µg/mL) was added to the samples to exclude dead cells from sorting.

The T cells were sorted for CD8-FITC, multimer PE, and/or multimer APC or for the unlabeled or labeled Pro5 R MHC class I Pentamers specific for the peptide in question and placed in a tube filled with 500 µLof human AB serum. Samples and sorted cells were transported on ice.

4.3.8 Limiting Dilution

After sorting the CD8+ cells, they were expanded using limited dilution to single out the most promising clones.

To do so, each well of a 96-well plate received a single T cell in 200 µL of T-cell medium along with anti-CD3 (30 ng/mL), 10^5 irradiated LCL (100 Gray), and $5x10^4$ irradiated Pool-PBMCs (30 Gray). Additionally, 100 U/mL IL-2 and 2 ng/mL IL-15 were mixed into the T-cell medium. The single T cell was assigned statistically to a well based on the number of sorted cells in a predetermined medium volume.

After a week, the T cells were re-stimulated by replacing half of the medium and the cytokines.

4.3.9 T-Cell Expansion

T cells (at least $5x10^4$ cells) were resuspended in a 25 mL T-cell medium. Irradiated LCL (100 Gray, $5x\ 10^6$ cells/flask) and Pool-PBMCs of 4 healthy donors (30 Gray, $2,5\ x\ 10^7$) were added as feeder cells. Furthermore, 30 ng/mL of Anti-CD3 was added immediately. One day after the start of the expansion, IL-2 (100 U/mL) and IL-15 (2ng/mL) were mixed into the suspension.

Afterward, cytokines were refreshed every two days, and the medium was replaced whenever necessary.

4.4 Identifying specific T cell clones

4.4.1 ELISpot Assay

One day before starting the protocol, adherent cells were stimulated with 100 U/mL INFy to increase their HLA presentation.

On the first day, 50 µL of the required antibody solution (capture antibody mAb 1-D1K and PBS) was carefully pipetted into each well of the ELISpot plate and incubated for the night at 4°C.

On the second day, T2 cells, if utilized, were pulsed with the peptide that needed to be tested and the FLU-negative control for two hours, mixed continuously, and washed three times with T-cell medium. The ELISpot plates were dumped, washed four times with 200µL PBS/well in 10-minute refrigerated intervals, and then blocked for unspecific binding by T-cell medium (150µL/well) for 60 minutes. The plate was then emptied out again.

Meanwhile, the T cells to be tested were counted and washed three times with T-cell medium. 50 µL of T-cell medium containing the required number of T cells (e.g., 1000 or 5000 T cells) was put into each well and incubated for 30 minutes at 37°C. Target cells were also counted and washed twice with T cell medium. Subsequently, 20,000 T2 and target cells/well were added in another 50 µL of T-cell medium by layering it on top of the T cells without mixing and incubated for 20 hours at 37°C.

On the third day, the plates were emptied again and washed six times with PBS mixed with 0.05% Tween. 100 µL of the detection antibody (7-B6-1-Biotin in PBS and 5% BSA) was added to each well and incubated for 2 hours at 37°C. Afterward, the plates were washed again with PBS and 0,05% Tween, and 100 µL of streptavidin-horseradish peroxidase in PBS, and 5% BSA was pipetted into each well.

After incubating for one hour, away from light and at room temperature, the plates were again washed three times using PBS Tween and three times with normal PBS.

Finally, 100 µL of development solution (see 3.5.3) was added to each well. The reaction was halted after approximately 10 minutes or when spots were visible by rinsing the plates under running water.

The plates were dried to analyze the plates using the ELISpot reader.

4.4.2 Flow Cytometry

The desired cells were counted. Per staining, 2 to 4 x 10^5 cells were added into a 96-well round bottom plate and then centrifuged at 1500 rpm for 5 minutes. Cells were resuspended in 50 µL of staining buffer. Next, 3µL of the appropriate antibody

was added, and the plate was incubated for 30 minutes at 4°C. Afterward, the plate was washed. For that, 100 µL of staining buffer was added to the samples and centrifuged at 1500 rpm for 5 minutes. The washing step was then repeated. The samples were then transferred into 300 µL PBS for the analysis.

4.5 Sequencing TCRs

4.5.1 RNA Isolation

To isolate RNA from a sample, 1 mL TriReagent solution was used to homogenize 5-10 x 10^6 cells. The homogenate was then incubated at room temperature for 5 minutes.

100 µL BCP was added for every milliliter of TriReagent solution, mixed, and then again incubated at room temperature for 5 - 15 minutes. After the time elapsed, the solution was centrifuged at 12000 g at 4 °C for 10 - 15 minutes.

500 µL isopropanol was added per 500 µL of the solution's aqueous phase, vortexed for a few seconds, and then again incubated at room temperature. The centrifuge was used again at 12000 g for 8 min at 4 – 25 °C. Afterward, the supernatant was discarded, 1 mL of 75% ethanol per 1 mL solution was added, and the mix was centrifuged at 7500 g for 5 min. After removing the ethanol, the RNA pellet was air-dried and then liquefied in 30 – 40 µL DEPC H20.

The concentration of RNA was tested with a nanophotometer.

4.5.2 cDNA Synthesis

The High-Capacity Reverse Transcription Kit was used to transcribe RNA into cDNA.

First, 2 PCR master mixes were prepared. Their composition is listed in Table 14 and 15.

Table 14 Mix A

Buffer	2 µL
Primer	2 µL
dNTPs	0,8 µL

Reverse Transcriptase	1 µL
	5,8 µL

Table 15 Mix B

RNA	1 µg
DEPC - H20	X µL
	14,2 µL

Secondly, the 20 µL combination of both master mixes was processed in a thermocycler. The settings are given in Table 16.

***Table 16** Phases and Temperatures in Thermocycler*

Phase	Temperature (°C)	Duration (min)
1	25	10
2	37	60
3	37	60
4	85	5
5	4	∞

The concentration of DNA was tested in a nanophotometer.

4.5.3 Vαβ-Repertoire Analysis

The AccuPrime™ Taq DNA Polymerase System was used to analyze the Vα – and Vβ-repertoire of the T cell clones.

A PCR was performed after RNA was isolated from the desired clone (5.7.1) and transcribed into cDNA (5.7.2).

To amplify the TCR repertoire, 34 alpha chain-specific primers and 38 beta chain-specific primers, and two internal controls per chain were used. These variable primers attach to the 5'-end of the different TCR variable chains. 3' TCα and 3' CβII were used as the respective 3’-primers. They correspond to a constant region close to the variable chain. The internal controls P-5`αST and P-3`αST and P-5`βST and P-3`βST are binding in the constant regions of their respective chains.

The primer sequences can be found in Chapter 3.9.

Again, a PCR master mix was prepared according to Table 17.

Table 17 PCR ingredients

10x Buffer I	2,5 µL
H20	18,5 µL
Primer P-5`αST/ P-5`βST	0,5 µL
Primer P-3`αST/ P-3`βST	0,5 µL
Primer 3`TCα/ 3`CβII	1 µL
Primer Vαx/Vβx	1,5 µL
AccuPrimeR Taq DNA Polymerase	0,5 µL

The PCR was conducted using a thermocycler using the settings listed in Table 18 and with phases 2-4 conducted for 40 cycles.

Table 18 Phases and Temperatures PCR in Thermocycler

Phase	Temperature (°C)	Duration (min)
1	94	6
2	94	1
3	54	1
4	68	1
5	68	7
6	4	∞

4.5.4 Gel Electrophoresis and Sample Extraction

The fragments of the Vαβ-Repertoire analysis were separated in 2 % agarose using gel electrophoresis.

The gel was cast after adding 0.02 µL/mL ethidium bromide.

The DNA solutions were mixed with 6x loading dye and pipetted into the gel slots. A 1 kb plus ladder was also running in the electrophoresis to determine the size of the fragments, which was performed at a voltage of 5 – 10 V/cm.

Promising fragments were then cut from the gel under UV light with the help of a scalpel and could then be extracted from the gel via the Strataprep DNA gel extraction kit.

300 µL extraction buffer was pipetted into an epi containing the gel cube and dissolved at 50°C for approximately 10 minutes.

The solution was then placed into a micro spin cup in a 2 mL tube and centrifuged for 30 seconds. The flow-through was discarded, and 750 µL wash buffer was added to the micro spin cup, which was again centrifuged for 30 seconds.

After transferring into another 1.5 mL Epi, pipetting 50 µL DEPC-H20 onto the fiber matrix, and incubating for 5 minutes at room temperature, the tube was centrifuged for 30 seconds a last time.

A nanophotometer measured the concentration of the DNA in the flow-through.

4.5.5 TCR sequencing

Sequiserve in Vaterstetten sequenced all samples using the corresponding primers. The Basic Local Alignment Search Tool (BLAST) and the open reading frame finder (ORFfinder) were used to analyze the sequencing results.

4.5.6 Single-Cell RNA Sequencing

Single-cell RNA sequencing was performed with the help of Sabrina Wagner from the Institute for Medical Microbiology, Immunology and Hygiene, Technical University Munich, Germany.

4.6 Data Analyses and Statistics

GraphPad Prism 10 and FlowJo were utilized to analyze data and create graphics.

Where applicable, ELISpot assays were analyzed with a two-tailed T-test, and Error Bars indicate the results from duplicate experiments. A p-value of <0.05 was seen as statistically significant.

The methods were implemented according to protocols used in our laboratory, which can lead to similarities with previous work published by members of our laboratory. For example, the methods were previously described in (Blaeschke, 2016; Kirschner, 2017; Pirson, 2010; Storz, 2020).

5 Results

5.1. LIPI

Two pre-generated T-cell clones targeting LIPI (Lipase 1), a protein that plays a significant role in oncogenesis and metastasis (Mahlendorf & Staege, 2013; Staege et al., 2004), were re-evaluated for their specificity and functionality.

Both clones were stained with FITC CD8, the specific LIPI multimer, and an unspecific STEAP1 multimer for comparison. The staining results (see Figure 2 A) clearly showed that the clones are CD8 positive, confirming their identity as T cells. They also showed positive binding to the specific LIPI-multimer, whereas the unspecific STEAP1 multimer did not bind, indicating that these clones are specific for the LIPI-peptide.

Following this, two ELISpot assays (see Figure 2 B) were performed to test further peptide specificity, HLA-A*0201 restriction, and the ability of the T-cell clones to recognize Ewing sarcoma cell lines in IFNγ ELISpot assays.

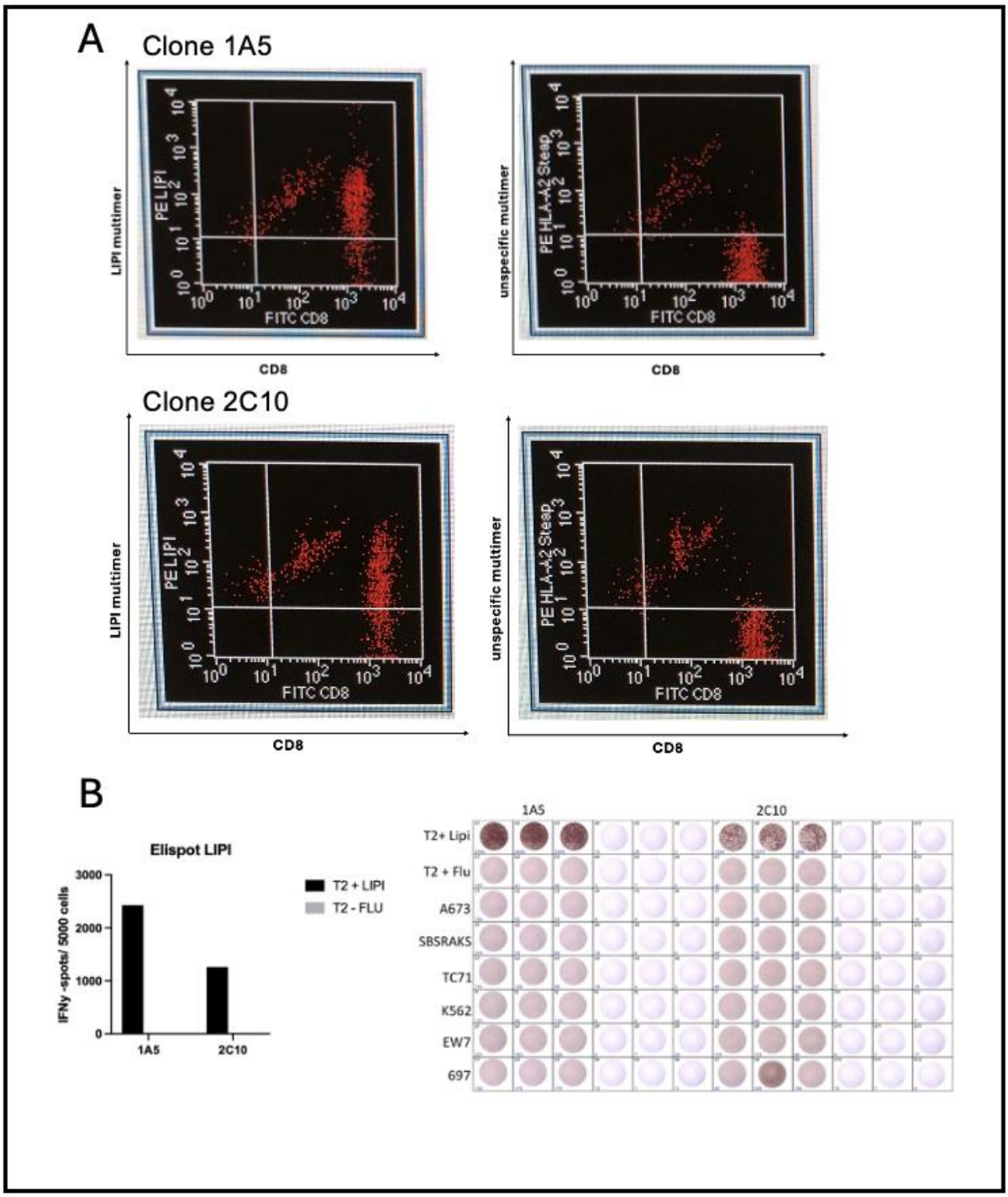

Figure 2 LIPI clones 1A5 & 2C10 are peptide-specific in FACS and ELISpot analysis but neglect EwS-tumor cell lines *(A) Cells were stained for FITC CD8+ and a LIPI-specific PE-multimer as a positive control (left) and with FITC CD8+ and a STEAP1-specific PE-multimer as a negative control (right) (B) The clones were tested in an IFNy ELIspot for peptide specificity and HLA-A*0201 restriction and their ability to identify EwS cell lines. LIPI-pulsed T2 cells served as the positive control, while FLU-pulsed T2 cells served as the negative control for peptide specificity. EwS cell lines A673, TC71, EW7: HLA-A*0201+ EwS served as a positive control, while SB-KMS-KS: HLA-A*0201- EwS, 697: HLA-A*0201+ pediatric cALL and K562: MHC- NK cell control were used as a negative control, regarding peptide specificity and HLA-A*0201 restriction.*

The ELISpot assays confirmed the flow cytometry results, showing significant T-cell activity in wells containing target cells loaded with the LIPI peptide and almost none in wells with irrelevant FLU-control peptide. However, LIPI clones 1A5 and 2C10, although able to recognize peptide-pulsed T2 cells, did not recognize any Ewing sarcoma cell lines, specifically A673, TC71, or EW7, suggesting that LIPI may not be expressed on the tested tumor cell lines. Consequently, these clones were not pursued further.

5.2 PAX7

Next, PAX7 was analyzed as a potential target. It is linked to cancer growth and is also present in alveolar rhabdomyosarcoma and synovial sarcoma (Baldauf et al., 2018; Charville et al., 2017).

5.2.1 In Silico Analysis

An *in silico* analysis was conducted to identify PAX7 peptides suitable for processing and presentation via HLA-A*0201 (see Chapter 4.2.1). The analysis, which can be found in Table 19, suggested four peptides with high scores in binding strength, including PAX7 489, PAX7 280, PAX7 3, and PAX7 374. Importantly, these peptides showed no hits in the cross-reactivity scan. These peptides were selected for further evaluation and commissioned.

Table 19 In silico prediction of binding scores & cross-reactivity identifies 4 PAX7 nonamers (using SYFPEITHY & ScanProsite). *PAX7-peptides were tested in silico using SYFPEITHY & ScanProsite for a high binding score and no hits in the cross-reactivity test. Four promising peptides were chosen for further evaluation. Table was sorted by binding score in descending order.*

Position	Sequence	Score (SYFPEITH)	Hits (Cross-reactivity)
280	QLAAFNHLL	24	no hit
489	CLFMESYKV	24	no hit
3	ALPGTVPRM	23	no hit
374	HMNPVSGL	23	no hit

*5.2.2 PAX7-HLA-A*0201-Binding Assay*

A T2/HLA-A*0201 peptide binding assay (see Figure 3) was performed as described in Chapter 4.2.2 to analyze the binding properties of the four peptides relative to an influenza peptide (GILFGFVFTL). The PAX7 489 peptide (CLFMESYKV) emerged as a promising HLA-A*0201 binder, comparable to the influenza peptide, the positive control, and was selected for further use. An increased binding affinity could also be observed with higher peptide concentrations.

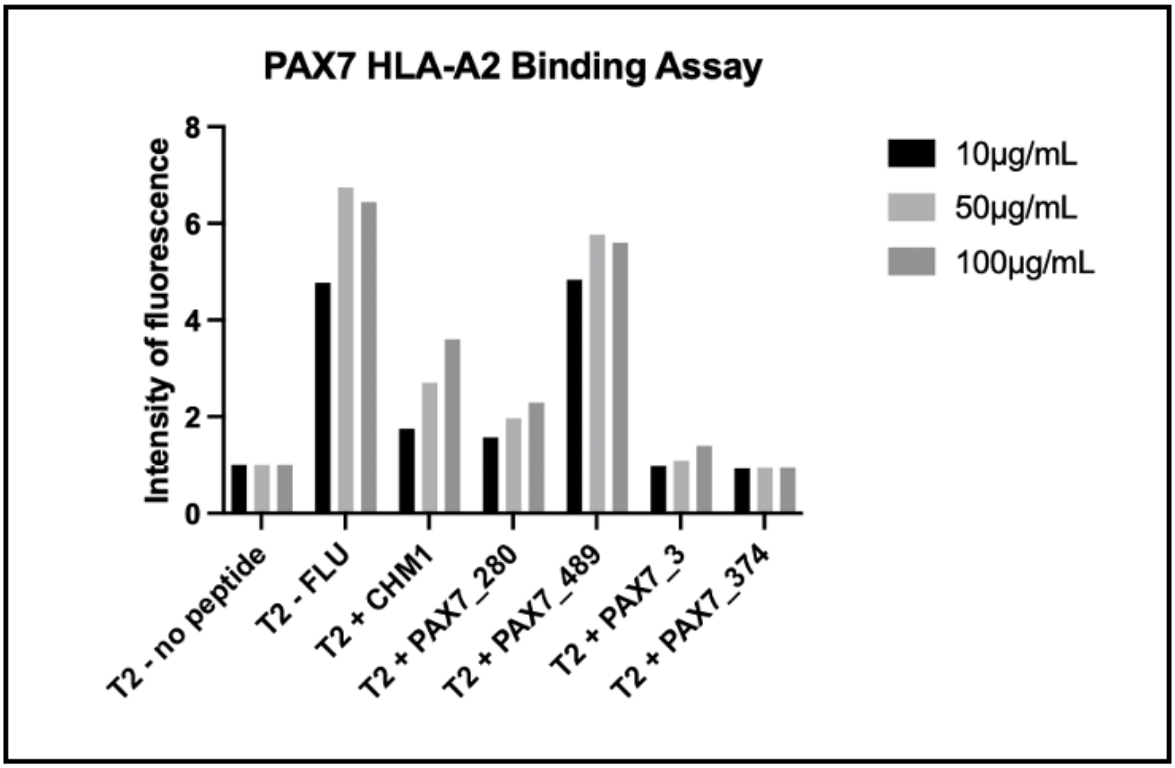

Figure 3 HLA-A2 Binding Assay via FACS analysis identifies PAX7 489 as a good binding peptide. *Nonamers identified in in silico testing were tested for their HLA-A2*0201 binding capacities. The fluorescence intensity in comparison to FLU (positive control) and an intensity increase associated with a higher peptide concentration were evaluated.*

5.2.3. Generation of PAX7 specific T cell clones

To generate allo-restricted, PAX7-specific cytotoxic T cells, CD8+ HLA-A*0201+ T cells were co-cultured with PAX7 489-pulsed DCs for 14 days. The maturation status of DCs was confirmed by the presence of CD83, CD86, and HLA-DR markers (see Figure 4).

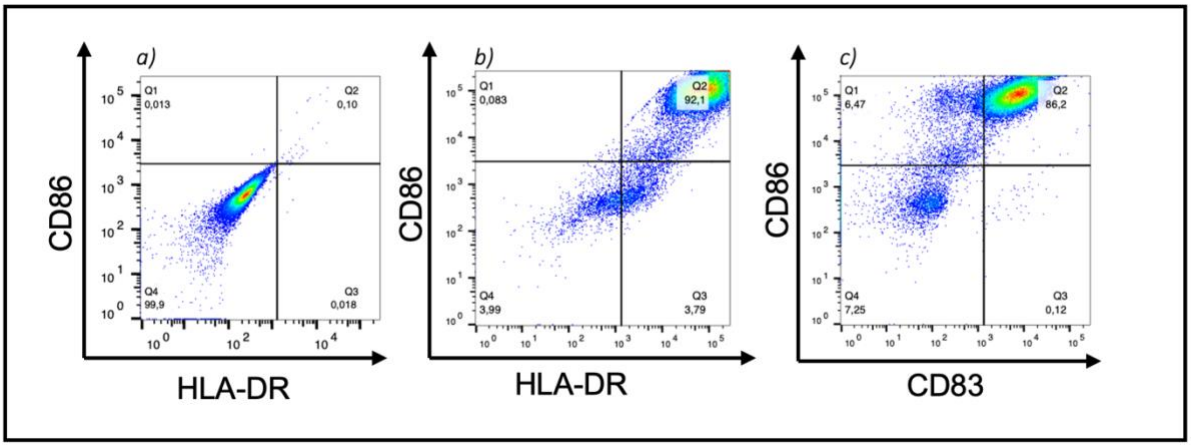

Figure 4 DCs were considered mature when positive for CD86, HLA-DR, and CD83 *DCs were tested for their maturity level in a FACS analysis, either a) unstained, or b) & c) stained with CD86 FITC, HLA-DR PE, and CD83 APC.*

After 14 days, the CD8+ HLA-A2*0201 + T cells were stained with CD8 and the PAX7 multimer. Alternatively, unlabeled Pro5 R MHC class I Pentamers specific for PAX7 and made visible by the Pro5 Fluorotag R-PE, or the labeled Pro5 R MHC class I Pentamer specific for PAX7 were used for staining. Typically, 2 x 10^7 cells were used. Double-positive cells were sorted at the Institute for Medical Microbiology, Immunology and Hygiene, Technical University Munich, Germany (exemplary see Figure 6 A) and expanded using limiting dilution (see Chapter 4.3.8).

Several runs were conducted to increase the likelihood of identifying promising cells, adjusting different variables. For example, various colors (APC vs. PE) and multimers (CD8 vs. CD3 and CD4) were used for staining to avoid potential interference with the peptide-specific multimer. Furthermore, a labeled Pro5 R MHC class I Pentamer and then an unlabeled Pro5 R MHC class I Pentamer were tested, in contrast to the previously used multimer, hoping for better binding properties. Moreover, HLA-A*0201+ blood from a known young donor was used instead of Buffy coats from unknown donors to increase the probability of selecting young, vital cells.

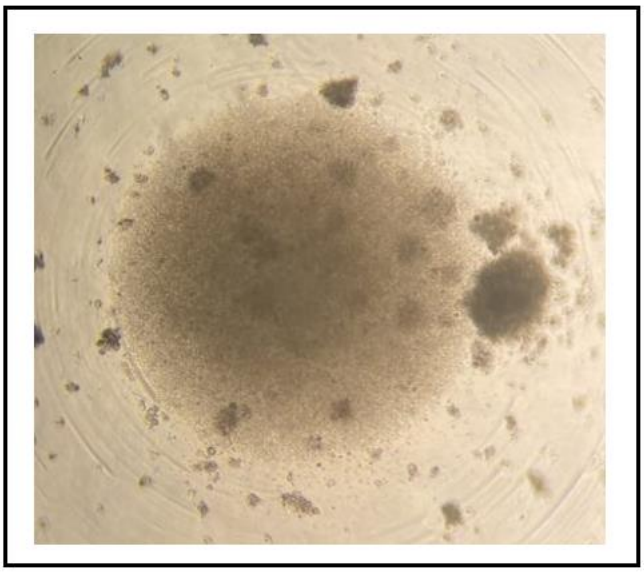

Figure 5 T cells were chosen for further testing based on a crown-like clonal T-cell growth pattern on the bottom of the well*. Following the sorting and a 2-week limiting dilution process, the cells were evaluated microscopically regarding their growth pattern.*

After two weeks of expansion (see Chapter 4.3.8), the T cells were always tested in screening ELISpots for their ability to recognize target peptides. Cell populations for the screening ELISpot were selected based on their growth pattern, meaning a dense crown on the bottom of the wells (see Figure 5). One such screening ELISpot can be found in Figure 6 B.

Clones were selected and considered specific depending on their ability to identify the positive control, T2 cells pulsed with the PAX7-peptide. Furthermore, the non-recognition of the negative control, T2 cells pulsed with a FLU-peptide, was considered.

Clones showing a strong response to PAX7-peptide-pulsed T2 cells and minimal response to a FLU-peptide control in the screening ELISpot were selected for further expansion (see Chapter 4.3.9). PAX7 clone 6E12 showed the best recognition of loaded T2 cells but also some cross-reactivity with FLU-pulsed T2 cells.

Figure 6 (C,D,E) shows the results of the Confirmation ELISpot of the most promising clone, 6E12. The T-cell clone 6E12 showed a good recognition of the positive control, suggesting a peptide specificity. Some potential cross-reactivity was observed, as the clone also recognized the negative control (FLU-pulsed T2 cells) but to a lesser degree.

Moreover, 6E12 was able to recognize Ewing sarcoma cancer cell lines, notably the HLA-A201+ A673 and TC71 tumor cell lines, much better than the HLA-A201- SB-KMS-KS cell line, implying an HLA-A*201 restriction.

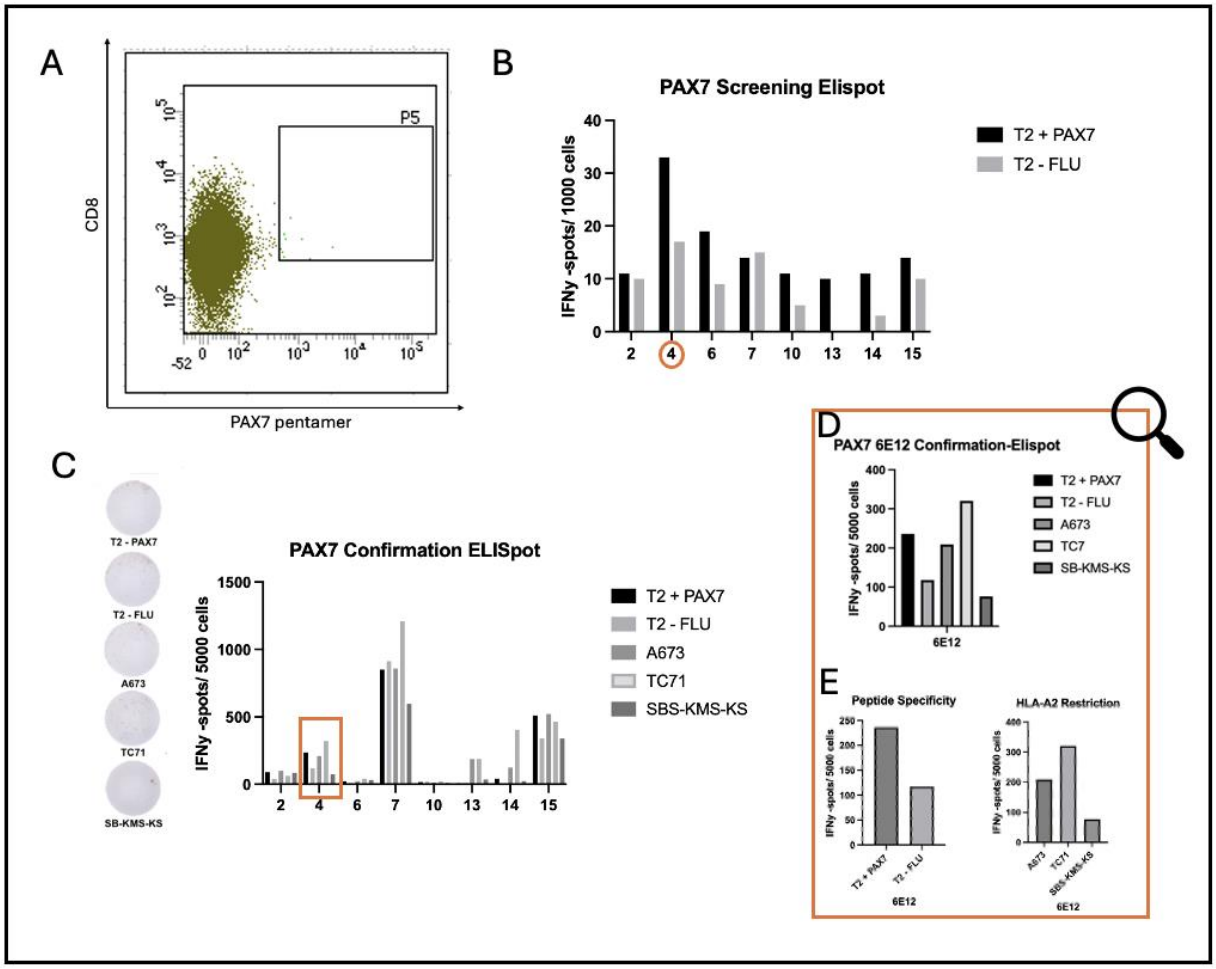

Figure 6 PAX7 T cell-sorting - identified PAX7 clone 6E12 recognized PAX7-loaded T2 cells and EwS cancer cell lines in IFNy ELISpot. *(A) In vitro primed CD8 + T cells were stained for FITC CD8 and PE Pentamer/Multimer. Double-positive cells were gated (P5) and subsequently sorted. (B,C,D,E) After the limiting dilution process, the T cell clones were tested in IFNy ELIspots for peptide specificity, HLA-A*0201 restriction, and their ability to identify EwS cell lines. PAX7-pulsed T2 cells served as the positive control, while FLU-pulsed T2 cells served as the negative control for peptide specificity. EwS cell lines A673 and TC71: HLA-A*0201+ EwS served as a positive control, while SB-KMS-KS: HLA-A*0201- EwS was used as a negative control regarding HLA-A*0201 restriction. Clones eliminated after the screening ELISpot not shown.*

Based on these findings, this clone was chosen for further investigation and expanded to generate enough cells to potentially identify a TCR.

Despite initial promising results, the specificity and viability of clone 6E12 could not be replicated over time. A FACS analysis and an additional ELISpot assay

was performed to investigate this phenomenon. The results are shown in

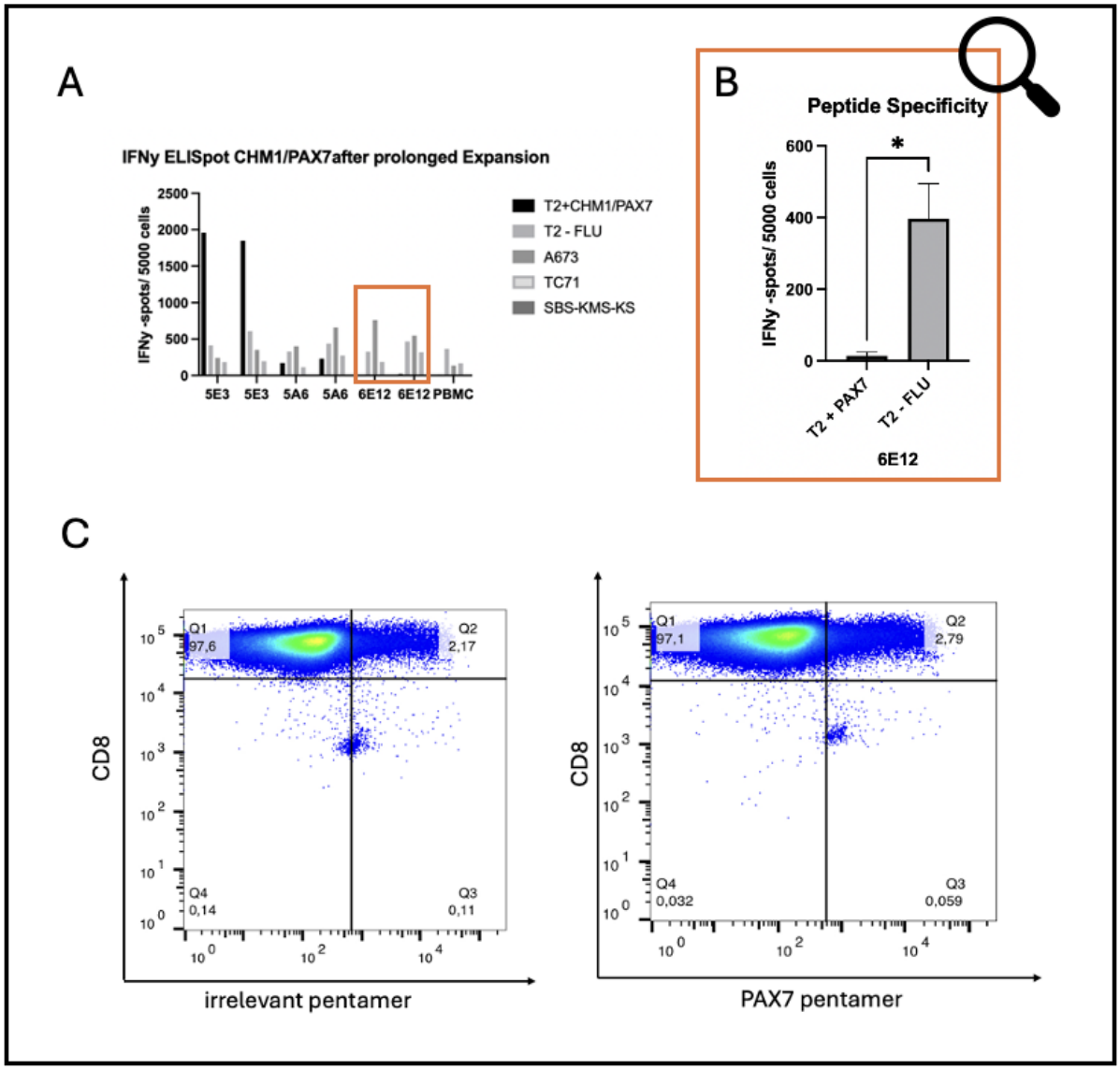

Figure **7**.

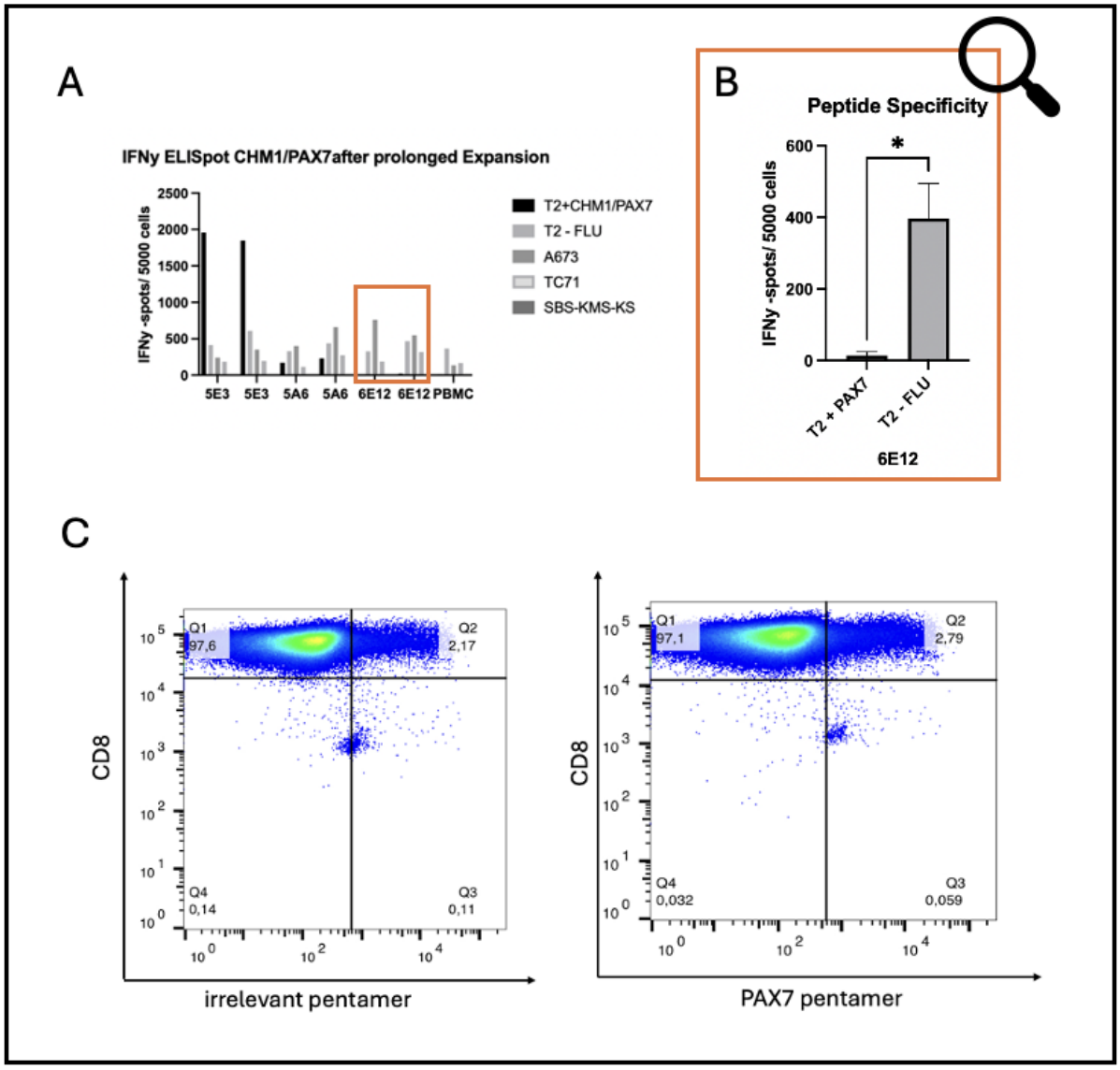

Figure 7 IFNy ELISpot and FACS analysis of T-cell clone 6E12 show little remaining PAX7-peptide-specificity and many non-viable cells. *(A, B) PAX7- (& CHM1) specific T cell clones were tested again in IFNy ELIspots for peptide specificity, HLA-A*0201 restriction, and their ability to identify EwS cell lines after a prolonged culture time. PAX7- (& CHM1-) pulsed T2 cells served as the positive control, while FLU-pulsed T2 cells served as the negative control for peptide specificity. EwS cell lines A673 and TC71: HLA-A*0201+ EwS served as a positive control, while SB-KMS-KS: HLA-A*0201- EwS was used as a negative control regarding HLA-A*0201 restriction. (C) T cells were stained with specific PAX7-PE-pentamer and FITC CD8, pictured on the right, and with an unspecific CHM1-PE-multimer and FITC CD8 as control, pictured on the left. (Error bars indicate the standard deviation of a duplicate, * p <0,0332)*

The peptide specificity suggested in the conducted ELISpots could not be replicated, neither in an additional ELISpot assay, which showed barely any recognition of PAX7-pulsed T2 cells, nor in a FACS analysis, as no significant difference between the relevant (PAX7) and irrelevant (CHM1) staining could be identified. Furthermore, a large amount of cell debris or non-viable cells was observed.

As a result, further investigation of this clone was halted. Attempts to generate another promising PAX7 clone were unsuccessful. However, the initial ELISpot results suggest potential for future efforts, particularly with approaches like scRNAseq that may reduce cultivation time and minimize cell death and overgrowth.

5.3 GPR64

GPR64, which is involved in tumor progression and metastasis, was also investigated. It is over-expressed in several cancers, including Ewing sarcoma. (Richter et al., 2013; Schirmer et al., 2018)

5.3.1 Background

Previously, GPR64-862-specific clones were generated in our laboratory, but a TCR was never isolated, and no clone was preserved. Therefore, a new attempt to generate a GPR64-862-specific clone was initiated. Our group previously identified the target peptide, GPR64-862.

5.3.2 Generation of GPR64 specific T-Cell Clones

To generate allo-restricted, GPR64-specific, cytotoxic T cells, CD8+ HLA-A*0201 + T cells were co-cultured with GPR64-862-pulsed DCs for 14 days.

The DCs' maturation status was always checked before adding the adjusted amount, depending on the percentage of mature DCs. DCs were considered mature when positive for CD83, CD86, and HLA-DR (see Figure 4, equivalent to PAX7-generation).

After 14 days, the CD8+ HLA-A2*0201 + T cells were stained with CD8 and the GPR64-multimer. Typically, 2 x 10^7 cells were used. Double-positive cells were sorted at the Institute for Medical Microbiology, Immunology and Hygiene, Technical University Munich, Germany (exemplary see Figure 8 A). Subsequently, they were expanded using limiting dilution (see Chapter 4.3.8).

After two weeks of expansion (see Chapter 4.3.8), the T cells were tested in screening ELISpots for their target recognition. Cell populations for the screening ELISpot were selected based on their growth pattern, characterized by a dense crown on the bottom of the wells (see Figure 5, equivalent to PAX7-generation).

One such screening ELISpot, containing the most promising clones, can be found in Figure 8 B.

Clones were selected depending on their ability to identify the positive control - T2 cells pulsed with the GPR64-peptide. Furthermore, the non-recognition of the negative control - T2 cells pulsed with a FLU peptide, was considered.

Promising clones identified in the screening ELISpot were then further expanded (see Chapter 4.3.9). Figure 8 C, D, and E shows the results of the confirmation ELISpot for the most promising clone, C520.

Clone C520 demonstrated good recognition of the positive control, indicating peptide specificity. However, it did not recognize Ewing sarcoma cancer cell lines better than the negative control. Despite this, the HLA-A*0201+ A673 and TC71 tumor cell lines were better identified than the HLA-A*0201- SB-KMS-KS cell line, suggesting potential HLA-A*0201 restriction.

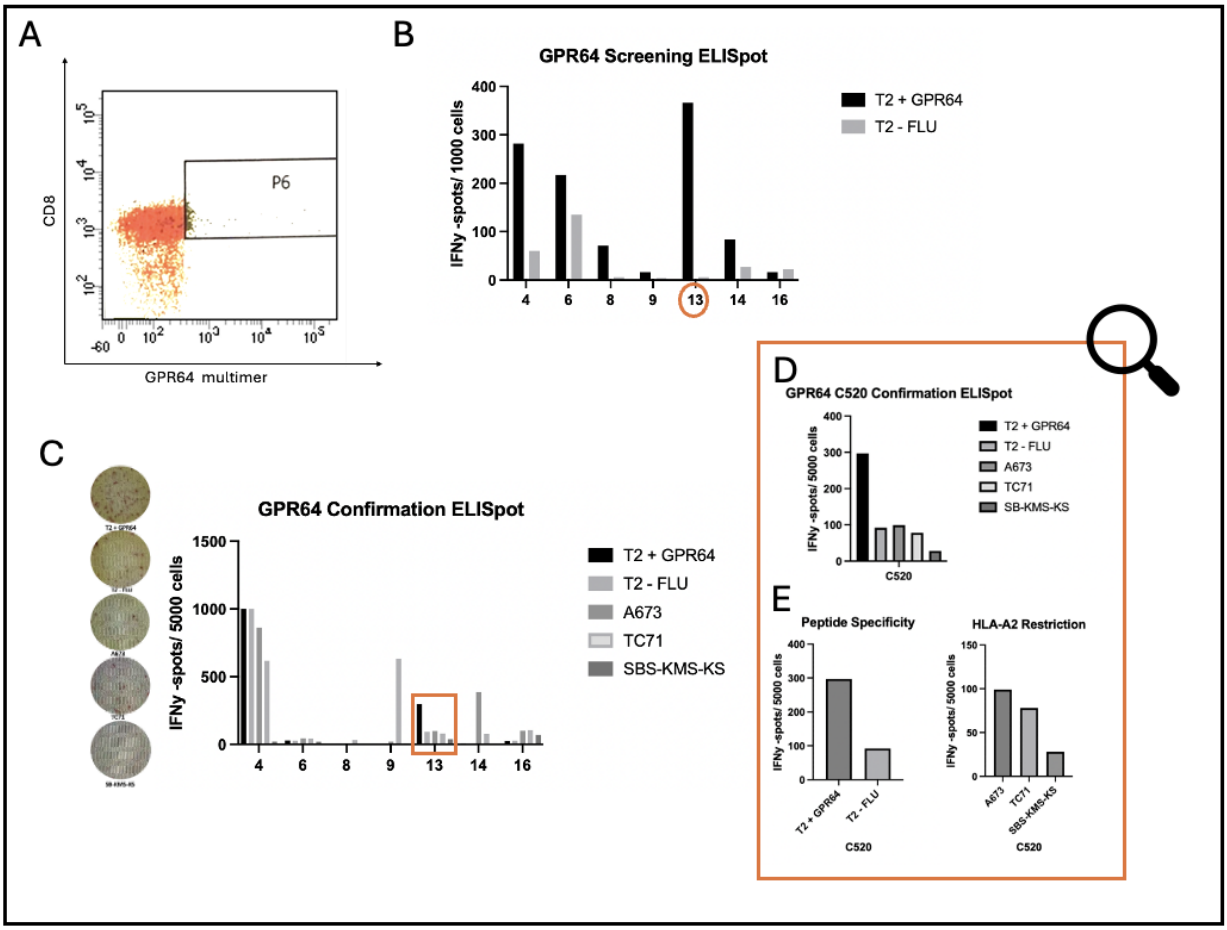

Figure 8 GPR64 T cell-sorting – identified GPR64 clone C520 recognized GPR64-loaded T2 cells and HLA-A*0201 positive cell lines in IFNγ ELISpot. *(A) In vitro primed CD8 + T cells were stained for FITC CD8 and PE Pentamer/Multimer. Double-positive cells were gated (P6) and subsequently sorted. (B,C,D,E) After the limiting dilution process, the T cell clones were tested for peptide specificity, HLA-A*0201 restriction, and their ability to*

*identify EwS cell lines in IFNy ELISpots. GPR64-pulsed T2 cells served as the positive control, while FLU-pulsed T2 cells served as the negative control for peptide specificity. EwS cell lines A673 and TC71: HLA-A*0201+ EwS served as a positive control, while SB-KMS-KS: HLA-A*0201- EwS, was used as a negative control HLA-A*0201 restriction. Clones eliminated after the screening ELISpot not shown.*

Due to slow growth, a FACS analysis was not performed to ensure sufficient cells for RNA isolation.

5.3.3 Identification of TCR Chains

RNA was isolated (see Chapter 4.5.1) and transcribed into cDNA (see Chapter 4.5.2). Gel electrophoresis was performed to identify the relevant Vα and Vβ chains for a potential TCR.

Specific bands were found at a height of 300 to 500 bp. The results are shown in Figure 9.

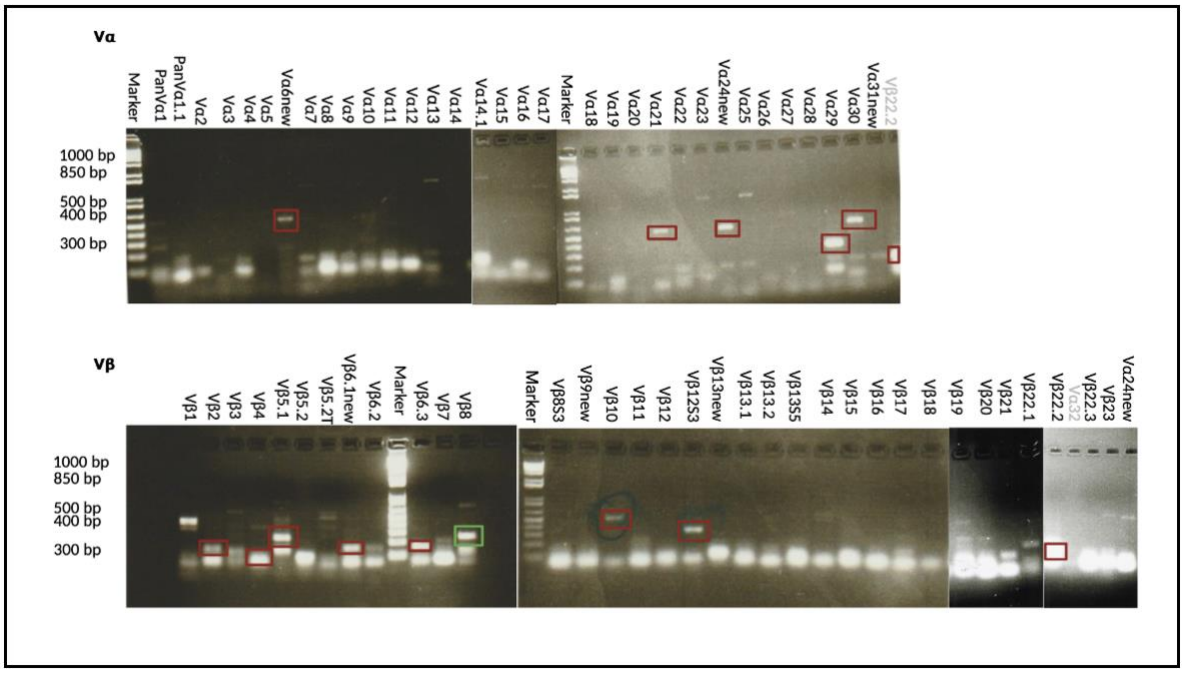

***Figure 9 TCR PCR identifies several PCR products representing potential Vα & Vβ chains for the identification of the GPR64-862 TCR sequence**. Different primers were used to amplify the expressed alpha- and beta-chains in the GPR64 clone. Bands between 500 – 300 bp (red boxes) were cut and sent for sequencing. The green box refers to the primer, that identified a TCR chain. Green boxes represent a successfully sequenced chain.*

The bands representing potentially promising sequences (red boxes) were cut from the gel and sent for sequencing.

The analysis at Sequiserve in Vaterstetten and a comparison with the BLAST and the ORFfinder identified only one Vβ chain. The BLAST results corresponding to the relevant primers containing the complete sequences and analysis, identifying the sequences as α- and ß-chains of TCRs can be found in Appendix 2.

The relevant primer, Vβ8, can be found in Table 20.

Table 20 *Vß8 was identified as the relevant primer for the Vß-chain.*

Primer	Primer-Sequence
Vβ8	ATT TAC TTT AAC AAC AAC GTT CCG

Attempts to generate a different GPR64 clone have not yet been successful. Future efforts using techniques like scRNAseq, which allow for shorter cultivation times, may reduce cell death and overgrowth, thereby increasing the chances of successful clone generation.

5.4 CHM1

CHM1 mediates metastasis in Ewing Sarcoma, especially into the lung. It is a downstream target of EWS-FLI1. (Blaeschke et al., 2016; Charville et al., 2017; U. Thiel et al., 2011; von Heyking et al., 2017)

5.4.1 Background

CHM1 is a promising target due to its already successful experimental use in patients (Thiel et al., 2017). Generating a new CHM1 clone could expand the available TCR options for patient treatment and potentially shed light on the issues encountered with the other targets in this thesis.

An *in silico* analysis (see Chapter 4.2.1) identified suitable CHM1 peptides that could be processed within cells and presented via HLA-A*0201. Table 21 lists six interesting peptides with the highest predicted binding strength: CHM1 47, CHM1 10, CHM1 54, CHM1 34, CHM1 45, and CHM1 77. Importantly, no cross-reactivity was observed. These peptides were selected for further evaluation and commissioned.

Table 21 In silico prediction of binding scores & cross-reactivity identifies 6 CHM1 nonamers (using SYFPEITHY & ScanProsite). *CHM1-peptides were tested in silico using SYFPEITHY & ScanProsite for a high binding score and no hits in the cross-reactivity test. Six promising peptides were chosen for further evaluation. Table was sorted by binding score in descending order.*

Position	Sequence	Score (SYFPEITHI)	Hits (Cross-reactivity)
47	LISGAVLLL	27	no hit
10	IALVGPDDV	20	no hit
54	LLFGAIGAF	20	no hit
34	SSPARLLKV	19	no hit
45	VVLISGAVL	19	no hit
77	YTMSINGKL	19	no hit

5.4.2 CHM1 Binding Assay

A T2/HLA-A*0201 peptide binding assay was performed (see Chapter 4.2.2) to analyze the binding properties of the six peptides compared to an influenza peptide (GILFGFVFTL). None of the peptides showed promising binding properties - except for CHM1 319, the established nonamer previously used in our laboratory to discover a TCR and successfully create a transgenic T cell (Blaeschke et al., 2016; U. Thiel et al., 2011). For CHM1 319, binding properties were comparable to FLU and increased with an increased peptide concentration. The results can be found in Figure 10.

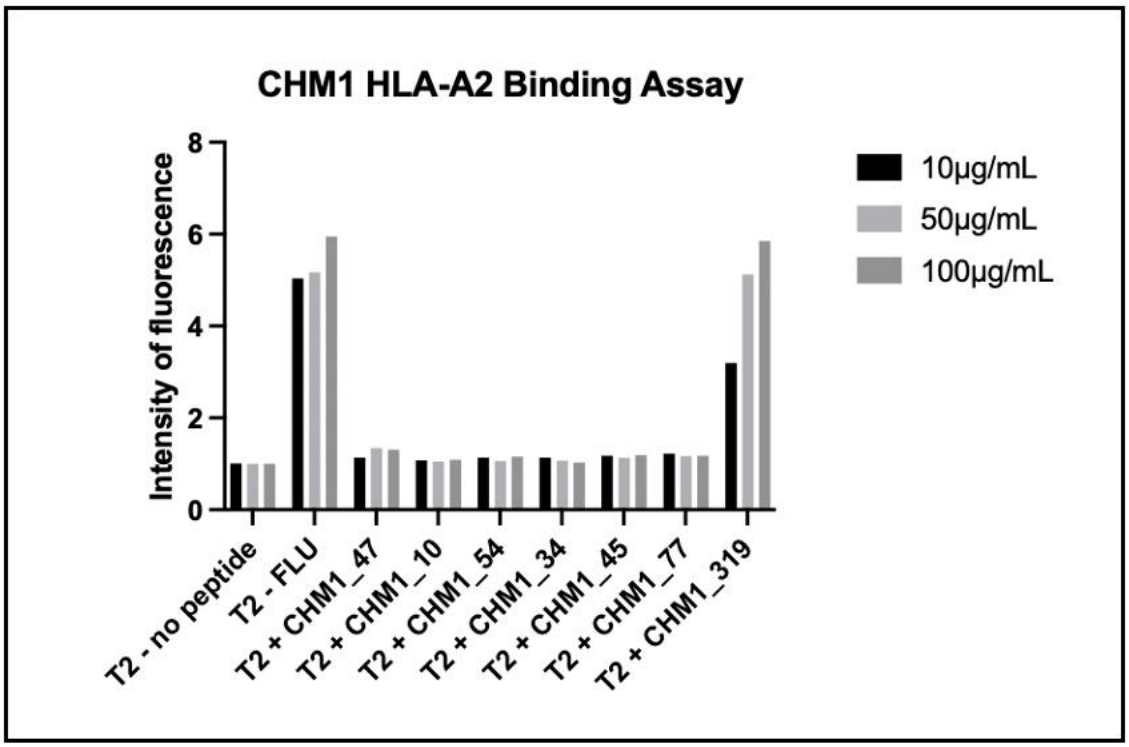

Figure 10 HLA-A2 Binding Assay via FACS analysis confirms only CHM1 319 as a good binding peptide. *Nonamers identified in in silico testing were tested for their HLA-A2*0201 binding capacities. The fluorescence intensity in comparison e to FLU (positive control) and an intensity increase associated with a higher peptide concentration were evaluated.*

Work began to generate another clone targeting the known CHM1 nonamer (VIMPCSWWV), aiming to establish a "clone library" with varying TCR characteristics for patient treatment, for example, regarding affinity to the target. Furthermore, the nonamer could function as a positive control, especially considering the multiple failures regarding the generation of a PAX7-specific and subsequent sequencing of the TCR.

5.4.3 Generation of CHM1-specific T cell clones

To generate allo-restricted, CHM1 319-specific cytotoxic T cells, CD8+ HLA-A*0201+ T cells were co-cultured with CHM1 319-pulsed DCs for 14 days. The maturation status of DCs was confirmed by CD83, CD86, and HLA-DR markers (see Figure 4, equivalent to PAX7-generation).

After 14 days, the CD8+ HLA-A2*0201 + T cells were stained with CD8 and the CHM1 multimer, the unlabeled Pro5 R MHC class I Pentamers specific for CHM1 and made visible by the Pro5 Fluorotag R-PE, or the labeled Pro5 R MHC class I Pentamer specific for CHM1. Typically, 2 x 10^7 cells were used. Double-positive cells were sorted at the Institute for Medical Microbiology, Immunology, and Hygiene, Technical University Munich, Germany (exemplary see Figure 11 A). Subsequently, they were expanded using limiting dilution (see Chapter 4.3.8).

Again, several runs were conducted to increase the likelihood of identifying promising cells, adjusting different variables. For example, various colors (APC vs. PE) and multimers (CD8 vs. CD3 and CD4) were used for staining to avoid potential interference with the peptide-specific multimer. Furthermore, a labeled Pro5 R MHC class I Pentamer and then an unlabeled Pro5 R MHC class I Pentamer were tested, in contrast to the previously used multimer, hoping for better binding properties. Moreover, HLA-A*0201+ blood from a known young donor was used instead of Buffy coats from unknown donors to increase the probability of selecting young, vital cells.

After two weeks of expansion (see Chapter 4.3.8), the T-cells were tested in screening ELISpots for their target recognition (see Figure 11 B). Cell populations for the screening ELISpot were selected based on their growth pattern, characterized by a dense crown on the bottom of the wells (see Figure 5, equivalent to PAX7-generation).

Clones were selected depending on their ability to identify the positive control, T2 cells pulsed with the CHM1-peptide. Furthermore, the non-recognition of the negative control, T2 cells pulsed with a FLU-peptide, was considered. CHM1 clone 5E3 showed the best recognition of loaded T2 cells and very little cross-reactivity (T2-FLU).

Promising clones identified in the screening ELISpot were then further expanded (see Chapter 4.3.9). The results of the confirmation ELISpot of the most promising clone, namely 5E3, can be found in Figure 11 C and D.

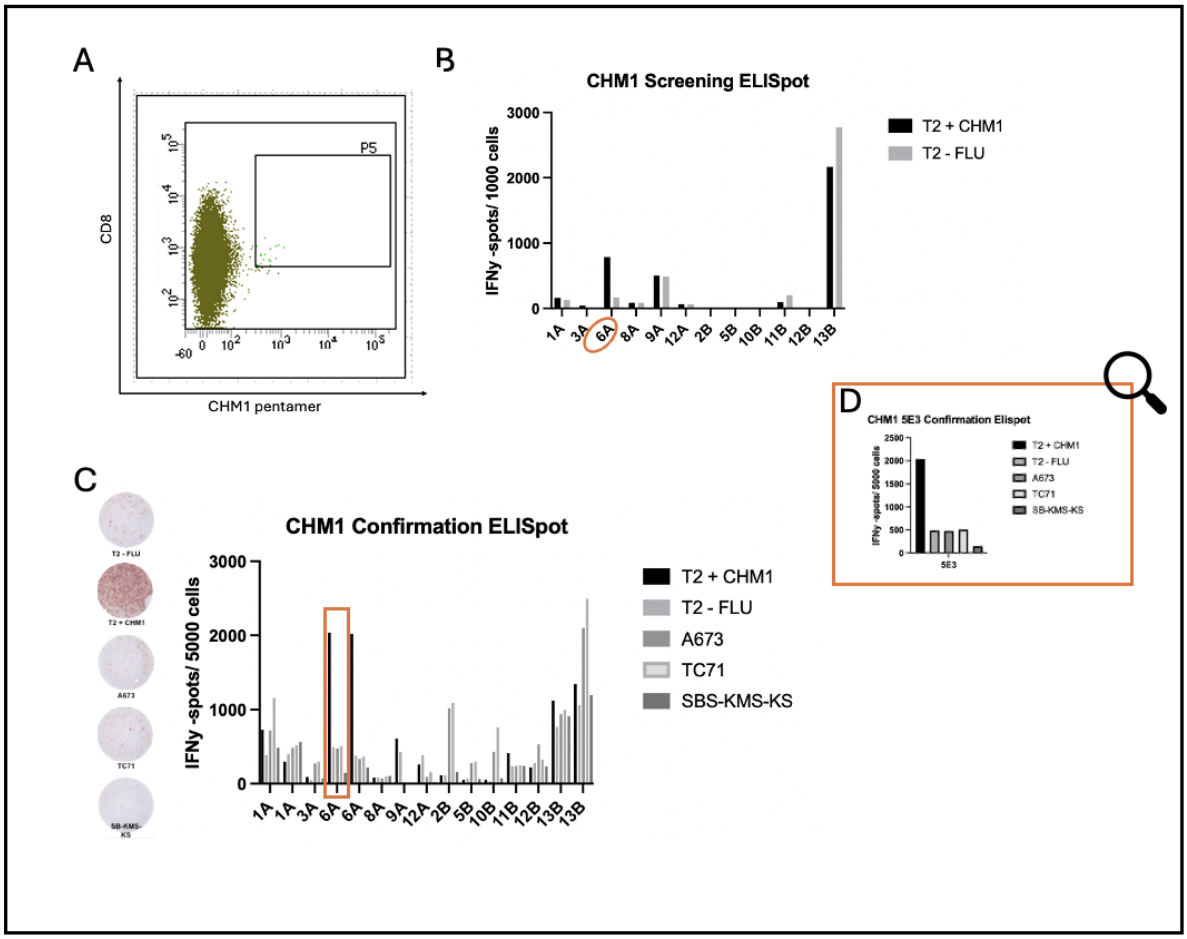

Figure 11 CHM1 T cell-sorting – identified CHM1 clone 5E3 recognized CHM1-loaded T2 cells and HLA-A*0201 positive cell lines to some extent in IFNγ ELISpot. *(A) In vitro primed CD8 + T cells were stained for FITC CD8 and PE Pentamer/Multimer. Double-positive cells were gated (P5) and subsequently sorted. (B, C, D) After the limiting dilution process, the T cell clones were tested again for peptide specificity, HLA-A*0201 restriction, and their ability to identify EwS cell lines in IFNγ ELISpots. GPR64-pulsed T2 cells served as the positive control, while FLU-pulsed T2 cells served as the negative control for peptide specificity. EwS cell lines A673 and TC71: HLA-A*0201+ EwS served as a positive control, while SB-KMS-KS: HLA-A*0201- EwS, was used as a negative control regarding HLA-A*0201 restriction. Clones eliminated after the screening ELISpot not shown.*

Clone 5E3 demonstrated good recognition of the positive control, indicating peptide specificity. However, it did not recognize Ewing sarcoma cancer cell lines better than the negative control. Despite this, the HLA-A*0201+ A673 and TC71 tumor cell lines were better identified than the HLA-A*0201- SB-KMS-KS cell line, suggesting potential HLA-A*0201 restriction. Based on these findings, this clone was chosen for further investigation and expansion.

A FACS analysis was performed (see Figure 12 C). It showed a partial CD8+ T cell population shift, suggesting a CHM1-peptide specificity. An unspecific HLA-A*0201-multimer, PAX7, served as the negative control. Additionally, the FACS

analysis also showed some non-viable cells. Another IFNy ELISpots after a prolonged expansion period confirmed the peptide specificity for CHM1, the EwS cell line recognition, and HLA-A*0201 restriction (see Figure 12 A and B).

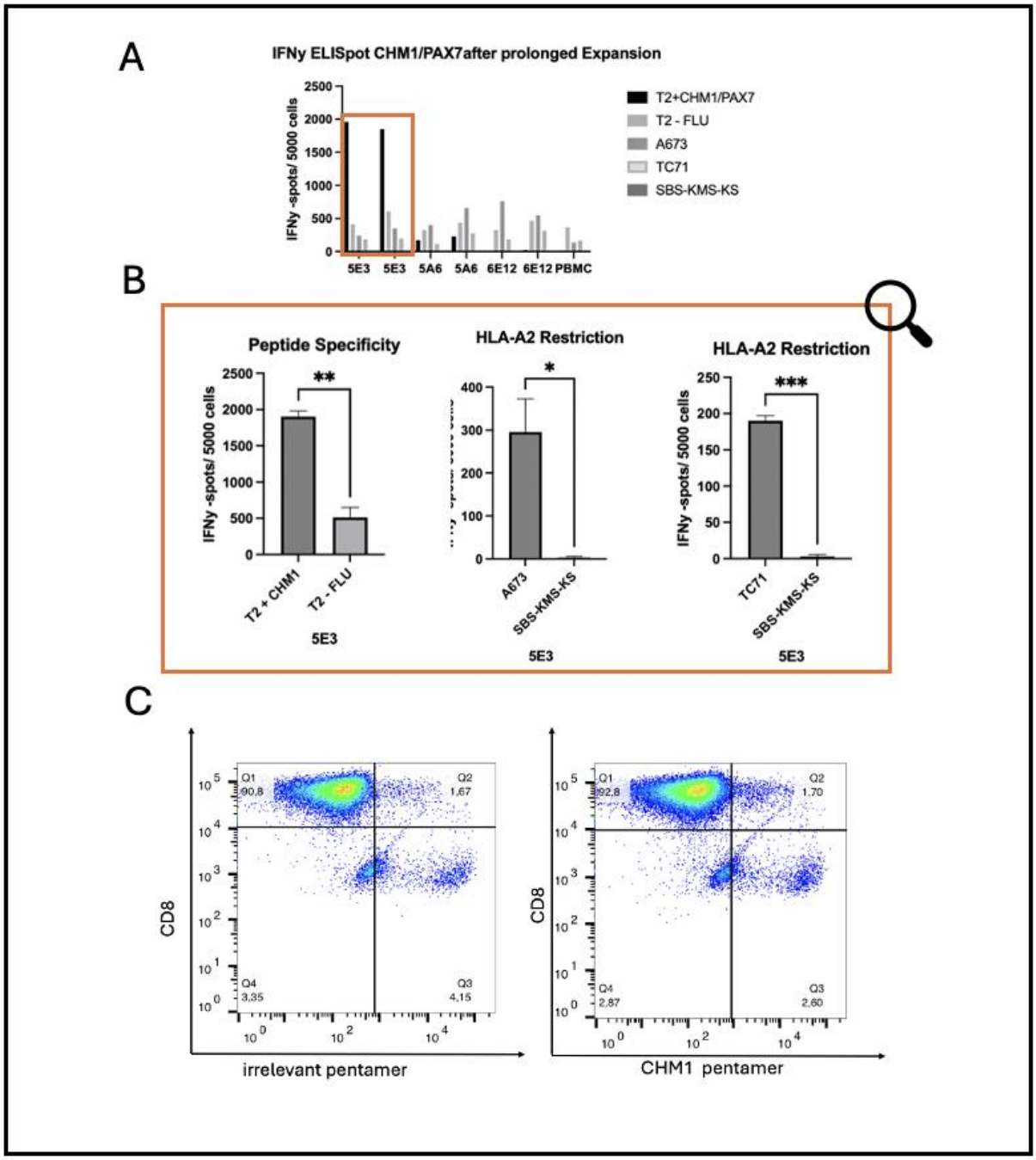

Figure 12 FACS analysis, depicting a partial shift of CD8+ T-cell population, and IFNy ELISpot of CHM1-specific T cell clone 5E3 confirm peptide-specificity and HLA-A*0201 restriction. *(A,B) CHM1- (&PAX7) specific T cell clones were tested again in IFNy ELIspots for peptide specificity, HLA-A*0201 restriction, and their ability to identify EwS cell lines after a prolonged culture time. CHM1- (& PAX7-) pulsed T2 cells served as the positive control, while FLU-pulsed T2 cells served as the negative control for peptide specificity. EwS cell lines A673 and TC71: HLA-A*0201+ EwS served as a positive control, while SB-KMS-KS: HLA-A*0201- EwS was used as a negative control regarding HLA-A*0201 restriction. (C) T cells were stained with specific CHM1-PE-pentamer*

*and FITC CD8, pictured on the right, and with an unspecific PAX7-PE-pentamer and FITC CD8 as control, pictured on the left. (Error bars indicate the standard deviation of a duplicate, * p <0,0332, ** p<0,0021, ***p<0,0002)*

5.4.4 Identification of TCR Chains

RNA was isolated (see Chapter 4.5.1) and transcribed into cDNA (see Chapter 4.5.2). Gel electrophoresis was performed to identify the relevant Vα and Vβ chains for a potential TCR.

Specific bands were found at a height of 300 to 500 bp. The results can be found in Figure 13.

The bands representing potentially promising sequences (red boxes) were cut from the gel and sent for sequencing.

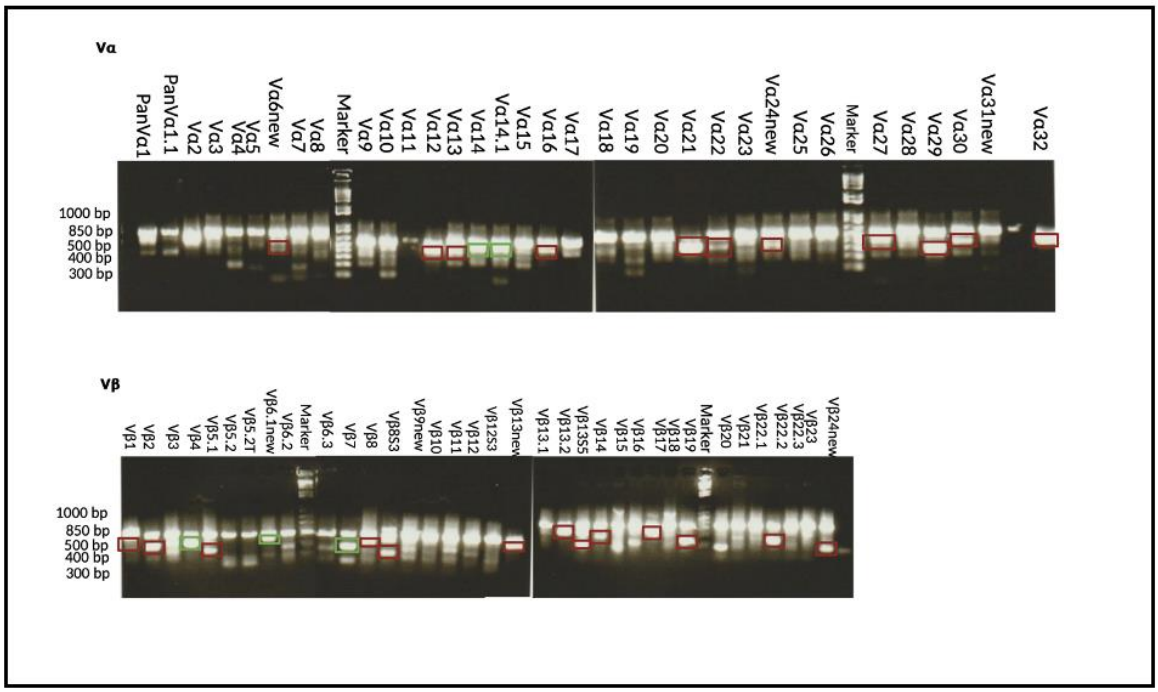

Figure 13 TCR PCR identifies several PCR products representing potential Vα & Vβ chains for the identification of the CHM1-319 TCR sequence*. To amplify the expressed alpha- and beta-chains in the CHM1 clone, different primers were used. Bands between 500 – 300 bp (red boxes) were cut and sent for sequencing. Green boxes refer to the primers that identified a TCR chain. Green boxes represent a successfully sequenced chain.*

The analysis at Sequiserve in Vaterstetten as well as a comparison with the BLAST and the ORFfinder identified 2 Vα -chains and 3 Vβ-chains, suggesting a lack of monoclonality in the sample.

The BLAST results corresponding to the relevant primers containing the complete sequences and analysis, identifying the sequences as α- and ß-chains of TCRs can be found in Appendix 3. The relevant primers can be found in Table 22.

Table 22 *Relevant primers identified for a possible TCR.*

Primer	Primer-Sequence
Vα14.1	CAG TCC CAG CCA GAG ATG TC
Vα14	CAG TCT CAA CCA GAG ATG TC
Vβ4	ACA TAT GAG AGT GGA TTT GTC ATT
Vβ6.1new	GCC CAG AGT TTC TGA CTT ACT TC
Vβ7	CCT GAA TGC CCC AAC AGC TCT C

5.5 Single Cell RNA Sequencing

To compare and verify the sequences found for GPR64 and CHM1 and asses the possibility of doing future experiments with a different approach, a sample of CHM1 5E3 and GPR64 C520 was also sequenced using single-cell RNA sequencing with the help of Sabrina Wagner from the German Cancer Consortium in the Institute for Medical Microbiology, Immunology and Hygiene of the Technical University Munich.

For GPR64, no full TCR sequence was identified either. After sample preparation, there was only one GPR64 cell detectable, and it proved negative for CD8 and CD3 and therefore considered irrelevant (see Figure 14).

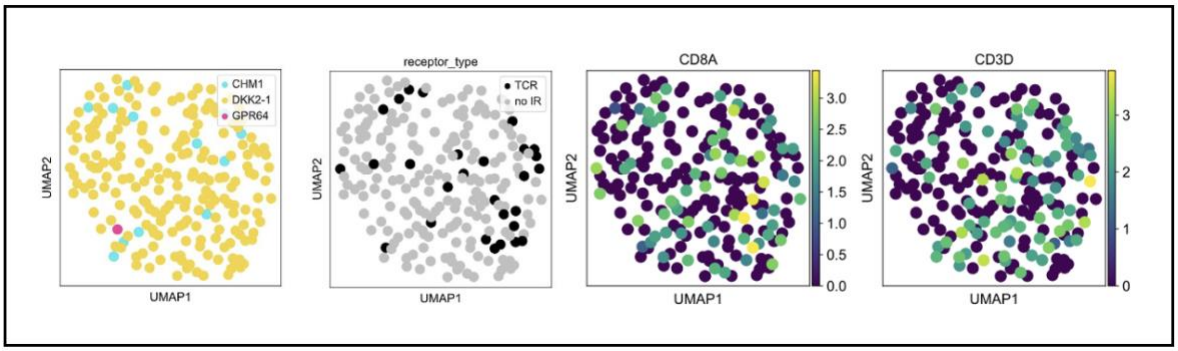

Figure 14 scRNAseq identifies CHM1-CD8-positive T-cell clones. *T cells in the sample were tested for TCR expression and T cell markers. TCR+ (black), CD8A+, and CD3D+ cells could be found in the samples for CHM1 (turquoise). Only one GPR64+ cell (pink) was found, negative for TCR-, CD8-, and CD3-. The identified CHM1-*

specific cells (turquoise) were sequenced (Figure from Sabrina Wagner, German Cancer Consortium in the Institute for Medical Microbiology, Immunology and Hygiene of the Technical University Munich).

For CHM1, an α- and ß-chain corresponding to one cell could be identified. The result can be found in Table 23.

Table 23 A full TCR could be identified via scRNAseq targeting CHM1, highlighted in red. *The black sequences show another target (DKK2) that was also investigated by our group and tested in the same experiment.*

Clone ID	Clone size	Sample name	Alpha V chain	Alpha J chain	CDR3 region alpha chain	Beta V chain	Beta J chain	CDR3 region beta chain
0	17	DKK2-1	TRAV20	TRAJ13	CAVQAASGGYQKVTF	TRBV7-9	TRBJ2-1	CASSFYNEQFF
1	8	DKK2-1	nan	nan	nan	TRBV7-9	TRBJ2-1	CASSFYNEQFF
2	2	DKK2-1	TRAV20	TRAJ13	CAVQAASGGYQKVTF	nan	nan	nan
3	1	CHM1	TRAV25	TRAJ20	CARLPWNDYKLSF	TRBV6-2	TRBJ2-7	CASSQLGHYEQYF

This analysis shows yet another TCR sequence distinct from those found with the traditional method. Nevertheless, the nature of scRNAseq, which sequences only one cell at a time and groups them, suggests that this is a full TCR, meaning there is no mispairing between alpha—and beta-chains and that, at least in this sample, there was only one clone with only one TCR.

This sequence can now be used for the generation of transgenic T cells presenting the identified TCR. This is now being done in our laboratory using retroviral transduction as well as CRISPR/Cas9. While it was not yet possible to identify TCRs for LIPI, GPR64, and PAX7, this study has successfully identified a TCR targeting an Ewing sarcoma-specific antigen, namely CHM1, which is essential for tumor metastasis and/or tumor survival. This is a vital step in the process of creating TCR transgenic T cells. Furthermore, introducing scRNAseq in the process helps streamline future attempts.

6 Discussion

6.1 The Current Treatment

Through the introduction of a multimodal therapy regime, which includes a combination of chemotherapy, surgery, and radiation, progress has been made over the last decades. Yet, Ewing Sarcoma still remains a therapeutical challenge. Survival rates for patients with localized disease are plateauing at 70-80%, while survival rates for patients with advanced disease are far worse at <30%. Moreover, the treatments are associated with severe toxicities, highlighting the need for better and less toxic treatment options. (Balamuth & Womer, 2010; Grünewald et al., 2018; Hesla et al., 2021; Zöllner et al., 2021)

To reiterate, patients are usually included in clinical trials for treatment. The most common treatment protocols focus on multiagent chemotherapy, including agents like vincristine, doxorubicin, cyclophosphamide, ifosfamide, and etoposide (see 1.1.6). (Anderton et al., 2020; Bernstein et al., 2006; Hesla et al., 2021)

In advanced or relapsed cases, auto-SCT or allo-SCT in combination with high-dose chemotherapy in different constellations has been tested as a treatment option. While some studies have reported improved outcomes in relapsed or refractory patients and a possible Graft versus Tumor effect, the success rate differs, and event-free long-term survival remains a challenge, especially considering the accompanying toxicities. (Bernstein et al., 2006; Burdach et al., 2000; U. Thiel et al., 2011; U Thiel et al., 2011)

The other treatment pillars also have complications, which can be separated into acute and late effects. (Grünewald et al., 2018)

The effects of chemotherapy can further be divided into more general and agent-dependent side effects. Anthracyclines such as doxorubicin are known to be cardiotoxic. Alkylating agents, such as cyclophosphamide and ifosfamide, are also associated. Moreover, they are associated with infertility, which is especially important and life-altering, as patients are usually young, and family planning is still in their future. (Bernstein et al., 2006; Hudson, 2010; Simbre et al., 2005) In the short term, chemotherapy can induce nausea, vomiting, and most agents commonly used in treatment regimens have at least a moderate to high emetogenic potential. An

increased infection risk due to myelosuppression, which usually limits agent dosage, is well documented. (Friberg et al., 2002; Grünewald et al., 2018; Hesketh, 2008)

Both radiation and chemotherapy can cause secondary malignancies. Occurrences of secondary malignancies have been well documented for EwS-long-term survivors, with Caruso et al. (2019) listing incidences of up to 20,5% after 30 years. Solid tumors, especially osteosarcoma, were the most common, while leukemia presented the largest entity. (Bernstein et al., 2006; Caruso et al., 2019; Fuchs et al., 2003; Grünewald et al., 2018; Paulino & Fowler, 2005) Radiation can further damage the surrounding tissue and cause pulmonary fibrosis and growth impairment in pediatric patients. (Fuchs et al., 2003; Grünewald et al., 2018; Hesla et al., 2021; Zöllner et al., 2021) Bone healing problems, fractures, and infection risks accompany surgery. Especially, endoprostheses in limb-sparing surgeries carry risks like loosening, mechanical failure, and periprosthetic infections. (Hardes et al., 2010; Hesla et al., 2021; Zöllner et al., 2021) The main complication in allo-SCT is GvHD, which is when the donor cells attack the recipient's tissues. It can lead to severe complications, including death, as well as long-term complications, such as non-malignant organ dysfunction and a loss of quality of life. Infections are not only a cause of morbidity but also mortality, caused by neutropenia and a diminished T-cell response even more than a year after engraftment. This is further exacerbated by the clinically needed immunosupression. (Burdach et al., 2000; DANIEL KELLY BENJAMIN et al., 2002; Mohty & Mohty, 2011; Ruutu et al., 2012)

To sum it up, patients suffering from advanced Ewing sarcoma still have poor outcomes, while the adverse effects of current treatments are substantial. Therefore, future research is required to develop safer and more effective treatment strategies, leading to better patient outcomes and general improvement in the quality of life.

As mentioned in the introduction, adoptive T Cell therapy could be a possible approach. Especially, considering that while allo-SCT has not been able to achieve a breakthrough in advanced EwS-treatment, its tentatively described effects indicate that other immunotherapeutic approaches may be worth pursuing. Immunotherapy, including targeted therapy, in general, has revolutionized cancer treatment and has shown promising results across various cancer types. Adoptive cell therapy, in particular, includes TIL, TCR-T Therapy, and CAR-T Therapy, which leverage the immune system to target and eliminate cancer cells. More targeted approaches like

TCR T cell therapy, might even be able to separate the unwanted Graft versus Host-effect from the wanted Graft-versus-Tumor effect in an allogenic setting. (Blaeschke et al., 2016; Nicholson et al., 2012; Rohaan et al., 2019)

In light of this, in this thesis, I aimed to identify specific TCRs that can be utilized for adoptive transfer treating Ewing Sarcoma.

But why might the TCR Therapy approach be better than CAR-T Therapy for the treatment of Ewing Sarcoma?

6.2 CAR-T Therapy and TCR Therapy

CARs were developed as monoclonal antibodies plus intracellular T-cell activation domains. (Leko & Rosenberg, 2020) This informs their structure as a synthetic receptor with an extracellular antigen-binding domain, a hinge region, a transmembrane domain, and an intracellular signaling domain. (Sterner & Sterner, 2021)

Based on antibodies, CARs can identify surface antigens without relying on MHC molecules for antigen presentation. (Sterner & Sterner, 2021) While limited to extracellular antigens, CARs are also able to recognize non-proteins like carbohydrates or glycolipids. (June et al., 2018; Sadelain et al., 2009)

CARs have proven successful in treating hematologic malignancies, such as B-cell leukemia or lymphoma. (Huang et al., 2020; Sterner & Sterner, 2021) Maude et al. (2014) were able to produce high remission rates in relapsed and refractory ALL patients. Porter et al. (2011) treated CLL patients with CART19 infusions, resulting in remissions that were sustained for at least ten months. (Maude et al., 2014; Porter et al., 2011) These and other reports of remarkable clinical outcomes and long-term survival in patients' bodies established CAR-T cells as “living drugs” and a powerful therapeutic option, although low persistence of CAR-T cells has also been reported. (Huang et al., 2020; Mohanty et al., 2019)

One of the major advantages of CAR-T therapy is the MHC-independent T-cell activation. (June et al., 2018; Sterner & Sterner, 2021)

This makes CAR-T therapy suitable for a broader spectrum of patients, irrespective of their HLA type and genetic backgrounds. (Baulu et al., 2023; Shafer et al., 2022; Wachsmann et al., 2022)

Moreover, CARs are highly potent effector cells, killing efficiently and producing cytokines abundantly, at least in the short term. However, in situations of continuing or large quantities of antigen, CAR-T cells run the risk of activation-induced cell death. Engineered TCR T-cells, on the other hand, are able to retain a central memory pool. (Wachsmann et al., 2022)

CAR-T therapy also has other limitations. The fact that CAR-T cells can only target surface antigens is one of them. Therefore, their application is limited to cases where such antigens are present. Many tumors, especially solid or pediatric tumors, may not express suitable antigens or if they do only in a very heterogeneous manner. (Baulu et al., 2023; Greenbaum et al., 2021; Gröbner et al., 2018; Marofi et al., 2021; Shafer et al., 2022)

Antigen escape is another issue for CAR-T therapy. Tumors can fully or partially lose antigens, especially targeted during treatment rendering it ineffective. (Sterner & Sterner, 2021) However, this is also true for TCR Therapy, but maybe to a lesser extent, as T cells theoretically only need one antigen to elicit a response, whereas CARs need many. (Shafer et al., 2022) However, CAR-T cells, being MHC-independent, do not run the risk of the loss of MHC-associated antigen presentation through MHC-class I downregulation, a main mechanism of immune escape. (Garrido et al., 2017; June et al., 2018; Muenst et al., 2016; Seliger, 2005)

The immunosuppressive environment of solid tumors and problematic tumor infiltration also pose a substantial hurdle for both CAR-T therapy and TCR therapy. (Greenbaum et al., 2021; Marofi et al., 2021; Shafer et al., 2022; Sterner & Sterner, 2021; Wei et al., 2022)

Additionally, CAR-T therapy can cause severe side effects and toxicities. Cytokine release syndrome, CRS, caused by a massive cytokine release of the CAR-T cells, can manifest as an influenza-like syndrome with fever or even organ dysfunction and death. (June et al., 2018; Neelapu et al., 2018; Sterner & Sterner, 2021) Neurotoxicity is also a common occurrence with patients developing seizures, delirium, cerebral edema, or hemorrhage. (June et al., 2018; Neelapu et al., 2018; Sterner & Sterner, 2021)

For TCR-T Therapy, T cells can also be engineered to express a TCR capable of identifying a specific antigen. (Shafer et al., 2022) Similar to natural T cells, a TCR alpha- and beta chain are introduced into the T cell and facilitate the desired specificity together with the endogenous CD3 complex. (Shafer et al., 2022)

As indicated above, in contrast to CAR T-cells, TCR T-cells can only detect antigens that have been processed and are being presented by MHC molecules. (Shafer et al., 2022) However, the MHC presentation makes it possible for TCR T-cells to also recognize intracellular antigens. (Baulu et al., 2023; Shafer et al., 2022) In the case of Ewing Sarcoma, given that it is a solid tumor with a low mutation burden characterized by an intracellular fusion protein EWS-FLI1, this seems to be an advantage. (Crompton et al., 2014; Gröbner et al., 2018)

TCR T cells are highly sensitive towards their target antigen. They are 100 times more sensitive to their specific antigen than CAR-T cells, meaning a lower antigen density is enough to elicit a response. (Baulu et al., 2023; Salter et al., 2021; Shafer et al., 2022; Wachsmann et al., 2022) Furthermore, being MHC-dependent, TCR T cells engage more natural signaling pathways, possibly resulting in better tumor detection and killing while elevating T cell persistence. (Baulu et al., 2023; Wu et al., 2020)

In conclusion, TCRs seem to be the better choice for a solid tumor like Ewing Sarcoma. This is due to TCR-T cells' ability to recognize intracellular and extracellular antigens, allowing for targeting a broader range of antigens, their greater sensitivity to their target epitope, especially in situations with lower antigen concentrations, a potentially more physiological downstream signalling that may prevent exhaustion and drive survival and a reduced risk of CRS. (Baulu et al., 2023; Chruściel et al., 2020; Shafer et al., 2022; Wei et al., 2022)

6.3 Target Selection

With TCR Therapy as the chosen approach, suitable targets have to be selected. Targets with constant, high expression should be preferred to ensure that the TCRs can efficiently and sustainably recognize and eliminate cancer cells. Tumor biology and the role the targets play in it need also be considered; targets involved in essential pathways for tumor growth, survival, and metastasis are prioritized, as they

will most likely impact tumor progression and, therefore, influence the development of the disease. Of particular interest in this context are driver mutations, especially if they are shared by patients and homogenously expressed. (Leko & Rosenberg, 2020; Rath & Arber, 2020; Shafer et al., 2022; Thiel et al., 2017)

Another key factor is the specificity of the target antigen. Targets with minimal expression in normal tissues should be selected to reduce the risk of off-tumor on-target effects and toxicity. TCRs specific for the antigen will optimally only target cancer cells, minimizing the damage to healthy tissues and the risk of GvHD frequently experienced in allo-SCT. (Hinrichs & Restifo, 2013; Leko & Rosenberg, 2020; Rath & Arber, 2020; Shafer et al., 2022; U. Thiel et al., 2011)

To give an example, CHM1 is overexpressed in Ewing Sarcoma cells. Furthermore, CHM1 is involved in metastasis. Disrupting it could impact important biological processes that support tumor spread, especially lung metastasis, and, therefore, influence the progress of the disease. Moreover, the limited expression of CHM1 in normal tissues reduces the risk of “on-target, off-tumor” effects, making CHM1 a safer target for TCR-based therapy, as the TCRs would primarily attack the cancer cells, as they are the only ones expressing it. All of this, taken together, makes CHM1 a suitable target for TCR Therapy. (U. Thiel et al., 2011; Thiel et al., 2017; von Heyking et al., 2017) The other targets were evaluated similarly (see 1.2.5.).

It is important to remember that Ewing sarcoma is a rather non-immunogenic tumor, showing very low somatic mutation rates and, therefore, not providing many neoantigens that could be used as possible targets for immunotherapy. That is why we focused on overexpressed antigens and non-mutated cancer-specific genes, only expressed during embryogenesis or immune-privileged germline, such as the testis, which lacks HLA-class 1, reducing the risk for off-tumor toxicity. (Crompton et al., 2014; Gröbner et al., 2018; Shafer et al., 2022)

6.4 The findings

LIPI, PAX7, GPR64, and CHM1 were evaluated as targets for T cell-based immunotherapy in Ewing Sarcoma.

6.4.1. LIPI

The two preexisting LIPI clones, 1A5 and 2C10, were confirmed as a LIPI/HLA-A*0201 restricted CD8+ T cell line in a FACS analysis, as they were able to be stained by a LIPI-specific multimer and not by an irrelevant one. Moreover, both LIPI-specific T cell clones targeted LIPI-pulsed T2 cells while neglecting the FLU-pulsed negative control in IFN-γ ELISpots. This indicates that the clones were specific for the LIPI nonamer. However, they demonstrated no Ewing sarcoma cell-specific recognition.

Lacking EwS-cell line recognition has been observed several times in our research group. Several reasons were proposed back then. First, these specific clones could not detect the epitope on the cell lines. Other clones might be capable of doing that. Second, the antigen density is lower on cell lines compared to pulsed T2 cells, a concern, especially in case of a possible low avidity clone, which therefore cannot target the cell lines, as avidity plays a central role in TCR sensitivity. On the other hand, a too-high avidity clone might be less effective in low-dose peptide:MHC-situations, and the density with which each target is exhibited is unclear. This is related to third, the cell line expresses the antigen but presents it badly, or fourth, the epitope is not processed at all. This can be tested by COS7 transfection, for example. We assumed the fourth variant at that point – a possible lacking expression on the cancer cell lines, at least of that protein isoform. (Campillo-Davo et al., 2020; Pirson, 2010; U. Thiel et al., 2011)

Regarding the peptide presentation on cell lines, it is important to consider, that cell lines progress in culture. Ben-David et al. (2018) showed that established cancer cell lines exhibit clonal and genetic diversity. This is associated with different cellular properties, cellular function, and morphology. It could even be shown that this had a major impact on drug response. Hughes et al. (2007) corroborate this, especially when cells are in culture for a long time and passaged often. Cells might experience genetic drift or selective pressure and, therefore, demonstrate different key functions.
All this introduces variability in cell behavior and elicited responses, making it more difficult to understand and reproduce experimental data or even produce wrong results. (Ben-David et al., 2018; Hughes et al., 2007; Pamies et al., 2022)

An additional concern is inter- and intraspecies contamination, as more than one-third of cell cultures are supposed to contain cross-contamination. Microbial

contamination, especially mycoplasma, can often be found. It can distort experiments by introducing unwanted variables and interfering with most aspects of cell physiology, including cell growth. (Hughes et al., 2007; Masters et al., 2001; Pamies et al., 2022; Uphoff & Drexler, 2011; Young et al., 2010)

In light of this, phenotypic variability, which is even detectable when genetic and environmental differences are minimized, which they were possibly inadvertently not in the experiments, needs to be considered – especially concerning peptide presentation or growth rates. (Ben-David et al., 2018; Geiler-Samerotte et al., 2013; Pamies et al., 2022)

This could be a reason why tumor cell lines were not recognized by LIPI clones and not well recognized in the ELISpot assays of GPR64 and CHM1 clones. Maybe the cells did not express the peptide on their surface at the time, did so badly, or exhibited impurities.

It is also important to consider that proteins can have isoforms. This includes peptides derived from LIPI and might also be an explanation for their missing cell line recognition if the cell lines were to express another isoform. Protein isoforms are based on the same gene but exhibit different amino acid sequences and occur due to splicing, mutations, or post-translational modifications. (Mann & Jensen, 2003; Psatha et al., 2017; Sinitcyn et al., 2023; Torrens-Fontanals et al., 2021) These isoforms could affect the binding affinity and recognition of the peptides by TCRs and, therefore, the final success of a possible therapy. Post-translational modifications, for example, influence the activation, location, the turnover, and even protein-protein-interactions. (Mann & Jensen, 2003) It may be pertinent in future studies to consider protein isoforms during the development of TCRs so that they can specifically recognize and function effectively against peptides, as well as their isoforms. The lack of protein isoform exploration is common in proteomic studies, for example due to missing suitable methods, representing a field that needs to be further explored. (Mann & Jensen, 2003; Psatha et al., 2017; Sinitcyn et al., 2023)

Moreover, as mentioned above, the chosen target has to be processed and expressed on the tumor cell. COS cells have the ability to express a specific protein for a limited period (Aruffo, 1998; Edwards & Aruffo, 1993). Consequently, transducing COS7 cells with HLA-A2- and peptide-cDNA would have demonstrated whether the peptides are physiologically processed and presented on the cell surface. Furthermore, this method could have confirmed the ability of TCRs to recognize the

peptides. In fact, T cells release IFN-y when confronted with double-transfected COS-7 cells if the epitope is present. (Pirson, 2010; U. Thiel et al., 2011) Nevertheless, the step of transducing COS7 cells with HLA-A2 and peptides was omitted. Only for CHM1-319 has the peptide processing been confirmed by this method before. (Pirson, 2010; U. Thiel et al., 2011) However, this approach might have clarified the issues with poor recognition of tumor cells, such as the LIPI clones. COS7 cell transduction could have given an indication of whether the problem lay with the T cells, the peptides and their presentation, or the tumor cells.

6.4.2 PAX7

In contrast, the PAX7-specific clone 6E12 was able to detect EwS-cell lines, as well as the PAX7-pulsed T2 cells, *in vitro*, indicated by IFN-γ release in ELISpot Assays. Unfortunately, the initial specificity could not be replicated over time, and the clone population became increasingly unviable. For that reason, a TCR sequence for this antigen could not be identified yet. Besides, generating any PAX7 clone proved very difficult with many unsuccessful runs, with sometimes not a single clone being able to recognize PAX7-pulsed T2 cells in the Screening IFN-γ ELISpots. Possible reasons for that, adjustments we made to find this one initially specific clone, and possible reasons for the specificity loss and demise of it could be related to the chosen original cells or the sorting and staining process.

A vital step in T-cell generation is choosing the best possible cells to generate T cells.

T cells are isolated from PBMCs, which can be easily obtained from healthy donor blood or buffy coats, which are leukocyte concentrates and a by-product from Blood Banks. Due to this, they are convenient, readily available, and commonly used in research settings. (Kleiveland, 2015)

Importantly, the physiological status (nutrition, hormones, infections) influences the composition of the PBMCs, which can lead to experimental variations (Kleiveland, 2015). It could, therefore, be assumed that using fresh blood from young, healthy donors to win PBMCs is more likely to garner high-functioning cells. They are less likely to be affected by age-related changes or environmental factors, as the donor is young and known.

Moreover, fresh blood was utilized immediately, while the buffy coats used in our laboratory were older. The buffys even traveled to our laboratory from Ulm to Munich by train. A study by Mondragão-Rodrigues et al. (2023) showed that monocytes from Fresh Buffy Coats – blood collection and processing on the same day - were better at functioning as antigen-presenting cells and activating Natural Killer cells than monocytes from Overnight Buffys – collecting and processing on different days. While not directly testing the impact on T-cell functionality, this indicates that even short storage times can have an effect on the cells. Furthermore, we also used PBMCs from the Buffys to generate DCs in our experiments, highlighting the potential impact even more. (Mondragão-Rodrigues & Macedo, 2023)

Additionally, all steps in handling PBMCs, including the collection, possible cryopreservation, thawing, and culture, influence T-cell viability and immunogenicity. For example, a relation between anticoagulant, post-venipuncture processing time, temperature - interesting also in relation to the train journey - and PBMC viability and functionality has been postulated. (Browne et al., 2024) This could also be controlled better when fresh blood from a young, known donor is used.

In conclusion, fresh blood samples could increase the likelihood that T cells are in the best possible condition for expansion and activation, hopefully improving the overall success of generating specific T cells. In our case, the sorting yields increased after switching from buffy coats to fresh blood.

Moreover, after priming, the T cells must be sorted to isolate the relevant antigen-specific T cells. The “right” T cell must be expanded to identify the “right” TCR later. Fluorescence-activated cell sorting (FACS) was used to analyze and sort single cells with the desired characteristics - CD8-positivity, and the ability to bind the MHC multimer/pentamer in our case. This was based on the detection of the specific antibodies or MHC- multimers/pentamers, respectively. (Davis et al., 2011; Givan, 2011; Orfao & Ruiz-Arguelles, 1996; Picot et al., 2012)

Cells are sorted if they are detected in a pre-drawn sort region. This is called gating.

Importantly, different gating strategies lead to different outcomes. Gating is a manual process that selects zones of interest from bivariate graphs. Thereby, the analyzer sets thresholds for the detection of the desired markers to distinguish between target and non-target cells. However, different gating strategies lead to different results, especially quantitatively. (Anchang et al., 2014; Givan, 2011; Perfetto et al., 2004)

Setting the gate more strictly or loosely, therefore, affects the yield when sorting. This, in turn, impacts the probability of isolating a desired cell. Nevertheless, it can also affect the level of avidity of the isolated cells, as the selection depends, among others, on the binding strength to the MHC multimer. The optimal level of avidity of T cells in potential future therapies is yet to be determined. (Anchang et al., 2014; Baulu et al., 2023; Britten et al., 2009; Campillo-Davo et al., 2020; Davis et al., 2011; Schmid et al., 2010; Shafer et al., 2022) In our case, setting a slightly less stringent sorting gate, obviously led to more sorted cells that could be tested and allowed us to have positive results in IFNγ Screening ELISpots. Maybe sorting too stringently only sorted highly avid cells, which exhausted too quickly and lost their effector functions, like IFNγ release. Additionally, lower affinity TCRs which would be more frequently included when gating more loosely, are, as mentioned above, more sensitive in low-dose peptide: MHC-situations, and the density with which each of the targets was exhibited, especially on the chosen EwS cell lines, is unclear. This is more important in the context of LIPI, GPR64, and CHM1 cell line recognition, but mentioned here for comprehensiveness. (Baulu et al., 2023; Campillo-Davo et al., 2020)

The choice of multimer versus pentamer in the sorting process could also have influenced the detection of specific T cells and the avidity levels of sorted ones. In this study, we utilized MHC-multimers and pentamers specific for the respective target.

They are peptide-MHC complexes that are multimerized. The multimeric structure improved the binding between TCR and the MHC complex, which is usually characterized by low affinity. This made it possible to detect and isolate specific T cells using FACS. Monomers would not have survived the process due to the fast off-rate of TCR/pMHC interaction. (Altman et al., 1996; Chang, 2021; Davis et al., 2011; Rudolph et al., 2006)

MHC multimers, particularly tetramers, are widely used for TCR identification and immunological research. While already relatively sensitive, they may have a disadvantage in identifying lower affinity TCRs. (Chang, 2021; Davis et al., 2011)
Pentamers, also multimers, consist of five MHC molecules. Due to their higher valency, they might have an increased binding avidity, for all MHC molecules can bind to CD8+ T cells. The enhanced sensitivity could reduce the risk of false negatives and, therefore, enable a more efficient and reliable identification of relevant TCRs. A study conducted in different labs by Britten et al. (2009) showed that CD8+ T cells specific

for two different antigens derived from PBMC from five different donors were more likely detected when pentamers were utilized compared to tetramers (81% vs. 61% responses). Moreover, pentamers are supposed to profit from great long-term stability. The use of pentamers has been validated in more than 1800 scientific publications. (Britten et al., 2009; Chang, 2021; Davis et al., 2011; ProImmune, 2024)

This is consistent with the experiences gained during this study. Switching from multimers to pentamers produced improved yields with more positive clones in Screening ELISpot assays, or even any yield at all during sorting.

Additionally, newer FACS machines can distribute the sorted cells into individual wells of a 96-well plate automatically. We seeded cells manually, which leads to a random settling of the sorted cells and possibly more than one cell per well by chance, facilitating the potential suppression of one clone by another. Therefore, the mechanical seeding could be the basis for a more controlled and precise way of limiting dilution. (Lindström & Andersson-Svahn, 2012; Lu et al., 2018) This could also constitute a possible reason why several alpha and beta chains could be detected when sequencing the CHM1 clone 5E3. Maybe there were several cells in one well, with only one facilitating the specificity. This can also be the basis for the hypothesized overgrowth and specificity loss of the PAX7 clone 6E12. (Lu et al., 2018)
In conclusion, sorting and gating parameters can be adjusted to influence the yield and purity of T cells specific for the desired target. Under optimal sorting conditions, higher proportions should be specific for the target antigen.

Nevertheless, the PAX7-489 nonamer was identified as a good binding peptide through in silico prediction and a PAX7-HLA-A*0201-Binding Assay, including comparable results to the FLU-positive control and a peptide-concentration dependent increase in HLA-A*0201 expression. These results taken together with the fact that a specific clone could be identified at first, recommend PAX7 as a promising therapeutic target, especially since PAX7 is not only overexpressed on Ewing Sarcoma, but also synovial sarcoma and alveolar rhabdomyosarcoma. (Baldauf et al., 2018; Charville et al., 2017) A potential TCR could, therefore, be used for patients with different types of cancers.

6.4.3 GPR64

For GPR64, there were already several more or less successful generation attempts in our laboratory (Pirson, 2010). However, a TCR was never isolated.
While a promising clone emerged, we were also unsuccessful in sequencing a TCR.
The identified GPR64-clone C520 was able to recognize GPR64-pulsed T2 cells while detecting the FLU-pulsed negative cells significantly less in IFN-γ ELISpots, suggesting a peptide-specific recognition. Interestingly, the HLA-A*0201+ cell lines A673 and TC71 were detected only as well as the negative control. However, the HLA-A*0201- cell line SB-KMS-KS was barely detected, suggesting a potential HLA-A*201 restriction.
Such a recognition pattern is not unheard of in our research group. In the work of Blaeschke et al. (2016), a similar pattern can be observed, with around 400-500 IFN-γ spots/1000 T cells for T2 & FLU and TC71 and A673. They also acknowledged that the IFN-γ release of T cells targeting pulsed T2 cells is more pronounced than in co-culture with cancer cell lines, postulating a non-physiological setting. They explained the background IFN-γ release in the well with FLU-pulsed T2 cells as a possible weak allo-recognition amplified by the very dense presentation of peptide/MHC-complexes on T2 cells and the activation of T cells is associated with the epitope density. Back then, they could not detect any cross-reactivity in subsequent tests. Therefore, we still went ahead with this clone. (Blaeschke et al., 2016; Campillo-Davo et al., 2020)

Unfortunately, the clone did not expand as hoped.

Our T cells were often in culture for an extended period of time, most often due to a cell number that was too small to proceed with subsequent experiments in a timely manner. We suspect that this played a substantial role with regard to the problem of identifying more specific TCRs. The failure of T cell clones to grow to sufficient numbers is well documented in the conventional process of T cell cloning. Martkamchan et al. (2016) mention three weeks as the appropriate time period for cell expansion (Martkamchan et al., 2016). According to Sudarsanam et al. (2022), most protocols mention 7-14 days as standard culture periods, at least for CAR T cell expansion (Sudarsanam et al., 2022). This was exceeded.

Long-cultivation problems introduce additional problems to an already problematic T-cell expansion. These include competition for space in the case of overgrowth, nutrients, and growth factors or the accumulation of metabolic waste

products. This reduces cell viability and can ultimately lead to cell death. (Lu et al., 2018; Martkamchan et al., 2016; Pamies et al., 2022; Rathmell et al., 2000) Jeurink et al. (2008) showed that the number of non-viable cells increased steadily from day to day up to day 7 in culture after polyclonal stimulation, and in our case, the cells were in culture much longer (Jeurink et al., 2008). This supports the large number of non-viable cells we identified in the FACS analyses, especially in the one from PAX7.

Overgrowth and prolonged culture times could also mean the growth of an unspecific clone (especially remembering the manual seeding process or cross-contamination with another clone from another well or flask) and, consequently, the suppression of the specific desired one. This might be an explanation for the specificity loss observed in the PAX7 clone 6E12. (Pamies et al., 2022)

Moreover, there can be temporary alterations in the TCR expression of T cells during T-cell activation, as surface TCRs can cycle between intracellular compartments (internalization) and the plasma membrane. These TCR expression levels influence the T-cell responses to a certain antigen, and the longer the cultivation time, the more likely differences in expression are. Three reasons for TCR downregulation are proposed by Schrum et al. 2003. Two are interesting in our case. First, the cells are actively signaling or not ‘resting’ due to growth factors, which were supplied continuously. Second, the utilized TCR ligand is very strong. Anti-CD3 would be an example of that and was used in our T-cell expansion protocol. TCR downregulation can be sustained for several days. (Schrum et al., 2003) This could have led to different, sometimes diminished, specificities and effectiveness levels of T cell populations over time and in different tests. Both up- and downregulation of surface TCR influences the signaling potential of T cells. However, some TCR expression on the cell surface always remains. Moreover, changing avidities can be observed as surface TCRs undergo avidity maturation. (Labrecque et al., 2001; Schrum et al., 2003) This is also an important point to consider, when thinking about the specificity loss observed in the PAX7 clone.

Additionally, T cells can become exhausted, which is associated with the loss of effector functions, such as decreased cytokine production or diminished cytotoxic activity, and the expression of inhibitory receptors. Exhaustion is known to contribute to the fact that T cells do not grow enough to proceed with the TCR identification progress. (Dunsford et al., 2020; Lu et al., 2018; Wherry, 2011) All of this could have introduced a potential variability in the reproducibility of specificity results, and as

mentioned above, T cell growth was not only an issue in the GPR64 clones mentioned here but also in a lot of other generation attempts that were conducted. Furthermore, a member of our laboratory showed that at least retrovirally transduced T cells lost all effector functions after 54 days in culture, underlining our observations here, that a prolonged culture time results in T cell exhaustion. (Xue, 2022) It could also constitute another possible reason for our inability to reproduce PAX7 specificity after some culture time.

Strategies addressing these challenges could include the adjustment of nutrient concentrations and stimuli, keeping the culture time as short as possible, and including rest periods to prevent exhaustion and TCR downregulation. (Dunsford et al., 2020; Pamies et al., 2022; Schrum et al., 2003; Sudarsanam et al., 2022; Wherry, 2011)

Considering this, it might be worth looking at the T-cell stimulation and expansion protocols and two highly relevant players.

DCs are professional antigen-presenting cells. They capture and process antigens to exhibit them as MHC-peptide complexes and stimulate T cells to initiate immune responses. They also provide co-stimulatory signals required for the activation of T cells. Moreover, they play an important role in the regulation of T cells and the immune system, for example, with regard to T cell tolerance and the negative selection of autoreactive cells. (Banchereau & Steinman, 1998; Steinman, 2003)

Cytokines also play an essential role in T-cell stimulation (Bachmann & Oxenius, 2007; Banchereau & Steinman, 1998; Steinman, 2003). IL-2, for example, is crucial for the immune response, progressing the T-cell cell cycle and encouraging T cells to proliferate, grow, and differentiate. It is routinely used in cell cultures, including ex vivo expansion of T cells. (Bachmann & Oxenius, 2007; Smith, 1988; Sudarsanam et al., 2022) This is also true for our laboratory, where it is utilized for T-cell priming and expansion protocols.

Proleukin is the recombinant form of IL-2. Although its effects should be similar to natural IL-2, it is a more homogeneous product and may offer enhanced stability. It is used clinically to treat cancer patients, such as renal cell carcinoma or melanoma, and viral infections like HIV. (Baigent, 2002)

In this study, dendritic cells and IL-2, later Proleukin, were used to expand T cells. T cells were usually primed two times with DCs and cytokines, but more frequent stimulation (e.g., three times) could enhance the efficacy of T-cell priming. Continual and repeated stimulatory signals at the right time maintain T cells in an activated state,

promote their survival, and sustain their function. It has been shown that strong or weak stimulation is correlated with the number of activation events in T cells. (Bachmann & Oxenius, 2007; Richard et al., 2021; Smith, 1988; Sudarsanam et al., 2022) Nevertheless, the stimulation frequency needs to be balanced against overstimulation. Overstimulation or stimulation at the wrong time can lead to T-cell exhaustion – marked by a loss of the capacity to perform effector activities and the expression of inhibitory receptors – activation-induced cell death, or toxicity. (Bachmann & Oxenius, 2007; Dunsford et al., 2020; Martkamchan et al., 2016; Sudarsanam et al., 2022; Wherry, 2011; Wherry & Kurachi, 2015)

Maybe a different stimulation regimen could have improved the viability and effectiveness of the T cells.

Additionally, single-cell sequencing may provide a chance to decrease the culture times—and, therefore, the risks associated with prolonged ones—and may further provide insights into cellular and genomic heterogeneity, thus helping identify issues related to TCR expression and T-cell exhaustion. (Lu et al., 2021; Lu et al., 2018; Schrum et al., 2003; Szabo et al., 2019; Wherry, 2011; Wherry & Kurachi, 2015)

Nevertheless, the cell number was enough for one sequencing round. Sadly, only a beta-chain could be identified using traditional sequencing, and no relevant GPR64 cell was detectable by the time we tried to utilize scRNAseq. This could all be related to the problems associated with the long cultivation times given above, or due to sequencing problems described in the next section.

However, GPR64 still presented itself as a viable target, as detection was possible at first. This is especially true as GPR64 is also highly expressed in nephroblastoma. (Richter et al., 2013)

6.4.4 CHM1

In the case of CHM1, a new TCR was successfully identified. The clone 5E3 was confirmed as a CHM1/HLA-A*0201 restricted CD8+ T cell line in a FACS analysis, showing partial positivity to a CHM1-specific MHC-pentamer compared with an irrelevant PAX7-multimer. Notably, a lot of non-viable cells could also be detected, which we also interpreted as a result of a rather long T-cell cultivation time. The detection patterns observed in the IFN-γ-ELISpots were comparable to that of the GPR64 clone C520, and results were therefore interpreted analogously.

Moreover, while no other CHM1-nonamers could be identified as good binding peptides in the CHM1-HLA-A*0201-Binding Assay, despite in silico prediction, the known CHM1-319 nonamer (VIMPCSWWV) was reinforced as such.

The PCR and the traditional sequencing of clone 5E3 identified several alpha- and beta-chains, suggesting a non-clonality of the cell population. Reasons for that could be contamination or the seeding procedure during limiting dilution, as explained in the examples of clones specific for the other epitopes. Nevertheless, some T cells also naturally express multiple alpha chains. However, the phenomenon of multiple chains was also encountered by our research group before. ScRNAseq could provide a remedy for this. In our case, scRNAseq was able to identify one alpha- and one beta-chain, which we know belongs together, as it was sequenced in a single cell, reducing the risks of mispairing in subsequent engineering steps and connected unwanted issues like specificity loss or cross-reactivity. (Blaeschke, 2016; Lu et al., 2018)

As mentioned above, single-cell RNA sequencing could be an asset for identifying TCRs more efficiently. (Baulu et al., 2023; Shafer et al., 2022) It can provide a transcriptional analysis of individual cells and even provide information about their functional states. This enables scRNA to identify and describe cellular subpopulations. (Kolodziejczyk et al., 2015; Stubbington et al., 2017)

scRNAseq can identify the TCR of individual cells in a sample. It can further provide information about monoclonality or potential heterogeneity in a clone population by determining whether identical or different TCR sequences exist. Moreover, since the TCR is identified from a single cell, the likelihood of mismatched alpha- and beta-chains during subsequent engineering steps and associated problems such as specificity loss or cross-reactivity can be reduced. This is important as traditional sequencing, which we employed in a first step, comes with hurdles. Some TCRs cannot be amplified by PCR very well. Furthermore, it is known that up to 30% of T cells have two different TCRα chains, but only one leads to a specific TCR. (Lu et al., 2021; Lu et al., 2018) This also needs to be considered in the light of the fact that we could identify several alpha chains and beta chains during the traditional sequencing of the CHM1 clone and only a beta chain when sequencing the GPR64 clone. While there are also other explanations, such as previously mentioned overgrowth, contamination, or more than one cell per well, these amplification problems and multiple chains need to be examined as well, especially since the occurrence of multiple alpha and beta chains even after multiple limited dilution steps

was already observed in earlier works of our research group. (Blaeschke, 2016; Lu et al., 2018)
The value of scRNAseq in this regard is indicated by the fact that during the scRNAseq of the CHM1 clone 5E3, one TCR with one alpha- and one beta-chain from one cell could be identified, which can now be engineered with greater confidence.

Furthermore, in the future, the clone colonies can not only be sequenced more efficiently and more precisely but also be investigated regarding their functionality and activation state. Doing this may be crucial for effective TCR identification and the subsequent T-cell therapy development, as this aids in expanding and selecting the best cell subsets from a cell biology perspective, for example, those that have a high expression of effector cytokines like IFN-γ or IL-2. (Baulu et al., 2023; Lu et al., 2021; Lu et al., 2018; Shafer et al., 2022)

Moreover, as mentioned in the previous paragraph, analyzing the genetic information in a single cell might significantly reduce the time required in culture to expand T-cell clones. (Lu et al., 2021; Lu et al., 2018) This shorter culture time reduces the possibility of overgrowth, cell death, or exhaustion, and other problems associated with longer durations of culture – all of which I encountered during my study. (Lu et al., 2018)

Summarizing, while one CHM1-specific T cell could be identified, we struggled to generate more CHM1-specific T cells and failed to identify any for the other targets. While this is statistically possible, it is unlikely. We see the reasons for the problematic TCR identification mainly in the peptide presentation, especially on tumor cells, T cell characteristics, like affinity or exhaustion, T cell expansion, and sequencing strategies. Moreover, it is important to remember, that while some phenomena were explained mainly at the example of a clone specific for one epitope, all of them played a role in the hampered generation of clones from all entities.

6.5 Conclusion

PAX7, GPR64, and CHM1 are promising targets for adoptive immunotherapy in advanced EwS. PAX7 also overexpressed in synovial sarcoma and alveolar rhabdomyosarcoma, and GPR64, present in nephroblastoma, are especially interesting T-cell targets.

The successfully identified TCR sequence for CHM1 will now indeed provide parts of a toolbox for T-cell engineering within our research group. It could be part of a potential foundation of a TCR library enabling the delivery of highly specific, targeted therapy for advanced Ewing Sarcoma patients.

Nevertheless, more research and optimization are needed. Optimizing methods such as multimer/pentamer technologies, optimized DC stimulation, and single-cell RNA sequencing can enhance and simplify the identification, expansion, and possibly efficacy of TCRs.

Future research will focus on the identification of further targets and the re-exploration of those pursued in this thesis. The identified TCR sequence will be further investigated in *in vitro* experiments and a mouse model. Transgenic T cells expressing the identified TCR will be genetically engineered by retroviral transduction and CRISPR-Cas9.

7 Summary

Ewing sarcoma is a highly aggressive bone and soft tissue cancer that mostly affects children and adolescents. It is characterized by EWS/ETS fusion oncogenes, which encode aberrant transcription factors responsible for transactivation and transformation. At the time of diagnosis, 75% of patients with EwS display a local disease, including micro-metastases. However, 25% initially present with an already metastatic disease. These patients with metastatic disease, and especially with advanced Ewing sarcoma (≥ 2 bone metastases, and/or bone marrow involvement and/or relapse ≤ 2 years after diagnosis) still have a dismal prognosis.
Ewing Sarcoma is usually treated with a multimodal approach combining chemotherapy and local therapy, including surgery and/or irradiation.
Advanced Ewing sarcoma, in particular, is treated with a combination of high-dose chemotherapy and stem cell transplantation, albeit with varied results. However, current treatment protocols often lead to severe side effects. All of this, taken together, highlights the need for new therapeutic approaches.

We examined T cell-based adoptive immunotherapy against nonamers derived from the EwS-associated antigens LIPI, GPR64, PAX7, and CHM1.
To that end, nonamers selected in silico for their potential binding strength and lacking cross-reactivity were tested for their actual binding capacities in T2-HLA-A*02:01-binding assays. The selected peptides were then used to pulse HLA-A*02:01+ dendritic cells, which were employed to prime HLA-A*02:01- CD8+ T cells. After the two-week co-cultivation period, the T cells were stained with multimers and subsequently sorted. Afterward, the identified cells were expanded using a single-cell dilution process. Selected based on their growth pattern, the clones were evaluated for HLA-A*02:01-restriction, peptide specificity, and Ewing sarcoma cell line detection in ELISpot assays and FACS analyses. Promising candidates were further expanded to analyze the DNA sequences of their T cell receptors (TCR). This was done both by using gel electrophoresis and polymerase chain reaction and by single-cell RNA sequencing.
The T cells pulsed with LIPI antigen showed limited recognition of EwS, only targeting peptide-pulsed T2 cells as a positive control and failing to recognize EwS cell lines.

On the other hand, PAX7 and GPR64-specific T cells demonstrated peptide-specificity and the ability to target EwS cell lines *in vitro*, although PAX7 lost its specificity after an extended cultivation time. At the same time, a complete TCR sequence could not be identified for the GPR64-clone. Moreover, the CHM1-clone exhibited peptide-specificity and Ewing Sarcoma cell line specificity in ELISpot assays and FACS analyses. For the CHM1-specific T cell clone, a new TCR was successfully identified using both PCR and scRNAseq.

In conclusion, PAX7, GPR64, and CHM1 appear as promising targets for adoptive immunotherapy in advanced EwS. Notably, PAX7 is also overexpressed in synovial sarcoma and alveolar rhabdomyosarcoma, while GPR64 is in nephroblastoma, making these antigens particularly interesting as potential T cell targets. The discovered CHM1 TCR sequence will be further investigated in additional in vitro experiments and a mouse model. However, we struggled to identify TCRs for any other targets. The problematic identification of TCR may primarily be attributed to issues with peptide presentation, particularly on tumor cells. Factors such as T cell characteristics, including affinity or exhaustion, as well as T cell expansion and sequencing strategies, contribute to this challenge. Therefore, our future research will focus on revisiting PAX7 and GPR64, with an emphasis on scRNAseq, as this technique simplifies TCR identification, particularly after extended cell cultivation—a challenge encountered, particularly with PAX7 cells. These findings highlight the potential of targeted T cell therapy in addressing advanced EwS but stress the need for continued optimization of T cell manufacturing to make the generation of specific T cells for a wider variety of targets more efficient.

8 Zusammenfassung

Das Ewing-Sarkom ist ein hochaggressiver Knochen- und Weichteiltumor, der hauptsächlich Kinder und Jugendliche betrifft. Es ist durch EWS/ETS-Fusionsonkogene gekennzeichnet, die aberrante Transkriptionsfaktoren kodieren, die für Transaktivierung und Transformation verantwortlich sind. Zum Zeitpunkt der Diagnose zeigen 75 % der Patienten mit EwS eine lokale Erkrankung, einschließlich Mikrometastasen. Allerdings präsentieren sich 25 % der Patienten initial mit einer bereits metastasierten Erkrankung. Diese Patienten mit metastasierter Erkrankung und insbesondere mit fortgeschrittenem Ewing-Sarkom (≥ 2 Knochenmetastasen und/oder Knochenmarkbefall und/oder Rezidiv ≤ 2 Jahre nach Diagnose) haben weiterhin eine schlechte Prognose.

Das Ewing-Sarkom wird in der Regel mit einem multimodalen Ansatz behandelt, der eine Kombination aus Chemotherapie und lokaler Therapie, einschließlich Operation und/oder Bestrahlung, umfasst. Das fortgeschrittene Ewing-Sarkom wird insbesondere mit einer Kombination aus hochdosierter Chemotherapie und Stammzelltransplantation behandelt, wenn auch mit unterschiedlichen Ergebnissen. Die aktuellen Behandlungsprotokolle führen jedoch oft zu schweren Nebenwirkungen. All dies zusammen unterstreicht die Notwendigkeit neuer therapeutischer Ansätze.

Wir haben T-Zell-basierte adoptive Immuntherapien gegen Nonamere untersucht, die von den mit EwS assoziierten Antigenen LIPI, GPR64, PAX7 und CHM1 abgeleitet sind. Zu diesem Zweck wurden in silico ausgewählte Nonamere, die sich durch ihre potenzielle Bindungsstärke und fehlende Kreuzreaktivität auszeichnen, in T2-HLA-A*02:01-Bindungsassays auf ihre tatsächlichen Bindungskapazitäten getestet. Die ausgewählten Peptide wurden dann verwendet, um HLA-A*02:01+ dendritische Zellen zu generieren, die eingesetzt wurden, um HLA-A*02:01- CD8+ T-Zellen zu primen. Nach einer zweiwöchigen Kokulturzeit wurden die T-Zellen mit Multimeren gefärbt und anschließend sortiert. Danach wurden die identifizierten Zellen durch Einzelzelldilution expandiert. Auf der Grundlage ihres Wachstumsverhaltens wurden die Klone auf HLA-A*02:01-Restriktion, Peptidspezifität und Ewing-Sarkom-

Zelllinien detektion in ELISpot-Assays und FACS-Analysen untersucht. Vielversprechende Kandidaten wurden weiter expandiert, um die DNA-Sequenzen ihrer T-Zell-Rezeptoren (TCR) zu analysieren. Dies wurde sowohl durch Gel-Elektrophorese und Polymerase-Kettenreaktion als auch durch Einzelzell-RNA-Sequenzierung durchgeführt.

Die mit LIPI-Antigen gepulsten T-Zellen zeigten eine begrenzte Erkennung von EwS, indem sie nur die peptid-pulsierten T2-Zellen als positive Kontrolle angriffen und keine EwS-Zelllinien erkannten. Andererseits demonstrierten PAX7- und GPR64-spezifische T-Zellen Peptidspezifität und die Fähigkeit, EwS-Zelllinien in vitro zu erkennen, obwohl PAX7 nach längerer Kultivierungszeit seine Spezifität verlor. Gleichzeitig konnte für den GPR64-Klon keine vollständige TCR-Sequenz identifiziert werden. Darüber hinaus zeigte der CHM1-Klon Peptidspezifität und Spezifität für Ewing-Sarkom-Zelllinien in ELISpot-Assays und FACS-Analysen. Für den CHM1-spezifischen T-Zell-Klon wurde ein neuer TCR erfolgreich sowohl mittels PCR als auch scRNAseq identifiziert.

Zusammenfassend scheinen PAX7, GPR64 und CHM1 vielversprechende Ziele für die adoptive Immuntherapie bei fortgeschrittenem EwS zu sein. Bemerkenswert ist, dass PAX7 auch in Synovialsarkomen und alveolären Rhabdomyosarkomen überexprimiert wird, während GPR64 in Nephroblastomen vorkommt, was diese Antigene als potenzielle T-Zell-Ziele besonders interessant macht. Die entdeckte CHM1-TCR-Sequenz wird in weiteren in vitro-Experimenten und in einem Mausmodell weiter untersucht. Wir hatten jedoch Schwierigkeiten, TCRs für andere Ziele zu identifizieren. Die problematische Identifizierung von TCRs kann möglicherweise auf Probleme bei der Peptidpräsentation, insbesondere auf Tumorzellen, zurückgeführt werden. Faktoren wie T-Zell-Eigenschaften, einschließlich Affinität oder Erschöpfung, sowie T-Zell-Expansion und Sequenzierungsstrategien tragen zu dieser Herausforderung bei. Daher wird sich unsere zukünftige Forschung auf die erneute Untersuchung von PAX7 und GPR64 konzentrieren, mit einem Schwerpunkt auf scRNAseq, da diese Technik die TCR-Identifikation, insbesondere nach verlängerter Zellkultivierung, vereinfacht – eine Herausforderung, die insbesondere bei PAX7-Zellen auftrat. Diese Ergebnisse unterstreichen das Potenzial der zielgerichteten T-Zell-Therapie bei der Behandlung

fortgeschrittener EwS, betonen jedoch die Notwendigkeit einer kontinuierlichen Optimierung der T-Zell-Herstellung, um die Erzeugung spezifischer T-Zellen für eine breitere Vielfalt von Zielen effizienter zu gestalten.

References

Abboud, A., Masrouha, K., Saliba, M., Haidar, R., Saab, R., Khoury, N., Tawil, A., & Saghieh, S. (2021). Extraskeletal Ewing sarcoma: Diagnosis, management and prognosis. *Oncol Lett*, *21*(5), 354. https://doi.org/10.3892/ol.2021.12615

Aggen, D. H., Chervin, A. S., Schmitt, T. M., Engels, B., Stone, J. D., Richman, S. A., Piepenbrink, K. H., Baker, B. M., Greenberg, P. D., Schreiber, H., & Kranz, D. M. (2012). Single-chain VαVβ T-cell receptors function without mispairing with endogenous TCR chains. *Gene Ther*, *19*(4), 365-374. https://doi.org/10.1038/gt.2011.104

Altman, J. D., Moss, P. A., Goulder, P. J., Barouch, D. H., McHeyzer-Williams, M. G., Bell, J. I., McMichael, A. J., & Davis, M. M. (1996). Phenotypic analysis of antigen-specific T lymphocytes. *Science*, *274*(5284), 94-96. https://doi.org/10.1126/science.274.5284.94

Anchang, B., Do, M. T., Zhao, X., & Plevritis, S. K. (2014). CCAST: a model-based gating strategy to isolate homogeneous subpopulations in a heterogeneous population of single cells. *PLoS computational biology*, *10*(7), e1003664.

Anderton, J., Moroz, V., Marec-Bérard, P., Gaspar, N., Laurence, V., Martín-Broto, J., Sastre, A., Gelderblom, H., Owens, C., Kaiser, S., Fernández-Pinto, M., Fenwick, N., Evans, A., Strauss, S., Whelan, J., Wheatley, K., & Brennan, B. (2020). International randomised controlled trial for the treatment of newly diagnosed EWING sarcoma family of tumours - EURO EWING 2012 Protocol. *Trials*, *21*(1), 96. https://doi.org/10.1186/s13063-019-4026-8

Aruffo, A. (1998). Transient expression of proteins using COS cells. *Current Protocols in Neuroscience*, *2*(1), 4.7. 1-4.7. 7.

Bachmann, M. F., & Oxenius, A. (2007). Interleukin 2: from immunostimulation to immunoregulation and back again. *EMBO Rep*, *8*(12), 1142-1148. https://doi.org/10.1038/sj.embor.7401099

Baigent, G. (2002). Recombinant Interleukin-2 (rIL-2), aldesleukin. *J Biotechnol*, *95*(3), 277-280. https://doi.org/10.1016/s0168-1656(02)00019-6

Balamuth, N. J., & Womer, R. B. (2010). Ewing's sarcoma. *Lancet Oncol*, *11*(2), 184-192. https://doi.org/10.1016/s1470-2045(09)70286-4

Baldauf, M. C., Gerke, J. S., Kirschner, A., Blaeschke, F., Effenberger, M., Schober, K., Rubio, R. A., Kanaseki, T., Kiran, M. M., Dallmayer, M., Musa, J., Akpolat, N., Akatli, A. N., Rosman, F. C., Özen, Ö., Sugita, S., Hasegawa, T., Sugimura, H., Baumhoer, D., . . . Grünewald, T. G. P. (2018). Systematic identification of cancer-specific MHC-binding peptides with RAVEN. *Oncoimmunology*, *7*(9), e1481558. https://doi.org/10.1080/2162402x.2018.1481558

Banchereau, J., & Steinman, R. M. (1998). Dendritic cells and the control of immunity. *Nature*, *392*(6673), 245-252. https://doi.org/10.1038/32588

Baulu, E., Gardet, C., Chuvin, N., & Depil, S. (2023). TCR-engineered T cell therapy in solid tumors: State of the art and perspectives. *Sci Adv*, *9*(7), eadf3700. https://doi.org/10.1126/sciadv.adf3700

Ben-David, U., Siranosian, B., Ha, G., Tang, H., Oren, Y., Hinohara, K., Strathdee, C. A., Dempster, J., Lyons, N. J., Burns, R., Nag, A., Kugener, G., Cimini, B., Tsvetkov, P., Maruvka, Y. E., O'Rourke, R., Garrity, A., Tubelli, A. A., Bandopadhayay, P., . . . Golub, T. R. (2018). Genetic and transcriptional evolution alters cancer cell line drug response. *Nature*, *560*(7718), 325-330. https://doi.org/10.1038/s41586-018-0409-3

Bendle, G. M., Linnemann, C., Hooijkaas, A. I., Bies, L., de Witte, M. A., Jorritsma, A., Kaiser, A. D., Pouw, N., Debets, R., Kieback, E., Uckert, W., Song, J. Y., Haanen, J. B., & Schumacher, T. N. (2010). Lethal graft-versus-host disease in mouse models of T cell receptor gene therapy. *Nat Med*, *16*(5), 565-570, 561p following 570. https://doi.org/10.1038/nm.2128

Bernstein, M., Kovar, H., Paulussen, M., Randall, R. L., Schuck, A., Teot, L. A., & Juergens, H. (2006). Ewing's sarcoma family of tumors: current management. *Oncologist*, *11*(5), 503-519. https://doi.org/10.1634/theoncologist.11-5-503

Biele, E., Schober, S. J., Prexler, C., Thiede, M., Heyking, K. V., Gassmann, H., Eck, J., Xue, B., Burdach, S., & Thiel, U. (2021). Monocyte Maturation Mediators Upregulate CD83, ICAM-1 and MHC Class 1 Expression on Ewing's Sarcoma, Enhancing T Cell Cytotoxicity. *Cells*, *10*(11). https://doi.org/10.3390/cells10113070

Blaeschke, F. (2016). *Generation of Ewing's sarcoma antigens CHM1- and EZH2-selective and HLA-A*0201-restricted T-cell receptor transgenic T cells* [Ph.D.

Thesis, Technische Universität München]. https://mediatum.ub.tum.de/1253333

Blaeschke, F., Thiel, U., Kirschner, A., Thiede, M., Rubio, R. A., Schirmer, D., Kirchner, T., Richter, G. H. S., Mall, S., Klar, R., Riddell, S., Busch, D. H., Krackhardt, A., Grunewald, T. G., & Burdach, S. (2016). Human HLA-A*02:01/CHM1+ allo-restricted T cell receptor transgenic CD8+ T cells specifically inhibit Ewing sarcoma growth in vitro and in vivo. *Oncotarget*, *7*(28), 43267-43280. https://doi.org/10.18632/oncotarget.9218

Bosma, S., Ayu, O., Fiocco, M., Gelderblom, H., & Dijkstra, P. (2018). Prognostic factors for survival in Ewing sarcoma: a systematic review. *Surgical oncology*, *27*(4), 603-610.

Britten, C. M., Janetzki, S., Ben-Porat, L., Clay, T. M., Kalos, M., Maecker, H., Odunsi, K., Pride, M., Old, L., Hoos, A., & Romero, P. (2009). Harmonization guidelines for HLA-peptide multimer assays derived from results of a large scale international proficiency panel of the Cancer Vaccine Consortium. *Cancer Immunol Immunother*, *58*(10), 1701-1713. https://doi.org/10.1007/s00262-009-0681-z

Browne, D. J., Miller, C. M., & Doolan, D. L. (2024). Technical pitfalls when collecting, cryopreserving, thawing, and stimulating human T-cells. *Front Immunol*, *15*, 1382192. https://doi.org/10.3389/fimmu.2024.1382192

Burchill, S. A. (2003). Ewing's sarcoma: diagnostic, prognostic, and therapeutic implications of molecular abnormalities. *J Clin Pathol*, *56*(2), 96-102. https://doi.org/10.1136/jcp.56.2.96

Burdach, S. (2004). Treatment of advanced Ewing tumors by combined radiochemotherapy and engineered cellular transplants. *Pediatr Transplant*, *8 Suppl 5*, 67-82. https://doi.org/10.1111/j.1398-2265.2004.00186.x

Burdach, S., van Kaick, B., Laws, H. J., Ahrens, S., Haase, R., Körholz, D., Pape, H., Dunst, J., Kahn, T., Willers, R., Engel, B., Dirksen, U., Kramm, C., Nürnberger, W., Heyll, A., Ladenstein, R., Gadner, H., Jürgens, H., & Go el, U. (2000). Allogeneic and autologous stem-cell transplantation in advanced Ewing tumors. An update after long-term follow-up from two centers of the European Intergroup study EICESS. Stem-Cell Transplant Programs at Düsseldorf University Medical Center, Germany and St. Anna Kinderspital,

Vienna, Austria. *Ann Oncol*, *11*(11), 1451-1462. https://doi.org/10.1023/a:1026539908115

Campillo-Davo, D., Flumens, D., & Lion, E. (2020). The Quest for the Best: How TCR Affinity, Avidity, and Functional Avidity Affect TCR-Engineered T-Cell Antitumor Responses. *Cells*, *9*(7). https://doi.org/10.3390/cells9071720

Caruso, J., Shulman, D. S., & DuBois, S. G. (2019). Second malignancies in patients treated for Ewing sarcoma: A systematic review. *Pediatric Blood & Cancer*, *66*(11), e27938.

Chang, J. (2021). MHC Multimer: A Molecular Toolbox for Immunologists. *Molecules and Cells*, *44*(5), 328-334. https://doi.org/https://doi.org/10.14348/molcells.2021.0052

Charville, G. W., Wang, W. L., Ingram, D. R., Roy, A., Thomas, D., Patel, R. M., Hornick, J. L., van de Rijn, M., & Lazar, A. J. (2017). EWSR1 fusion proteins mediate PAX7 expression in Ewing sarcoma. *Mod Pathol*, *30*(9), 1312-1320. https://doi.org/10.1038/modpathol.2017.49

Chruściel, E., Urban-Wójciuk, Z., Arcimowicz, Ł., Kurkowiak, M., Kowalski, J., Gliwiński, M., Marjański, T., Rzyman, W., Biernat, W., Dziadziuszko, R., Montesano, C., Bernardini, R., & Marek-Trzonkowska, N. (2020). Adoptive Cell Therapy-Harnessing Antigen-Specific T Cells to Target Solid Tumours. *Cancers (Basel)*, *12*(3). https://doi.org/10.3390/cancers12030683

Cotterill, S. J., Ahrens, S., Paulussen, M., Jürgens, H. F., Voûte, P. A., Gadner, H., & Craft, A. W. (2000). Prognostic factors in Ewing's tumor of bone: analysis of 975 patients from the European Intergroup Cooperative Ewing's Sarcoma Study Group. *J Clin Oncol*, *18*(17), 3108-3114. https://doi.org/10.1200/jco.2000.18.17.3108

Couzin-Frankel, J. (2013). Breakthrough of the year 2013. Cancer immunotherapy. *Science*, *342*(6165), 1432-1433. https://doi.org/10.1126/science.342.6165.1432

Crompton, B. D., Stewart, C., Taylor-Weiner, A., Alexe, G., Kurek, K. C., Calicchio, M. L., Kiezun, A., Carter, S. L., Shukla, S. A., Mehta, S. S., Thorner, A. R., de Torres, C., Lavarino, C., Suñol, M., McKenna, A., Sivachenko, A., Cibulskis, K., Lawrence, M. S., Stojanov, P., . . . Stegmaier, K. (2014). The genomic landscape of pediatric Ewing sarcoma. *Cancer Discov*, *4*(11), 1326-1341. https://doi.org/10.1158/2159-8290.Cd-13-1037

DANIEL KELLY BENJAMIN, J., Miller, W. C., Bayliff, S., Martel, L., Alexander, K. A., & Martin, P. L. (2002). Infections diagnosed in the first year after pediatric stem cell transplantation. *The Pediatric infectious disease journal*, *21*(3), 227-234.

Davis, M. M., Altman, J. D., & Newell, E. W. (2011). Interrogating the repertoire: broadening the scope of peptide-MHC multimer analysis. *Nat Rev Immunol*, *11*(8), 551-558. https://doi.org/10.1038/nri3020

Davis, M. M., & Bjorkman, P. J. (1988). T-cell antigen receptor genes and T-cell recognition. *Nature*, *334*(6181), 395-402. https://doi.org/10.1038/334395a0

Delattre, O., Zucman, J., Plougastel, B., Desmaze, C., Melot, T., Peter, M., Kovar, H., Joubert, I., de Jong, P., Rouleau, G., & et al. (1992). Gene fusion with an ETS DNA-binding domain caused by chromosome translocation in human tumours. *Nature*, *359*(6391), 162-165. https://doi.org/10.1038/359162a0

Dunsford, L., Thoirs, R., Rathbone, E., & Patakas, A. (2020). A Human In Vitro T Cell Exhaustion Model for Assessing Immuno-Oncology Therapies. In (pp. 89-101). https://doi.org/10.1007/978-1-0716-0171-6_6

Edwards, C. P., & Aruffo, A. (1993). Current applications of COS cell based transient expression systems. *Current Opinion in Biotechnology*, *4*(5), 558-563. https://doi.org/https://doi.org/10.1016/0958-1669(93)90077-A

Fayzullina, D., Tsibulnikov, S., Stempen, M., Schroeder, B. A., Kumar, N., Kharwar, R. K., Acharya, A., Timashev, P., & Ulasov, I. (2022). Novel Targeted Therapeutic Strategies for Ewing Sarcoma. *Cancers (Basel)*, *14*(8). https://doi.org/10.3390/cancers14081988

Foy, S. P., Jacoby, K., Bota, D. A., Hunter, T., Pan, Z., Stawiski, E., Ma, Y., Lu, W., Peng, S., Wang, C. L., Yuen, B., Dalmas, O., Heeringa, K., Sennino, B., Conroy, A., Bethune, M. T., Mende, I., White, W., Kukreja, M., . . . Mandl, S. J. (2023). Non-viral precision T cell receptor replacement for personalized cell therapy. *Nature*, *615*(7953), 687-696. https://doi.org/10.1038/s41586-022-05531-1

Friberg, L. E., Henningsson, A., Maas, H., Nguyen, L., & Karlsson, M. O. (2002). Model of chemotherapy-induced myelosuppression with parameter consistency across drugs. *Journal of clinical oncology*, *20*(24), 4713-4721.

Fuchs, B., Valenzuela, R. G., Inwards, C., Sim, F. H., & Rock, M. G. (2003). Complications in long-term survivors of Ewing sarcoma. *Cancer*, *98*(12), 2687-2692.

Garrido, F., Ruiz-Cabello, F., & Aptsiauri, N. (2017). Rejection versus escape: the tumor MHC dilemma. *Cancer Immunol Immunother*, *66*(2), 259-271. https://doi.org/10.1007/s00262-016-1947-x

Gaspar, N., Hawkins, D. S., Dirksen, U., Lewis, I. J., Ferrari, S., Le Deley, M. C., Kovar, H., Grimer, R., Whelan, J., Claude, L., Delattre, O., Paulussen, M., Picci, P., Sundby Hall, K., van den Berg, H., Ladenstein, R., Michon, J., Hjorth, L., Judson, I., . . . Oberlin, O. (2015). Ewing Sarcoma: Current Management and Future Approaches Through Collaboration. *J Clin Oncol*, *33*(27), 3036-3046. https://doi.org/10.1200/jco.2014.59.5256

Geiler-Samerotte, K., Bauer, C., Li, S., Ziv, N., Gresham, D., & Siegal, M. (2013). The details in the distributions: why and how to study phenotypic variability. *Current opinion in biotechnology*, *24*(4), 752-759.

Ghosh, S., Brown, A. M., Jenkins, C., & Campbell, K. (2020). Viral Vector Systems for Gene Therapy: A Comprehensive Literature Review of Progress and Biosafety Challenges. *Appl Biosaf*, *25*(1), 7-18. https://doi.org/10.1177/1535676019899502

Ginsberg, J. P., Goodman, P., Leisenring, W., Ness, K. K., Meyers, P. A., Wolden, S. L., Smith, S. M., Stovall, M., Hammond, S., Robison, L. L., & Oeffinger, K. C. (2010). Long-term survivors of childhood Ewing sarcoma: report from the childhood cancer survivor study. *J Natl Cancer Inst*, *102*(16), 1272-1283. https://doi.org/10.1093/jnci/djq278

Givan, A. L. (2011). Flow Cytometry: An Introduction. In T. S. Hawley & R. G. Hawley (Eds.), *Flow Cytometry Protocols* (pp. 1-29). Humana Press. https://doi.org/10.1007/978-1-61737-950-5_1

Goedhart, L. M., Gerbers, J. G., Ploegmakers, J. J., & Jutte, P. C. (2016). Delay in Diagnosis and Its Effect on Clinical Outcome in High-grade Sarcoma of Bone: A Referral Oncological Centre Study. *Orthop Surg*, *8*(2), 122-128. https://doi.org/10.1111/os.12239

Gomez, S., Tabernacki, T., Kobyra, J., Roberts, P., & Chiappinelli, K. B. (2020). Combining epigenetic and immune therapy to overcome cancer resistance.

Semin Cancer Biol, *65*, 99-113. https://doi.org/10.1016/j.semcancer.2019.12.019

Gonzalez-Galarza, F. F., Christmas, S., Middleton, D., & Jones, A. R. (2011). Allele frequency net: a database and online repository for immune gene frequencies in worldwide populations. *Nucleic Acids Res*, *39*(Database issue), D913-919. https://doi.org/10.1093/nar/gkq1128

Greenbaum, U., Dumbrava, E. I., Biter, A. B., Haymaker, C. L., & Hong, D. S. (2021). Engineered T-cell Receptor T Cells for Cancer Immunotherapy. *Cancer Immunol Res*, *9*(11), 1252-1261. https://doi.org/10.1158/2326-6066.Cir-21-0269

Gröbner, S. N., Worst, B. C., Weischenfeldt, J., Buchhalter, I., Kleinheinz, K., Rudneva, V. A., Johann, P. D., Balasubramanian, G. P., Segura-Wang, M., Brabetz, S., Bender, S., Hutter, B., Sturm, D., Pfaff, E., Hübschmann, D., Zipprich, G., Heinold, M., Eils, J., Lawerenz, C., . . . Pfister, S. M. (2018). The landscape of genomic alterations across childhood cancers. *Nature*, *555*(7696), 321-327. https://doi.org/10.1038/nature25480

Grünewald, T. G. P., Cidre-Aranaz, F., Surdez, D., Tomazou, E. M., de Álava, E., Kovar, H., Sorensen, P. H., Delattre, O., & Dirksen, U. (2018). Ewing sarcoma. *Nat Rev Dis Primers*, *4*(1), 5. https://doi.org/10.1038/s41572-018-0003-x

Haeusler, J., Ranft, A., Boelling, T., Gosheger, G., Braun-Munzinger, G., Vieth, V., Burdach, S., van den Berg, H., Juergens, H., & Dirksen, U. (2010). The value of local treatment in patients with primary, disseminated, multifocal Ewing sarcoma (PDMES). *Cancer*, *116*(2), 443-450. https://doi.org/10.1002/cncr.24740

Hardes, J., von Eiff, C., Streitbuerger, A., Balke, M., Budny, T., Henrichs, M. P., Hauschild, G., & Ahrens, H. (2010). Reduction of periprosthetic infection with silver-coated megaprostheses in patients with bone sarcoma. *J Surg Oncol*, *101*(5), 389-395. https://doi.org/10.1002/jso.21498

Hesketh, P. J. (2008). Chemotherapy-induced nausea and vomiting. *New England Journal of Medicine*, *358*(23), 2482-2494.

Hesla, A. C., Papakonstantinou, A., & Tsagkozis, P. (2021). Current Status of Management and Outcome for Patients with Ewing Sarcoma. *Cancers (Basel)*, *13*(6). https://doi.org/10.3390/cancers13061202

Hinrichs, C. S., & Restifo, N. P. (2013). Reassessing target antigens for adoptive T-cell therapy. *Nat Biotechnol*, *31*(11), 999-1008. https://doi.org/10.1038/nbt.2725

Hiraki, Y., & Shukunami, C. (2000). Chondromodulin-I as a novel cartilage-specific growth-modulating factor. *Pediatr Nephrol*, *14*(7), 602-605. https://doi.org/10.1007/s004670000339

Howe, S. J., Mansour, M. R., Schwarzwaelder, K., Bartholomae, C., Hubank, M., Kempski, H., Brugman, M. H., Pike-Overzet, K., Chatters, S. J., de Ridder, D., Gilmour, K. C., Adams, S., Thornhill, S. I., Parsley, K. L., Staal, F. J., Gale, R. E., Linch, D. C., Bayford, J., Brown, L., . . . Thrasher, A. J. (2008). Insertional mutagenesis combined with acquired somatic mutations causes leukemogenesis following gene therapy of SCID-X1 patients. *J Clin Invest*, *118*(9), 3143-3150. https://doi.org/10.1172/jci35798

Hsing, M., Wang, Y., Rennie, P. S., Cox, M. E., & Cherkasov, A. (2020). ETS transcription factors as emerging drug targets in cancer. *Med Res Rev*, *40*(1), 413-430. https://doi.org/10.1002/med.21575

Huang, R., Li, X., He, Y., Zhu, W., Gao, L., Liu, Y., Gao, L., Wen, Q., Zhong, J. F., Zhang, C., & Zhang, X. (2020). Recent advances in CAR-T cell engineering. *J Hematol Oncol*, *13*(1), 86. https://doi.org/10.1186/s13045-020-00910-5

Hudson, M. M. (2010). Reproductive outcomes for survivors of childhood cancer. *Obstet Gynecol*, *116*(5), 1171-1183. https://doi.org/10.1097/AOG.0b013e3181f87c4b

Hughes, P., Marshall, D., Reid, Y., Parkes, H., & Gelber, C. (2007). The costs of using unauthenticated, over-passaged cell lines: how much more data do we need? *Biotechniques*, *43*(5), 575, 577-578, 581-572 passim. https://doi.org/10.2144/000112598

Husby, G., Hoagland, P. M., Strickland, R. G., & Williams, R. C., Jr. (1976). Tissue T and B cell infiltration of primary and metastatic cancer. *J Clin Invest*, *57*(6), 1471-1482. https://doi.org/10.1172/jci108417

Jeurink, P. V., Vissers, Y. M., Rappard, B., & Savelkoul, H. F. (2008). T cell responses in fresh and cryopreserved peripheral blood mononuclear cells: kinetics of cell viability, cellular subsets, proliferation, and cytokine production. *Cryobiology*, *57*(2), 91-103. https://doi.org/10.1016/j.cryobiol.2008.06.002

June, C. H., O'Connor, R. S., Kawalekar, O. U., Ghassemi, S., & Milone, M. C. (2018). CAR T cell immunotherapy for human cancer. *Science*, *359*(6382), 1361-1365. https://doi.org/10.1126/science.aar6711

Khan, S., Abid, Z., Haider, G., Bukhari, N., Zehra, D., Hashmi, M., Abid, M., & Ibrahim, U. (2021). Incidence of Ewing's Sarcoma in Different Age Groups, Their Associated Features, and Its Correlation With Primary Care Interval. *Cureus*, *13*(3), e13986. https://doi.org/10.7759/cureus.13986

Kirschner, A. M. (2017). *Characterization and Cloning of Ewing Sarcoma Selective HLA-A*02:01 Restricted T Cell Receptors Directed Against ADRB3 and PAPPA* [Ph.D. Thesis, Technische Universität München]. https://mediatum.ub.tum.de/1327463

Kleiveland, C. R. (2015). Peripheral Blood Mononuclear Cells. In K. Verhoeckx, P. Cotter, I. López-Expósito, C. Kleiveland, T. Lea, A. Mackie, T. Requena, D. Swiatecka, & H. Wichers (Eds.), *The Impact of Food Bioactives on Health: in vitro and ex vivo models* (pp. 161-167). Springer

Copyright 2015, The Author(s). https://doi.org/10.1007/978-3-319-16104-4_15

Knies, D., Klobuch, S., Xue, S. A., Birtel, M., Echchannaoui, H., Yildiz, O., Omokoko, T., Guillaume, P., Romero, P., Stauss, H., Sahin, U., Herr, W., Theobald, M., Thomas, S., & Voss, R. H. (2016). An optimized single chain TCR scaffold relying on the assembly with the native CD3-complex prevents residual mispairing with endogenous TCRs in human T-cells. *Oncotarget*, *7*(16), 21199-21221. https://doi.org/10.18632/oncotarget.8385

Kolodziejczyk, A. A., Kim, J. K., Svensson, V., Marioni, J. C., & Teichmann, S. A. (2015). The technology and biology of single-cell RNA sequencing. *Mol Cell*, *58*(4), 610-620. https://doi.org/10.1016/j.molcel.2015.04.005

Labrecque, N., Whitfield, L. S., Obst, R., Waltzinger, C., Benoist, C., & Mathis, D. (2001). How Much TCR Does a T Cell Need? *Immunity*, *15*(1), 71-82. https://doi.org/https://doi.org/10.1016/S1074-7613(01)00170-4

Leko, V., & Rosenberg, S. A. (2020). Identifying and Targeting Human Tumor Antigens for T Cell-Based Immunotherapy of Solid Tumors. *Cancer Cell*, *38*(4), 454-472. https://doi.org/10.1016/j.ccell.2020.07.013

Lindström, S., & Andersson-Svahn, H. (2012). Single-cell culture in microwells. *Methods Mol Biol*, *853*, 41-52. https://doi.org/10.1007/978-1-61779-567-1_5

Liu, S., Galat, V., Galat, Y., Lee, Y. K. A., Wainwright, D., & Wu, J. (2021). NK cell-based cancer immunotherapy: from basic biology to clinical development. *J Hematol Oncol*, *14*(1), 7. https://doi.org/10.1186/s13045-020-01014-w

Lu, Y. C., Zheng, Z., Lowery, F. J., Gartner, J. J., Prickett, T. D., Robbins, P. F., & Rosenberg, S. A. (2021). Direct identification of neoantigen-specific TCRs from tumor specimens by high-throughput single-cell sequencing. *J Immunother Cancer*, *9*(7). https://doi.org/10.1136/jitc-2021-002595

Lu, Y. C., Zheng, Z., Robbins, P. F., Tran, E., Prickett, T. D., Gartner, J. J., Li, Y. F., Ray, S., Franco, Z., Bliskovsky, V., Fitzgerald, P. C., & Rosenberg, S. A. (2018). An Efficient Single-Cell RNA-Seq Approach to Identify Neoantigen-Specific T Cell Receptors. *Mol Ther*, *26*(2), 379-389. https://doi.org/10.1016/j.ymthe.2017.10.018

Mackintosh, C., Madoz-Gúrpide, J., Ordóñez, J. L., Osuna, D., & Herrero-Martín, D. (2010). The molecular pathogenesis of Ewing's sarcoma. *Cancer Biol Ther*, *9*(9), 655-667. https://doi.org/10.4161/cbt.9.9.11511

Mahlendorf, D. E., & Staege, M. S. (2013). Characterization of Ewing sarcoma associated cancer/testis antigens. *Cancer Biol Ther*, *14*(3), 254-261. https://doi.org/10.4161/cbt.23298

Mann, M., & Jensen, O. N. (2003). Proteomic analysis of post-translational modifications. *Nature Biotechnology*, *21*(3), 255-261. https://doi.org/10.1038/nbt0303-255

Mariuzza, R. A., Agnihotri, P., & Orban, J. (2020). The structural basis of T-cell receptor (TCR) activation: An enduring enigma. *J Biol Chem*, *295*(4), 914-925. https://doi.org/10.1074/jbc.REV119.009411

Marofi, F., Motavalli, R., Safonov, V. A., Thangavelu, L., Yumashev, A. V., Alexander, M., Shomali, N., Chartrand, M. S., Pathak, Y., Jarahian, M., Izadi, S., Hassanzadeh, A., Shirafkan, N., Tahmasebi, S., & Khiavi, F. M. (2021). CAR T cells in solid tumors: challenges and opportunities. *Stem Cell Res Ther*, *12*(1), 81. https://doi.org/10.1186/s13287-020-02128-1

Martkamchan, S., Onlamoon, N., Wang, S., Pattanapanyasat, K., & Ammaranond, P. (2016). The Effects of Anti-CD3/CD28 Coated Beads and IL-2 on Expanded T Cell for Immunotherapy. *Adv Clin Exp Med*, *25*(5), 821-828. https://doi.org/10.17219/acem/35771

Masters, J. R., Thomson, J. A., Daly-Burns, B., Reid, Y. A., Dirks, W. G., Packer, P., Toji, L. H., Ohno, T., Tanabe, H., Arlett, C. F., Kelland, L. R., Harrison, M., Virmani, A., Ward, T. H., Ayres, K. L., & Debenham, P. G. (2001). Short tandem repeat profiling provides an international reference standard for human cell lines. *Proc Natl Acad Sci U S A*, *98*(14), 8012-8017. https://doi.org/10.1073/pnas.121616198

Maude, S. L., Frey, N., Shaw, P. A., Aplenc, R., Barrett, D. M., Bunin, N. J., Chew, A., Gonzalez, V. E., Zheng, Z., Lacey, S. F., Mahnke, Y. D., Melenhorst, J. J., Rheingold, S. R., Shen, A., Teachey, D. T., Levine, B. L., June, C. H., Porter, D. L., & Grupp, S. A. (2014). Chimeric antigen receptor T cells for sustained remissions in leukemia. *N Engl J Med*, *371*(16), 1507-1517. https://doi.org/10.1056/NEJMoa1407222

Mazzotti, L., Gaimari, A., Bravaccini, S., Maltoni, R., Cerchione, C., Juan, M., Navarro, E. A., Pasetto, A., Nascimento Silva, D., Ancarani, V., Sambri, V., Calabrò, L., Martinelli, G., & Mazza, M. (2022). T-Cell Receptor Repertoire Sequencing and Its Applications: Focus on Infectious Diseases and Cancer. *Int J Mol Sci*, *23*(15). https://doi.org/10.3390/ijms23158590

Mohanty, R., Chowdhury, C. R., Arega, S., Sen, P., Ganguly, P., & Ganguly, N. (2019). CAR T cell therapy: A new era for cancer treatment. *Oncology reports*, *42*(6), 2183-2195.

Mohty, B., & Mohty, M. (2011). Long-term complications and side effects after allogeneic hematopoietic stem cell transplantation: an update. *Blood cancer journal*, *1*(4), e16-e16.

Mondragão-Rodrigues, I., & Macedo, M. F. (2023). Buffy Coat Processing Impacts on Monocytes' Capacity to Present Lipid Antigens. *Biomedicines*, *11*(3). https://doi.org/10.3390/biomedicines11030833

Morales, E., Olson, M., Iglesias, F., Dahiya, S., Luetkens, T., & Atanackovic, D. (2020). Role of immunotherapy in Ewing sarcoma. *J Immunother Cancer*, *8*(2). https://doi.org/10.1136/jitc-2020-000653

Morotti, M., Albukhari, A., Alsaadi, A., Artibani, M., Brenton, J. D., Curbishley, S. M., Dong, T., Dustin, M. L., Hu, Z., McGranahan, N., Miller, M. L., Santana-Gonzalez, L., Seymour, L. W., Shi, T., Van Loo, P., Yau, C., White, H., Wietek, N., Church, D. N., . . . Ahmed, A. A. (2021). Promises and challenges

of adoptive T-cell therapies for solid tumours. *Br J Cancer*, *124*(11), 1759-1776. https://doi.org/10.1038/s41416-021-01353-6

Muenst, S., Läubli, H., Soysal, S., Zippelius, A., Tzankov, A., & Hoeller, S. (2016). The immune system and cancer evasion strategies: therapeutic concepts. *Journal of internal medicine*, *279*(6), 541-562.

Neelapu, S. S., Tummala, S., Kebriaei, P., Wierda, W., Gutierrez, C., Locke, F. L., Komanduri, K. V., Lin, Y., Jain, N., Daver, N., Westin, J., Gulbis, A. M., Loghin, M. E., de Groot, J. F., Adkins, S., Davis, S. E., Rezvani, K., Hwu, P., & Shpall, E. J. (2018). Chimeric antigen receptor T-cell therapy - assessment and management of toxicities. *Nat Rev Clin Oncol*, *15*(1), 47-62. https://doi.org/10.1038/nrclinonc.2017.148

Nicholson, E., Ghorashian, S., & Stauss, H. (2012). Improving TCR Gene Therapy for Treatment of Haematological Malignancies. *Adv Hematol*, *2012*, 404081. https://doi.org/10.1155/2012/404081

Orfao, A., & Ruiz-Arguelles, A. (1996). General concepts about cell sorting techniques. *Clin Biochem*, *29*(1), 5-9. https://doi.org/10.1016/0009-9120(95)02017-9

Ozaki, T. (2015). Diagnosis and treatment of Ewing sarcoma of the bone: a review article. *Journal of Orthopaedic Science*, *20*, 250-263.

Pamies, D., Leist, M., Coecke, S., Bowe, G., Allen, D. G., Gstraunthaler, G., Bal-Price, A., Pistollato, F., de Vries, R. B. M., Hogberg, H. T., Hartung, T., & Stacey, G. (2022). Guidance document on Good Cell and Tissue Culture Practice 2.0 (GCCP 2.0). *Altex*, *39*, 30-70. https://doi.org/10.14573/altex.2111011

Paulino, A. C., & Fowler, B. Z. (2005). Secondary neoplasms after radiotherapy for a childhood solid tumor. *Pediatr Hematol Oncol*, *22*(2), 89-101. https://doi.org/10.1080/08880010590896459

Perfetto, S. P., Chattopadhyay, P. K., & Roederer, M. (2004). Seventeen-colour flow cytometry: unravelling the immune system. *Nat Rev Immunol*, *4*(8), 648-655. https://doi.org/10.1038/nri1416

Picot, J., Guerin, C. L., Le Van Kim, C., & Boulanger, C. M. (2012). Flow cytometry: retrospective, fundamentals and recent instrumentation. *Cytotechnology*, *64*(2), 109-130. https://doi.org/10.1007/s10616-011-9415-0

Pirson, S. (2010). *Generation of autologous and allorestricted cytotoxic T cell clones directed against Ewing Tumor antigens* [Ph.D. Thesis, Technische Universität München]. https://mediatum.ub.tum.de/737159

Pishesha, N., Harmand, T. J., & Ploegh, H. L. (2022). A guide to antigen processing and presentation. *Nat Rev Immunol*, *22*(12), 751-764. https://doi.org/10.1038/s41577-022-00707-2

Porter, D. L., Levine, B. L., Kalos, M., Bagg, A., & June, C. H. (2011). Chimeric antigen receptor-modified T cells in chronic lymphoid leukemia. *N Engl J Med*, *365*(8), 725-733. https://doi.org/10.1056/NEJMoa1103849

ProImmune. (2024). *Pro5® MHC Class I Pentamers*. https://www.proimmune.com/introduction-to-pentamers/

Psatha, K., Kollipara, L., Voutyraki, C., Divanach, P., Sickmann, A., Rassidakis, G. Z., Drakos, E., & Aivaliotis, M. (2017). Deciphering lymphoma pathogenesis via state-of-the-art mass spectrometry-based quantitative proteomics. *Journal of Chromatography B*, *1047*, 2-14. https://doi.org/https://doi.org/10.1016/j.jchromb.2016.11.005

Rath, J. A., & Arber, C. (2020). Engineering Strategies to Enhance TCR-Based Adoptive T Cell Therapy. *Cells*, *9*(6). https://doi.org/10.3390/cells9061485

Rathmell, J. C., Vander Heiden, M. G., Harris, M. H., Frauwirth, K. A., & Thompson, C. B. (2000). In the absence of extrinsic signals, nutrient utilization by lymphocytes is insufficient to maintain either cell size or viability. *Mol Cell*, *6*(3), 683-692. https://doi.org/10.1016/s1097-2765(00)00066-6

Restifo, N. P., Dudley, M. E., & Rosenberg, S. A. (2012). Adoptive immunotherapy for cancer: harnessing the T cell response. *Nat Rev Immunol*, *12*(4), 269-281. https://doi.org/10.1038/nri3191

Richard, A. C., Frazer, G. L., Ma, C. Y., & Griffiths, G. M. (2021). Staggered starts in the race to T cell activation. *Trends Immunol*, *42*(11), 994-1008. https://doi.org/10.1016/j.it.2021.09.004

Richter, G. H., Fasan, A., Hauer, K., Grunewald, T. G., Berns, C., Rössler, S., Naumann, I., Staege, M. S., Fulda, S., Esposito, I., & Burdach, S. (2013). G-Protein coupled receptor 64 promotes invasiveness and metastasis in Ewing sarcomas through PGF and MMP1. *J Pathol*, *230*(1), 70-81. https://doi.org/10.1002/path.4170

Rohaan, M. W., Wilgenhof, S., & Haanen, J. (2019). Adoptive cellular therapies: the current landscape. *Virchows Arch*, *474*(4), 449-461. https://doi.org/10.1007/s00428-018-2484-0

Rosenberg, S. A., & Restifo, N. P. (2015). Adoptive cell transfer as personalized immunotherapy for human cancer. *Science*, *348*(6230), 62-68. https://doi.org/10.1126/science.aaa4967

Rosenberg, S. A., Spiess, P., & Lafreniere, R. (1986). A new approach to the adoptive immunotherapy of cancer with tumor-infiltrating lymphocytes. *Science*, *233*(4770), 1318-1321. https://doi.org/10.1126/science.3489291

Rudolph, M. G., Stanfield, R. L., & Wilson, I. A. (2006). How TCRs bind MHCs, peptides, and coreceptors. *Annu Rev Immunol*, *24*, 419-466. https://doi.org/10.1146/annurev.immunol.23.021704.115658

Ruutu, T., Van Biezen, A., Hertenstein, B., Henseler, A., Garderet, L., Passweg, J., Mohty, M., Sureda, A., Niederwieser, D., & Gratwohl, A. (2012). Prophylaxis and treatment of GVHD after allogeneic haematopoietic SCT: a survey of centre strategies by the European Group for Blood and Marrow Transplantation. *Bone marrow transplantation*, *47*(11), 1459-1464.

Sadelain, M., Brentjens, R., & Rivière, I. (2009). The promise and potential pitfalls of chimeric antigen receptors. *Curr Opin Immunol*, *21*(2), 215-223. https://doi.org/10.1016/j.coi.2009.02.009

Sakimura, R., Tanaka, K., Nakatani, F., Matsunobu, T., Li, X., Hanada, M., Okada, T., Nakamura, T., Matsumoto, Y., & Iwamoto, Y. (2005). Antitumor effects of histone deacetylase inhibitor on Ewing's family tumors. *Int J Cancer*, *116*(5), 784-792. https://doi.org/10.1002/ijc.21069

Salter, A. I., Rajan, A., Kennedy, J. J., Ivey, R. G., Shelby, S. A., Leung, I., Templeton, M. L., Muhunthan, V., Voillet, V., Sommermeyer, D., Whiteaker, J. R., Gottardo, R., Veatch, S. L., Paulovich, A. G., & Riddell, S. R. (2021). Comparative analysis of TCR and CAR signaling informs CAR designs with superior antigen sensitivity and in vivo function. *Science Signaling*, *14*(697), eabe2606. https://doi.org/doi:10.1126/scisignal.abe2606

Schirmer, D., Storz, I., Wisskirchen, K., Feederle, R., Schmidt, O., Abken, H., Protzer, U., Burdach, S., & Richter, G. H. S. (2018). Abstract A09: GPR64-specific CAR-transgenic T cells selectively kill Ewing sarcoma in vivo. *Cancer*

Research, *78*(19_Supplement), A09-A09. https://doi.org/10.1158/1538-7445.Pedca17-a09

Schmid, D. A., Irving, M. B., Posevitz, V., Hebeisen, M., Posevitz-Fejfar, A., Sarria, J. C., Gomez-Eerland, R., Thome, M., Schumacher, T. N., Romero, P., Speiser, D. E., Zoete, V., Michielin, O., & Rufer, N. (2010). Evidence for a TCR affinity threshold delimiting maximal CD8 T cell function. *J Immunol*, *184*(9), 4936-4946. https://doi.org/10.4049/jimmunol.1000173

Schober, K., Müller, T. R., Gökmen, F., Grassmann, S., Effenberger, M., Poltorak, M., Stemberger, C., Schumann, K., Roth, T. L., Marson, A., & Busch, D. H. (2019). Orthotopic replacement of T-cell receptor α- and β-chains with preservation of near-physiological T-cell function. *Nat Biomed Eng*, *3*(12), 974-984. https://doi.org/10.1038/s41551-019-0409-0

Schober, S. J., Thiede, M., Gassmann, H., von Ofen, A. J., Knoch, P., Eck, J., Prexler, C., Kordass-Wally, C., Hauer, J., Burdach, S., Holm, P. S., & Thiel, U. (2024). TCR-transgenic T cells and YB-1-based oncolytic virotherapy improve survival in a preclinical Ewing sarcoma xenograft mouse model. *Front Immunol*, *15*, 1330868. https://doi.org/10.3389/fimmu.2024.1330868

Schreiber, R. D., Old, L. J., & Smyth, M. J. (2011). Cancer immunoediting: integrating immunity's roles in cancer suppression and promotion. *Science*, *331*(6024), 1565-1570. https://doi.org/10.1126/science.1203486

Schrum, A. G., Turka, L. A., & Palmer, E. (2003). Surface T-cell antigen receptor expression and availability for long-term antigenic signaling. *Immunol Rev*, *196*, 7-24. https://doi.org/10.1046/j.1600-065x.2003.00083.x

Scotlandi, K., Hattinger, C. M., Pellegrini, E., Gambarotti, M., & Serra, M. (2020). Genomics and Therapeutic Vulnerabilities of Primary Bone Tumors. *Cells*, *9*(4). https://doi.org/10.3390/cells9040968

Seliger, B. (2005). Strategies of tumor immune evasion. *BioDrugs*, *19*, 347-354.

Shafer, P., Kelly, L. M., & Hoyos, V. (2022). Cancer Therapy With TCR-Engineered T Cells: Current Strategies, Challenges, and Prospects. *Front Immunol*, *13*, 835762. https://doi.org/10.3389/fimmu.2022.835762

Shah, K., Al-Haidari, A., Sun, J., & Kazi, J. U. (2021). T cell receptor (TCR) signaling in health and disease. *Signal Transduct Target Ther*, *6*(1), 412. https://doi.org/10.1038/s41392-021-00823-w

Simbre, V. C., Duffy, S. A., Dadlani, G. H., Miller, T. L., & Lipshultz, S. E. (2005). Cardiotoxicity of cancer chemotherapy: implications for children. *Pediatric Drugs*, *7*, 187-202.

Sinitcyn, P., Richards, A. L., Weatheritt, R. J., Brademan, D. R., Marx, H., Shishkova, E., Meyer, J. G., Hebert, A. S., Westphall, M. S., Blencowe, B. J., Cox, J., & Coon, J. J. (2023). Global detection of human variants and isoforms by deep proteome sequencing. *Nature Biotechnology*, *41*(12), 1776-1786. https://doi.org/10.1038/s41587-023-01714-x

Smith, K. A. (1988). Interleukin-2: inception, impact, and implications. *Science*, *240*(4856), 1169-1176. https://doi.org/10.1126/science.3131876

Staege, M. S., Hutter, C., Neumann, I., Foja, S., Hattenhorst, U. E., Hansen, G., Afar, D., & Burdach, S. E. (2004). DNA microarrays reveal relationship of Ewing family tumors to both endothelial and fetal neural crest-derived cells and define novel targets. *Cancer Res*, *64*(22), 8213-8221. https://doi.org/10.1158/0008-5472.Can-03-4059

Steinman, R. M. (2003). Some interfaces of dendritic cell biology. *Apmis*, *111*(7-8), 675-697. https://doi.org/10.1034/j.1600-0463.2003.11107802.x

Sterner, R. C., & Sterner, R. M. (2021). CAR-T cell therapy: current limitations and potential strategies. *Blood Cancer J*, *11*(4), 69. https://doi.org/10.1038/s41408-021-00459-7

Storz, I. M. (2020). *Generation of transgenic, GPR64 tumor antigen-specific T cells and evaluation of their therapeutic efficacy in pediatric sarcoma* [Ph.D. Thesis, Technische Universität München]. https://mediatum.ub.tum.de/1506557

Stubbington, M. J. T., Rozenblatt-Rosen, O., Regev, A., & Teichmann, S. A. (2017). Single-cell transcriptomics to explore the immune system in health and disease. *Science*, *358*(6359), 58-63. https://doi.org/10.1126/science.aan6828

Sudarsanam, H., Buhmann, R., & Henschler, R. (2022). Influence of Culture Conditions on Ex Vivo Expansion of T Lymphocytes and Their Function for Therapy: Current Insights and Open Questions. *Front Bioeng Biotechnol*, *10*, 886637. https://doi.org/10.3389/fbioe.2022.886637

Szabo, P. A., Levitin, H. M., Miron, M., Snyder, M. E., Senda, T., Yuan, J., Cheng, Y. L., Bush, E. C., Dogra, P., Thapa, P., Farber, D. L., & Sims, P. A. (2019). Single-cell transcriptomics of human T cells reveals tissue and activation

signatures in health and disease. *Nat Commun*, *10*(1), 4706. https://doi.org/10.1038/s41467-019-12464-3

Szeto, C., Lobos, C. A., Nguyen, A. T., & Gras, S. (2020). TCR Recognition of Peptide-MHC-I: Rule Makers and Breakers. *Int J Mol Sci*, *22*(1). https://doi.org/10.3390/ijms22010068

Thiel, U., Pirson, S., Müller-Spahn, C., Conrad, H., Busch, D. H., Bernhard, H., Burdach, S., & Richter, G. H. (2011). Specific recognition and inhibition of Ewing tumour growth by antigen-specific allo-restricted cytotoxic T cells. *Br J Cancer*, *104*(6), 948-956. https://doi.org/10.1038/bjc.2011.54

Thiel, U., Schober, S. J., Einspieler, I., Kirschner, A., Thiede, M., Schirmer, D., Gall, K., Blaeschke, F., Schmidt, O., Jabar, S., Ranft, A., Alba Rubío, R., Dirksen, U., Grunewald, T. G. P., Sorensen, P. H., Richter, G. H. S., von Lüttichau, I. T., Busch, D. H., & Burdach, S. E. G. (2017). Ewing sarcoma partial regression without GvHD by chondromodulin-I/HLA-A*02:01-specific allorestricted T cell receptor transgenic T cells. *Oncoimmunology*, *6*(5), e1312239. https://doi.org/10.1080/2162402x.2017.1312239

Thiel, U., Wawer, A., Wolf, P., Badoglio, M., Santucci, A., Klingebiel, T., Basu, O., Borkhardt, A., Laws, H.-J., & Kodera, Y. (2011). No improvement of survival with reduced-versus high-intensity conditioning for allogeneic stem cell transplants in Ewing tumor patients. *Annals of oncology*, *22*(7), 1614-1621.

Toomey, E. C., Schiffman, J. D., & Lessnick, S. L. (2010). Recent advances in the molecular pathogenesis of Ewing's sarcoma. *Oncogene*, *29*(32), 4504-4516. https://doi.org/10.1038/onc.2010.205

Torrens-Fontanals, M., Stepniewski, T. M., Gloriam, D. E., & Selent, J. (2021). Structural dynamics bridge the gap between the genetic and functional levels of GPCRs. *Current Opinion in Structural Biology*, *69*, 150-159. https://doi.org/https://doi.org/10.1016/j.sbi.2021.04.005

Tsimberidou, A.-M. (2015). Targeted therapy in cancer. *Cancer chemotherapy and pharmacology*, *76*, 1113-1132.

Tsimberidou, A. M., Van Morris, K., Vo, H. H., Eck, S., Lin, Y. F., Rivas, J. M., & Andersson, B. S. (2021). T-cell receptor-based therapy: an innovative therapeutic approach for solid tumors. *J Hematol Oncol*, *14*(1), 102. https://doi.org/10.1186/s13045-021-01115-0

Tu, J., Huo, Z., Gingold, J., Zhao, R., Shen, J., & Lee, D. F. (2017). The Histogenesis of Ewing Sarcoma. *Cancer Rep Rev*, *1*(2). https://doi.org/10.15761/crr.1000111

Uphoff, C. C., & Drexler, H. G. (2011). Detecting mycoplasma contamination in cell cultures by polymerase chain reaction. *Methods Mol Biol*, *731*, 93-103. https://doi.org/10.1007/978-1-61779-080-5_8

Viret, C., & Janeway, C. A., Jr. (1999). MHC and T cell development. *Rev Immunogenet*, *1*(1), 91-104.

von Heyking, K., Calzada-Wack, J., Göllner, S., Neff, F., Schmidt, O., Hensel, T., Schirmer, D., Fasan, A., Esposito, I., Müller-Tidow, C., Sorensen, P. H., Burdach, S., & Richter, G. H. S. (2017). The endochondral bone protein CHM1 sustains an undifferentiated, invasive phenotype, promoting lung metastasis in Ewing sarcoma. *Mol Oncol*, *11*(9), 1288-1301. https://doi.org/10.1002/1878-0261.12057

Wachsmann, T. L. A., Wouters, A. K., Remst, D. F. G., Hagedoorn, R. S., Meeuwsen, M. H., van Diest, E., Leusen, J., Kuball, J., Falkenburg, J. H. F., & Heemskerk, M. H. M. (2022). Comparing CAR and TCR engineered T cell performance as a function of tumor cell exposure. *Oncoimmunology*, *11*(1), 2033528. https://doi.org/10.1080/2162402x.2022.2033528

Waldman, A. D., Fritz, J. M., & Lenardo, M. J. (2020). A guide to cancer immunotherapy: from T cell basic science to clinical practice. *Nat Rev Immunol*, *20*(11), 651-668. https://doi.org/10.1038/s41577-020-0306-5

Wei, F., Cheng, X. X., Xue, J. Z., & Xue, S. A. (2022). Emerging Strategies in TCR-Engineered T Cells. *Front Immunol*, *13*, 850358. https://doi.org/10.3389/fimmu.2022.850358

Wherry, E. J. (2011). T cell exhaustion. *Nat Immunol*, *12*(6), 492-499. https://doi.org/10.1038/ni.2035

Wherry, E. J., & Kurachi, M. (2015). Molecular and cellular insights into T cell exhaustion. *Nat Rev Immunol*, *15*(8), 486-499. https://doi.org/10.1038/nri3862

Widhe, B., & Widhe, T. (2000). Initial symptoms and clinical features in osteosarcoma and Ewing sarcoma. *J Bone Joint Surg Am*, *82*(5), 667-674. https://doi.org/10.2106/00004623-200005000-00007

Worch, J., Matthay, K. K., Neuhaus, J., Goldsby, R., & DuBois, S. G. (2010). Ethnic and racial differences in patients with Ewing sarcoma. *Cancer*, *116*(4), 983-988. https://doi.org/10.1002/cncr.24865

Wu, H.-C., Chang, D.-K., & Huang, C.-T. (2006). Targeted therapy for cancer. *J Cancer Mol*, *2*(2), 57-66.

Wu, L., Wei, Q., Brzostek, J., & Gascoigne, N. R. J. (2020). Signaling from T cell receptors (TCRs) and chimeric antigen receptors (CARs) on T cells. *Cell Mol Immunol*, *17*(6), 600-612. https://doi.org/10.1038/s41423-020-0470-3

Xue, B. (2022). *Comparison of T Cells Engineered With CRISPR/Cas9 or Retroviral Gene Transfer In Immunotherapy of Ewing Sarcoma* [Ph.D. Thesis, Technische Universität München]. https://mediatum.ub.tum.de/1656810

Xue, B., von Heyking, K., Gassmann, H., Poorebrahim, M., Thiede, M., Schober, K., Mautner, J., Hauer, J., Ruland, J., Busch, D. H., Thiel, U., & Burdach, S. E. G. (2022). T Cells Directed against the Metastatic Driver Chondromodulin-1 in Ewing Sarcoma: Comparative Engineering with CRISPR/Cas9 vs. Retroviral Gene Transfer for Adoptive Transfer. *Cancers (Basel)*, *14*(22). https://doi.org/10.3390/cancers14225485

Young, L., Sung, J., Stacey, G., & Masters, J. R. (2010). Detection of Mycoplasma in cell cultures. *Nat Protoc*, *5*(5), 929-934. https://doi.org/10.1038/nprot.2010.43

Zöllner, S. K., Amatruda, J. F., Bauer, S., Collaud, S., de Álava, E., DuBois, S. G., Hardes, J., Hartmann, W., Kovar, H., Metzler, M., Shulman, D. S., Streitbürger, A., Timmermann, B., Toretsky, J. A., Uhlenbruch, Y., Vieth, V., Grünewald, T. G. P., & Dirksen, U. (2021). Ewing Sarcoma-Diagnosis, Treatment, Clinical Challenges and Future Perspectives. *J Clin Med*, *10*(8). https://doi.org/10.3390/jcm10081685

AI Declaration

During the preparation of this dissertation, I utilized ChatGPT-4 and Aithor.com to assist with literature research (Scholar GPT), drafting sections and brainstorming ideas (introduction and discussion), translations, and editing to enhance readability and language, as well as Grammarly to

improve grammar and style. All content generated or suggested by these tools was based on my input and critically evaluated, modified, rewritten, and edited by me, and I take full responsibility for the content of the dissertation. This Declaration was made after consulting the “Stellungnahme des Präsidiumsder Deutschen Forschungsgemeinschaft (DFG) zum Einfluss generativer Modelle für die Text- und Bilderstellung auf die Wissenschaften und das Förderhandeln der DFG” from September 2023.

9 Appendix

Appendix 1

Table 24 Full table of binding scores & cross-reactivity of various PAX7 peptides (in silico using SYFPEITHY & ScanProsite). *Four peptides (highlighted in green) showed a high binding score and no hits in the cross-reactivity test and were ordered for further analysis. Table was sorted by binding score in descending order.*

Position	Sequence	Score (SYFPEITHI)	Hits (Cross-Reactivity)
381	G L S P Q V M S I	27	Big-1 (bacterial Ig-like domain 1) domain profile : >PS51127|BIG1 (profile) Big-1 (bacterial Ig-like domain 1)
151	G L V S S I S R V	25	Biopterin-dependent aromatic amino acid hydroxylase family profile : >PS51410|BH4_AAA_HYDROXYL_2 (profile) Biopterin-dependent aromatic amino acid hydroxylase family profile :
191	I L G D K G N R L	25	Big-1 (bacterial Ig-like domain 1) domain profile : >PS51127|BIG1 (profile) Big-1 (bacterial Ig-like domain 1) domain profile :
224	F T A E Q L E E L	25	Protein prenyltransferases alpha subunit repeat profile : >PS51147|PFTA (profile) Protein prenyltransferases alpha subunit repeat profile : 1 - 9: score=4.592 [low confidence] -------FTAEQLEEL---------- ADF-H domain profile : >PS51263|ADF_H (profile) ADF-H domain profile : 1 - 9: score=5.084 [low confidence] ---------- ----------FTAEQLEEL---------- QLQ domain profile : >PS51666|QLQ (profile) QLQ domain profile : 1 - 9: score=8.107 [low confidence] -FTAEQLEEL----------
388	S I L G N P S A V	25	Big-1 (bacterial Ig-like domain 1) domain profile : >PS51127|BIG1 (profile) Big-1 (bacterial Ig-like domain 1) domain profile : 1 - 9: score=4.499 [low confidence] ---------- ----------SILGNPSAV-------- GTF2I-like repeat profile : >PS51139|GTF2I (profile) GTF2I-like repeat profile : 1 - 9: score=5.012 [low confidence] ----------SILGNPSAV----- ----------
255	K L T E A R V Q V	24	Big-1 (bacterial Ig-like domain 1) domain profile : >PS51127|BIG1 (profile) Big-1 (bacterial Ig-like domain 1) domain profile : 1 - 9: score=4.417 [low confidence] ----------KLT---EARVQV---------- ---------- Kininogen-type cystatin domain profile : >PS51647|CYSTATIN_KININOGEN (profile) Kininogen-type cystatin domain profile : 1 - 9: score=6.457 [low confidence]

			----------KLTEARVQV---------- ----------
280	Q L A A F N H L L	24	0 hit in 0 sequence
405	S I S P L H G G L	24	Ephrin receptor-binding (ephrin RBD) domain profile : >PS51551|EPHRIN_RBD_2 (profile) Ephrin receptor-binding (ephrin RBD) domain profile :
489	C L F M E S Y K V	24	0 hit in 0 sequence
3	A L P G T V P R M	23	0 hit in 0 sequence
374	H M N P V S N G L	23	0 hit in 0 sequence
470	C L V P W A S P V	22	Reelin domain profile : >PS51019|REELIN (profile) Reelin domain profile : >USERSEQ1 (9 aa) CLVPWASPV 1 - 9: score=6.984 [low confidence]
54	H I R H K I V E M	21	Protein prenyltransferases alpha subunit repeat profile : >PS51147|PFTA (profile) Protein prenyltransferases alpha subunit repeat profile : >USERSEQ1 (9 aa) HIRHKIVEM 1 - 9: score=4.610 [low confidence]
287	L L P G G F P P T	21	CobBQ-type GATase domain profile : >PS51274|GATASE_COBBQ (profile) CobBQ-type GATase domain profile : 1 - 9: score=7.727 [low confidence] ----------LLPGGFPPT------- ---------- ---------- ---------- PfpI endopeptidase domain profile : >PS51276|PEPTIDASE_C56_PFPI (profile) PfpI endopeptidase domain profile : 1 - 9: score=6.969 [low confidence]
408	P L H G G L D S A	21	GMP synthetase ATP pyrophosphatase (GMPS ATP-PPase) domain profile : >PS51553|GMPS_ATP_PPASE (profile) GMP synthetase ATP pyrophosphatase (GMPS ATP-PPase) domain profile : >USERSEQ1 (9 aa) PLHGGLDSA 1 - 9: score=7.859 [low confidence]
75	Q L R V S H G C V	20	Paired DNA-binding domain profile : >PS51057|PAIRED_2 (profile) Paired DNA-binding domain profile : >USERSEQ1 (9 aa) QLRVSHGCV 1 - 9: score=7.474 [low confidence]
338	G L A A A A A A A	20	Big-1 (bacterial Ig-like domain 1) domain profile : >PS51127|BIG1 (profile) Big-1 (bacterial Ig-like domain 1) domain profile : >USERSEQ1 (9 aa) GLAAAAAAA 1 - 9: score=4.623 [low confidence]
33	L G Q G R V N Q L	19	Big-1 (bacterial Ig-like domain 1) domain profile : >PS51127|BIG1 (profile) Big-1 (bacterial Ig-like domain 1) domain profile :

			>USERSEQ1 (9 aa) LGQGRVNQL 1 - 9: score=4.128 [low confidence]
30	S T P L G Q G R V	18	Big-1 (bacterial Ig-like domain 1) domain profile : >PS51127|BIG1 (profile) Big-1 (bacterial Ig-like domain 1) domain profile : >USERSEQ1 (9 aa) STPLGQGRV 1 - 9: score=5.016 [low confidence]
148	V P S G L V S S I	18	Big-1 (bacterial Ig-like domain 1) domain profile : >PS51127|BIG1 (profile) Big-1 (bacterial Ig-like domain 1) domain profile : >USERSEQ1 (9 aa) VPSGLVSSI 1 - 9: score=4.479 [low confidence]
304	Q L P D S T Y P T	18	Big-1 (bacterial Ig-like domain 1) domain profile : >PS51127|BIG1 (profile) Big-1 (bacterial Ig-like domain 1) domain profile : >USERSEQ1 (9 aa) QLPDSTYPT 1 - 9: score=4.210 [low confidence]

Appendix 2

Table 25 BLAST results - Sequence of the identified Vβ chain of the GPR64 TCR*. Only a Vβ -chain could be identified, after electrophoresis, PCR, and sequencing. The name sequence of the corresponding relevant primer is highlighted in yellow. Also listed is the identification of the sequence as TCR sequence. Also explained is the ORF and the number of ORFs (derived from BLAST & ORFfiner)*

Primer	Identified Sequence	number of ORFs	relevant ORF	identified as…
>6-GPR64\(Vb-8><3CbII)	ATTTACTTTAACAACAACGTTCCGATAGATGATTCAGGGATGCCCGAGGATCGATTCTCAGCTAAGATGCCTAATGCATCATTCTCCACTCTGAAGATCCAGCCCTCAGAACCCAGGGACTCAGCTGTGTACTTCTGTGCCAGCACCCTAGAGCCTCAGCCCCAGCATTTTGGTGATGGGACTCGACTCTCCATCCTAGAGGACCTGAACAAGGTGTTCCCACCCGAGGTCGCTGTGTTTGAGCCATC	2 (ORF2 negative strand)	MPEDRFSAKMPNASFSTLKIQPSEPRDSAVYFCASTLEPQPQHFGDGTRLSILEDLNKVFPPEVAVFEP	Homo sapiens T cell receptor beta chain (TCRBV8S1-TCRBJ1S5) mRNA, complete cds

Appendix 3

Table 26 BLAST results - Sequences of the identified Vα and Vβ chains of the CHM1 TCR. *Several Vα- and Vβ-chains could be identified via electrophoresis, PCR, and sequencing, indicating viable T cells in the sample but calling monoclonality into question. The name sequence of the corresponding relevant primer is highlighted in yellow. Also listed is the identification of the sequence as TCR sequence. Also explained is the ORF and the number of ORFs (derived from BLAST & ORFfiner)*

Primer	Identified Sequence	number of ORFs	relevant ORF	identified as…	RecName	AltName	Short	Flags
>CHM1-Va-14\(Va-14)	TGTGCAGGAGGCAGAGACYGTGACC CTGAGCTGCACAT ATGACACCAGTGAGAGTRATTATTAT TTRTTCTGGTACAA RCAGCCTCCCAGCAGGCAGATGATT CTCGTTATTCGCCAA GAAGCTTATAAGCAACAGAATGCAAC RGAGAATCGTTTCT CTGTGAACTTCCAGAAAGCAGCCAAA TCCTTCAGTCTCAA GATCTCAKACTCACAGCTGGGGGAT GCCGCGATGTATTTY TGTGCTTC	1	MILVIRQEAYKQ QNAT ENRFSVNFQKAA KSFS LKISXSQLGDAA MYFCA	Homo sapiens mRNA for T cell receptor alpha chain V-J-region, partial cds, isolate: Donor4-TRA1	Full=T cell receptor alpha variable 38-2/delta variable 8; Full=T cell receptor alpha chain MC.7.G5	Full=MC.7.G5 TRA; Full=TR alpha chain TRAV38-2DV8*01J31*01C*01		Flags: Precursor [Homo sapiens]
>CHM1-Va-14-1\(Va-14-1)	TGTGCAGGAGGCAGAGACYGTGACC CTGAGYTGCACATAT GACACCAGTGAGARTRATTATTATTT RTTCTGGTACAAGCA GCCTCCCAGCAGGCAGATGATTCTC GTTATTCGCCAAGAA GCTTATAAGCAACAGAATGCAACRGA GAATCGTTTCTCTG TGAACTTCCAGAAAGCAGCCAAATCC TTCAGTCTCAAGAT CTCAGACTCACAGCTGGGGGACAC	1	MILVIRQEAYKQ QNATEN RFSVNFQKAAKS FSLKIS DSQLGD	Homo sapiens mRNA for T cell receptor alpha chain V-J-region, partial cds, isolate: CM(3)-TRA151	Full=T cell receptor alpha variable 38-1; Full=T cell receptor alpha variable 38-2/delta variable 8; Full=T cell receptor alpha chain MC.7.G5	Full=MC.7.G5 TRA; Full=TR alpha chain TRAV38-2DV8*01J31*01C*01		Precursor [Homo sapiens]
>CHM1-Vb-4\(Vb-4><3Cbll)	ACATATGAGAGTGGATTTGTCATTGA CAAGTTTCCCATCAG CCGCCCAAACCTAACATTCTCAACTC TGACTGTGAGCAACA TGAGCCCTGAAGACAGCAGCATATAT CTCTGCAGCGTTGAAG ACCGGGGACCAGGCTATGGCTACAC CTTCGGTTCGGGGACCA GGTTAACCGTTGTAGAGGACCTGAAC AAGGTGTTCCCACCC GAGGTCGCTGTGTTTGAGCCATC	3 (ORF2+ORF3 negative strand)	MSPEDSSIYLCSVE D RGPGYGYTFGSGT RL TVVEDLNKVFPPEV AVFEP	Homo sapiens clone BC2 T cell receptor beta chain (TRB) mRNA, partial cds	Full=T cell receptor beta variable 29-1			Precursor [Homo sapiens]
CHM1-Vb-6-1\(Vb-6-1><3Cbll)	CACAATGAAGCTCAACTAGAAAAATC AAGGCTGCTCAG TGATCGGTTCTCTGCAGAGAGGCCTA AGGGATCTTTCT CCACCTTGGAGATCCAGCGCACAGA GCAGGGGGACTC GGCCATGTATCTCTGTGCCAGCAGCT CTTCAGTGGGTG GGGCCAACGTCCTGACTTTCGGGGC CGGCAGCAGGCTG ACCGTGCTGGAGGACCTGAAAAACG TGTCCCACCC	2 (ORF2 negative stra	MYLCASSSSVGGA NV LTFGAGSRLTVLED L KNVSH	Homo Sapiens mRNA for T-cell receptor beta chain (TRB gene), clone HA-1H Donor C TRBV7-9*01	Full=T cell receptor beta chain MC.7.G5	Full=TR beta chain TRBV25-1*01J2S3*01C2*01	MC.7.G5 TRB	Precursor [Homo sapiens]

		nd)						
>CHM1-Vb-7\(Vb-7><3Cbll)	CCTGAATGCCCCAACAGCTCTCTCTTAAACCTTCACCTACACGCCCTGCAGCCAGAAGACTCAGCCCCTGTATCTCTGCGCCAGCAGCCATCCCCGCCCTACGAGCAGTACTTCGGGCCGGGCACCAGGCTCACGGTCACAGAGGACCTGAAAAACGTGTTCCCACCCGAGGTCGCTGTGTTTGAGCCATC	1	MPQQLSLKPSPTRPAARRLSPVSLRQQPSPPYEQYFGPGTRLTVTEDLKNVFPPEVAVFEP	Homo sapiens clone 510 T cell receptor beta mRNA, partial cds	Full=T cell receptor beta chain MC.7.G5	Full=TR beta chain TRBV25-1*01J2S3*01C2*01	MC.7.G5 TRB	Precursor [Homo sapiens]

10 Acknowledgments

During the preparation of my research project at the Laboratory ‘Labor für krebskranke Kinder’, I met and could learn from a lot of great people.

I want to thank PD Dr. Uwe Thiel for allowing me to conduct my research and for his guidance and support. I also owe a huge thank you to Dr. Sebastian Schober, Dr. Hendrik Gaßmann, Dr. Kristina von Heyking, and Dr. Carolin Prexler for their patience and advice. Additionally, I am grateful to Melanie Thiede, Jennifer Eck, and Corazón Kordass for constantly answering all my questions.

Furthermore, I want to thank everyone for making my work experience not only instructive but also a lot of fun, especially Kira Schneider, who started with me at zero, and Sophia Laube, who shared the experience.

Lastly, I give thanks to all my family and friends, who listened to all my stories and complaints and accompanied me until the end.